The Dissertation Committee for Scott Anthony Kerr Certifies that this is the approved version of the following dissertation:

Host Range Trade-Offs in New World Arenaviruses and Discovery of Antibodies Against Ebola Virus and Norovirus

Committee:

George Georgiou, Supervisor

Sara L. Sawyer, Co-Supervisor

Kenneth A. Johnson

Christopher S. Sullivan

Jason L. Upton

Host Range Trade-Offs in New World Arenaviruses and Discovery of Antibodies Against Ebola Virus and Norovirus

by

Scott Anthony Kerr, B.S.

Dissertation

Presented to the Faculty of the Graduate School of

The University of Texas at Austin

in Partial Fulfillment

of the Requirements

for the Degree of

Doctor of Philosophy

The University of Texas at Austin

December 2016

Dedication

To Grandpa Sandy

“Do the best you can with the tools you have.”

Acknowledgements

I would like to acknowledge my parents for always pushing me to explore and giving me the tools to confidently go after the next big thing.

I would also like to acknowledge Celeste, Harmit, George and Sara for giving me an opportunity in their research groups. I cannot imagine a more thoughtful, caring, and inspiring group of mentors, it has been a true privilege.

Finally, I would like to acknowledge all my friends, family, and colleagues both inside and outside of graduate school. It has truly been a memorable ride. And Far West is not that far!

Host Range Trade-Offs in New World Arenaviruses and Discovery of Antibodies Against Ebola Virus and Norovirus

Scott Anthony Kerr, Ph.D.

The University of Texas at Austin, 2016

Supervisors: George Georgiou and Sara L. Sawyer

All biological life lives under the constant threat of viral infection. From the earliest homo sapiens until now well into the 21st century, the destruction brought on human life by viruses has been immense. Combating the viral threat has always required a combination of basic science and applied engineering. Scientific understanding of how viruses infect, propagate, and evolve is a pre-requisite for understanding how to go about preventing their activity. Of equal importance is the engineering of applications to take advantage of that knowledge to build solutions to the constant threat. The combination of hypothesis driven research and applied biotechnology lead to the first vaccines and the process continues to this day as we continue to build better diagnostic tools, safer vaccines, and more comprehensive strategies to combat the constant viral threat. Recent outbreaks of Ebola, Norovirus, Arenaviruses, novel Influenza strains, and Zika virus punctuate the ongoing need for understanding and application. Continuing in this tradition, the work describes both basic science and applied biotechnology approaches to: 1) understand host-viral evolution patterns in New World Arenaviruses, 2) identify Ebola specific antibodies for a diagnostic platform, and 3) characterize the immune profile following a Norovirus vaccine in clinical trials.

Table of Contents

List of Tables

List of Figures

Chapter 1: Introduction

Viruses are a constant threat to human health. They are naturally passed through fluids, air, and bodily contact. They infect both wild and domesticated species and some of them routinely hop into and through the human population. Viral infection and spread is exacerbated by the effects of large human migration movements, humans pushing into wildlands, and the general trend towards globalism. There is also the threat of bioterrorism using viruses. In addition to the known threat, more and more new viruses are routinely being discovered (Lipkin, 2010), (Datta et al., 2015). Major outbreaks and pandemics are likely to occur in the near future (Wolfe, 2011).

Combating existing and new viral threats requires both an understanding of how they work and the development of tools to combat them. A fundamental understanding of how viruses infect, spread, and evolve is required to inform a plan of action to take against viruses. Application of that knowledge leads to to better diagnostic tools and vaccines.

Here I focus on three different viruses which are having major impacts on human health. In this dissertation I describe work that I and others have done on New World Arenaviruses, Ebola-Reston Virus and Human Norovirus. These studies investigate viruses from both a basic science approach and an applied technology approach. In addition to multiple approaches, this work is highly collaborative, combining efforts in academia and industry and taking advantage of the numerous specialties available at the

University of Texas at Austin. In the TfR1-Machupo work (Chapter 2), I utilize a number of wet lab and virology techniques to demonstrate the effects the Transferrin Receptor 1 (TfR1) surface has on New World Arenavirus entry patterns. This work resulted in a collaboration with Eleisha Jackson in Claus Wilke's lab in which Eleisha was able to develop a Rosetta based computational model that was able to accurately predict the strength of the binding affinities that I characterized in the lab. In the Ebola work (Chapter 3), I work in parallel with a number of researchers at UT to identify novel antibodies that bind to the glycoproteins of Ebola. In that project we use novel Ebola VLPs that were designed and built at Rob Davies' lab at the Texas Biomedical Research Institute and we worked with Luminex in Austin, Texas to test our Ebola antibodies in a diagnostic assay based on their Magpix bead platform. In my ongoing Norovirus work (Chapter 4) I use two new technologies developed in the Georgiou lab to investigate the immune response in a donor who participated in a Phase 1 clinical vaccine trial with Takeda Pharmaceuticals.

NEW WORLD ARENAVIRUSES

The first New World Arenavirus zoonotic outbreak occurred in Junín, Argentina in 1958 (Agnese, 2007). Over the next fifty years four more New World Arenaviruses have infected humans; (Junín - 1958, Machupo - 1963, Guanarito - 1989, Sabia - 1990, Charpare – 2003) (Johnson and Wiebenga, 1965), (Delgado et al., 2008), (Salas et al., 1991), (Coimbra et al., 1994). New infections are reported yearly and outbreaks occur

every few years on a regular basis. In humans, viral infection leads to hemorrhagic fever and can have lethality rates as high as 30%. (Peters, 2002)

Small rodents throughout South and Central America carry New World Arenaviruses. Transmission from rodent to humans occurs through direct contact and/or aerosolization of virions in rodent feces and urine (LeDuc, 1989). Felines can also harbor the virus and a rodent-feline-human transmission pathway is likely occurring. Arenavirus transmission to humans is likely to increase as humans push further into wilderness areas within the host species range.

The New World Arenavirus phylogeny contains 29 species separated into four clades; A, B, C and A/B recombinant. The five New World Arenaviruses that infect humans are found in clade B of the arenavirus phylogeny (Nunberg and York, 2012) (Charrel et al., 2011). Clade B arenaviruses are unique in that their mechanism of entry into mammalian cells relies on the host encoded Transferrin Receptor 1 (TfR1) (Radoshitzky et al., 2007).

New World Arenaviruses are an emergent public health and bioterrorism threat due to their ability to infect humans and cause hemorrhagic fever. These viruses are categorized as BSL4, the most dangerous rating due to their lethality and lack to treatment options (NIAID website). The arenaviruses are very stable to desiccation, making them well-suited for terrorism and easy distribution.

Currently there are no FDA approved vaccines available for New World Arenaviruses. However, there is a Junin vaccine, Candid 1, which is available and in use

in South America. Candid 1 is an attenuated Junin strain, the virus was passaged through guinea pig, mouse brain and fetal rhesus monkey lung cells (Barrera Oro and McKee, 1991).

EBOLA VIRUS

The Ebola virus was first identified in a human outbreak in 1976. Since that time, regular outbreaks have occurred. It is an emerging virus and outbreaks have been reported periodically at 2-10 year intervals. Outbreaks occur primarily in Africa but other locations, including the US have experienced outbreaks of Ebola. The largest outbreak of Ebola was the most recent occurring in 2013-2015. Ebola outbreaks routinely have lethality rates of 50% and can be as high as 95% (Peters, 1996). Virus is spread by contact with blood or body fluids from infected individuals or animals, and is highly infectious. Due to it high lethality, Ebola virus is a BSL4 category pathogen

The primary animal reservoir is still unknown however, bats are hypothesized to be the reservoir (Leroy et al., 2005), (Amman et al., 2012). In addition to humans, Ebola virus can infect other primates and the virus has decimated gorilla populations in Africa (Bermejo et al., 2006). It has also been determined that Ebola can replicate in swine. Of particular interest is that infected swine are asymptomatic (Marsh et al., 2011) and there is evidence that Ebola was passed to human via swine in the Philippines (Barrette et al.,

2009). It has also been demonstrated that primates can pass Ebola to swine via aerosolization, (Weingartl et al., 2012).

Currently there are no vaccines approved for Ebola virus. However, there are candidates in clinical trials. The latest trial was run during the recent Ebola outbreak in West Africa. The vaccine consists of a replication competent vesicular stomatitis virus (VSV) pseudotyped with the glycoprotein of the Zaire strain of Ebola virus. In the phase 1 trail the vaccine was deemed safe and it was shown that trial volunteers were able to mount an immune response against the vaccine (Agnandji et al., 2015). Primate studies done with the same vaccine demonstrated that the vaccine was protective against live Ebola virus in those animals (Geisbert et al., 2008).

NOROVIRUS

Norovirus infects a number of species including human, mice, swine, and bovine. Norovirus strains are generally considered to be species specific and zooinotic events are rare (Mattison et al., 2007). The virus is typically spread though contaminated bodily fluids such as fecal matter and vomit. The transmission route is generally fecal-oral. There is also evidence that the virus can be aerosolized as well and presumably could lead to infection inhalation or oral uptake (Bonifait et al., 2015).

Norovirus is not particularly lethal but it does cause over 50% of the cases of gastroenteritis worldwide, and 21 million norovirus infections occur annually in the United States (Hall et al., 2011). The virus is particularly contagious in areas with tight

living quarters such as dormitories, cruise ships and military bases. Retirement home and elderly care facilities are particularly vulnerable as elderly patients are much more likely to be immunocompromised and develop chronic infections (Karin Bok, 2013).

Currently there are no approved vaccines for Norovirus. A VLP based vaccine has undergone phase 1 trials and was demonstrated to be safe and immunogenic however it failed to elicit long term protection (Treanor et al., 2014). One complication for developing a Norovirus vaccine is that, much like Influenza, Norovirus evolves quickly. This quick evolution is hypothesized to be driven by herd immunity within the human population. The process results in a new dominant Norovirus strain approximately every 2 years (Lindesmith et al., 2011).

SIGNIFICANCE AND HYPOTHESIS

New World Arenaviruses, Ebola virus, and Norovirus all present similar challenges. They have all started infecting humans in the last 70 years. They all have animal origins although it is unclear what the animal origins are, particularly for Ebola and Norovirus. New World Arenaviruses and Ebola have regular outbreaks in the human population and Norovirus continuously circulates through the human population. An active area of research investigates the process of how a virus undergoes a species switching event in which it begins to infect a species that it did not previously infect. (Sawyer and Elde, 2012)

It is imperative that we gain a better understanding how viruses evolve and switch species. Studying past species switching events provides valuable insight into what lead causes species switching to occur. Mechanistic insight will allow us to begin to predict what viral mutations can contribute to a species switching event. Further understanding and proper monitoring of viral evolution will lead to the identification of emerging viral species switching events and allow for proper action to be taken before a virus can cause large amounts of damage to humans or other species.

Similar to influenza, all three viruses studied here have RNA genomes. Viral replication is dependent on an RNA dependent RNA polymerase. The inability of RNA dependent RNA polymerases to proofread contributes to a high errors rate in the viral replication process. An error rate of ~1 in 10,000 bp occurs in RNA genomes. (Steinhauer and Holland, 1986) This high error rate accelerates the number of mutations that the virus can sample in evolutionary space and much like the influenza virus allows them to rapidly evolve as they explore various fitness landscapes.

In order for a virus to infect a new species it must have mutations that allow it access to spaces that it was formerly prevented in. For instance, in the case of receptor usage, the virus has higher chance of success if it acquires one or more mutations that allow it to bind to a receptor in a potential host that it was previously not able to interact with. Once this barrier is overcome, low levels of infection can occur and give the opportunity for more mutations to arise. This appears to be the case of the New World Arenaviruses. As described in Chapter 2, they utilize Transferrin Receptor 1 (TfR1) for

entry. Across the mammalian phylogeny, TfR1 has evolved in such a manner that some species TfR1's are permissive to a particular New World Arenavirus, such as Machupo, and others are not (Abraham et al., 2010) (Figure 1.1).

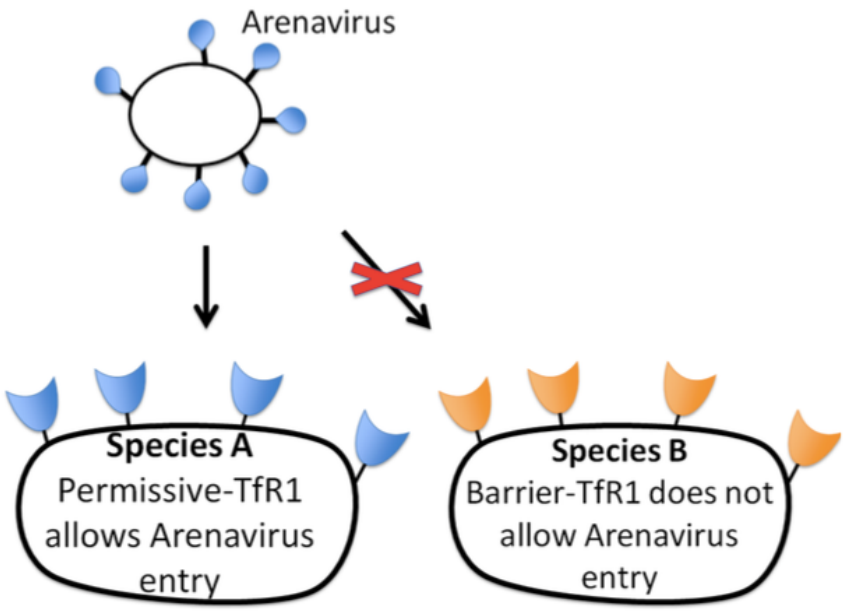

Figure 1.1 - Host Receptor Dynamics

The New World Arenavirus glycoproteins are compatible with receptors of some species and not others. Depicted here, the blue glycoprotein on the virus is able to bind the blue receptor on species A. Upon successful binding the virus can then be taken up by the cell. The virus is unable to enter Species B because it is unable to bind and interact with the Species B receptor, depicted in orange. Amino acid differences between the Species A and Species B receptor at the viral glycoprotein binding site contribute to whether the receptor is permissive to virus entry or a barrier to the virus. In order for the virus to gain entry through the Species B receptor, it must acquire mutations that allow to bind the receptor long enough for viral uptake to take place.

The focus of the work described here will remain primarily focused on the host-virus interactions that take place at the receptor binding interface; the reason for this is that viral entry, by definition, is the first event that occurs in a potential species switching

event. However, it should be noted that in addition to initial entry mediated by the viral glycoprotein, mutations that favor replication in the new species are selected for throughout the viral genome (Meyerson and Sawyer, 2011). This creates a more fit virus that overtime leads to a full species switching event in which the new virus has sufficient ability to successfully infect, replicate, avoid in innate immunes response, and transmit through the new host species. (Sawyer and Elde, 2012)

The concept of mutations being introduced to initiate a species switching event suggests two unique possibilities. The first is that these potential mutations arise by chance and are simply selected for when the virus with the rare mutations happens to interact with the cells of the new host species. The second is that there may be selective pressure creating mutations at the virus interface that interacts with the host receptor. The hypothesis addressed here is that pressure put upon the virus at the receptor binding site by the host immune mediated antibody response is selecting for mutations that, in addition to evading the immune response, confer the virus with a set of mutations that favor the initiation of a species switching event. (Figure 1.2)

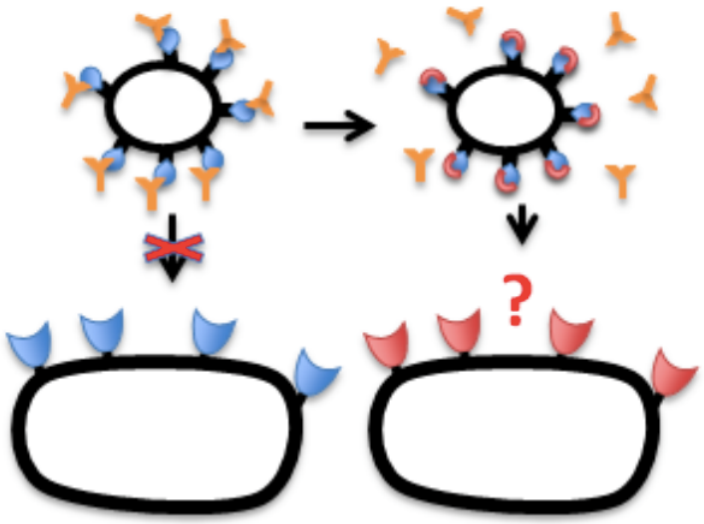

Figure 1.2 – Species Switching Hypothesis

During a viral infection, the host adaptive immune response produces antibodies that bind the virus, some of which directly bind the receptor bind site on the viral glycoprotein surface. The antibody block on the glycoprotein inhibits viral entry through the receptor and blocks viral infection. This block puts pressure on the viral genome to select for amino acid changes in the viral glycoprotein that prevent the antibodies from binding the receptor binding site on the virus. The overall hypothesis this work aims to test is that these mutations on the viral glycoprotein that block antibody binding are also leading the virus to interact with receptors of other species that it was previously unable to interact with.

In addition to the innate immune response, a spreading viral infection is attacked by the host adaptive immune response and in particular the antibodies that bind to the virus glycoproteins or viral capsid proteins. An effective way for antibodies to inhibit viral infections and spread is for the antibody to bind the viral glycoprotein or capsid protein at the interface that the virus uses to bind the host receptor protein. This is also a common strategy for developing vaccines. Chapter 4 discusses further work investigating a Norovirus vaccine that elicits an antibody response that physically blocks

the virus from interacting with the sugar groups required for viral entry and infection. (Treanor et al., 2014). Blocking the receptor site puts great pressure on the virus. It is hypothesized that Norovirus evolution is driven by the adaptive immune response. (Lindesmith et al., 2012) Mutations that arise in response to evading antibody binding to the receptor binding site will also modify how the virus binds the host receptor and potentially the receptors or other species that it does not infect thereby priming it for a species switching event.

Testing this hypothesis requires three experimental approaches. To test it requires host-virus system that can accurately assay the difference between a permissive and non-permissive receptor system. Chapter 2 works towards these goals and describes numerous successes demonstrating receptor permissiveness and non-permissiveness. The second aspect is identifying one or preferably more antibodies that can block viral entry by binding at the binding site.

Antibody discovery historically has been done using hybridoma technology. However this approach is time consuming, very inefficient with respect to how many antibodies can be isolated from it (Pirofski et al., 1990), and it also suffers from a multiple light chain problem (Zack et al., 1995), meaning that you may be dealing with an antibody that was not selected by the immune system. Additionally, non-natural antibodies are less than ideal when testing a hypothesis that is based on a natural immune response. Other antibody discovery technologies rely on constructing large libraries of antibody sequences expressed and selected in phage and yeast display systems (Smith,

1985), (Boder and Wittrup, 1997). These both suffer from the same problems as the hybridoma methodology in that the selected antibodies are not actual representatives from the immune response and are typically screened from large synthetic libraries or libraries derived from the heavy and light chain sequences pulled from pools of B-cells.

The Georgiou lab has developed a technology, VH:VL pairing that allows for the isolation and sequencing of immune system derived antibodies. VH:VL pairing is described in Chapter 3 and 4, and elsewhere. (DeKosky et al., 2013), (McDaniel et al., 2016) Antibodies against both Ebola glycoprotein and Norovirus capsid protein were identified using this approach. However, it was found that anti-Ebola antibodies described in Chapter 3 and elsewhere (Wang et al., 2015) did not block viral entry when tested and while useful for diagnostic and research purposes they are not sufficient to test the hypothesis presented here. Chapter 4 describes work to identify anti-Norovirus antibodies from an immune response that was demonstrated to contain antibodies that block viral interactions with host receptors. Identification of these blocking antibodies provides an ideal antibody to test if antibody escape by viruses contributes to their ability to switch species.

The final aspect of testing this hypothesis requires a viral evolution system in the lab that can reliably be used to select for viral variants that can switch species effectively and propagate those viruses. Ultimately the approach was unsuccessful and a proper viral-evolution system was not achieved.

References:

Abraham, J., Corbett, K.D., Farzan, M., Choe, H., Harrison, S.C., 2010. Structural basis for receptor recognition by New World hemorrhagic fever arenaviruses. Nature Publishing Group 17, 438–444. doi:10.1038/nsmb.1772

Agnandji, S.T., Huttner, A., Zinser, M.E., Njuguna, P., Dahlke, C., Fernandes, J.F., Yerly, S., Dayer, J.-A., Kraehling, V., Kasonta, R., Adegnika, A.A., Altfeld, M., Auderset, F., Bache, E.B., Biedenkopf, N., Borregaard, S., Brosnahan, J.S., Burrow, R., Combescure, C., Desmeules, J., Eickmann, M., Fehling, S.K., Finckh, A., Goncalves, A.R., Grobusch, M.P., Hooper, J., Jambrecina, A., Kabwende, A.L., Kaya, G., Kimani, D., Lell, B., Lemaître, B., Lohse, A.W., Massinga-Loembe, M., Matthey, A., Mordmüller, B., Nolting, A., Ogwang, C., Ramharter, M., Schmidt-Chanasit, J., Schmiedel, S., Silvera, P., Stahl, F.R., Staines, H.M., Strecker, T., Stubbe, H.C., Tsofa, B., Zaki, S., Fast, P., Moorthy, V., Kaiser, L., Krishna, S., Becker, S., Kieny, M.-P., Bejon, P., Kremsner, P.G., Addo, M.M., Siegrist, C.-A., 2015. Phase 1 Trials of rVSV Ebola Vaccine in Africa and Europe. New England Journal of Medicine 374, 1647–1660. doi:10.1056/NEJMoa1502924

Agnese, G., 2007. *"Una rara enfermedad alarma a la modesta población de O'Higgins*" Análisis del discurso de la prensa escrita sobre la epidemia de Fiebre Hemorrágica Argentina de 1958 Revista de Historia & Humanidades Médicas Vol. 3 No 1, Julio 2007

Amman, B.R., Carroll, S.A., Reed, Z.D., Sealy, T.K., Balinandi, S., Swanepoel, R., Kemp, A., Erickson, B.R., Comer, J.A., Campbell, S., Cannon, D.L., Khristova, M.L., Atimnedi, P., Paddock, C.D., Crockett, R.J.K., Flietstra, T.D., Warfield, K.L., Unfer, R., Katongole-Mbidde, E., Downing, R., Tappero, J.W., Zaki, S.R., Rollin, P.E., Ksiazek, T.G., Nichol, S.T., Towner, J.S., 2012. Seasonal Pulses of Marburg Virus Circulation in Juvenile Rousettus aegyptiacus Bats Coincide with Periods of Increased Risk of Human Infection. PLoS Pathogens 8, e1002877. doi:10.1371/journal.ppat.1002877

Barrera Oro, J.G., McKee, K.T., 1991. Toward a vaccine against Argentine hemorrhagic fever. Bulletin of PAH0 25(2), 1991

Barrette, R.W., Metwally, S.A., Rowland, J.M., Xu, L., Zaki, S.R., Nichol, S.T., Rollin, P.E., Towner, J.S., Shieh, W.-J., Batten, B., Sealy, T.K., Carrillo, C., Moran, K.E., Bracht, A.J., Mayr, G.A., Sirios-Cruz, M., Catbagan, D.P., Lautner, E.A., Ksiazek, T.G., White, W.R., McIntosh, M.T., 2009. Discovery of Swine as a Host for the Reston ebolavirus. Science 325, 204–206. doi:10.1126/science.1172705

Bermejo, M., Rodríguez-Teijeiro, J.D., Illera, G., Barroso, A., Vilà, C., Walsh, P.D., 2006. Ebola Outbreak Killed 5000 Gorillas. Science 314, 1564–1564. doi:10.1126/science.1133105

Bonifait, L., Charlebois, R., Vimont, A., 2015. Detection and quantification of airborne

norovirus during outbreaks in healthcare facilities. Clinical Infectious ….
Charrel, R.N., Coutard, B., Baronti, C., Canard, B., 2011. Arenaviruses and hantaviruses: from epidemiology and genomics to antivirals. Antiviral Research.
Coimbra, T.L.M., Nassar, E.S., de Souza, L.T.M., Ferreira, I.B., Rocco, I.M., Burattini, M.N., da Rosa, A.P.A.T., Vasconcelos, P.F.C., Pinheiro, F.P., LeDuc, J.W., Rico-Hesse, R., Gonzalez, J.-P., Tesh, R.B., Jahrling, P.B., 1994. New arenavirus isolated in Brazil. The Lancet 343, 391–392. doi:10.1016/S0140-6736(94)91226-2
Datta, S., Budhauliya, R., Das, B., Chatterjee, S., Vanlalhmuaka, Veer, V., 2015. Next-generation sequencing in clinical virology: Discovery of new viruses. World Journal of Virology 4, 265–276. doi:10.5501/wjv.v4.i3.265
DeKosky, B.J., Ippolito, G.C., Deschner, R.P., Lavinder, J.J., Wine, Y., Rawlings, B.M., Varadarajan, N., Giesecke, C., Dörner, T., Andrews, S.F., Wilson, P.C., Hunicke-Smith, S.P., Willson, C.G., Ellington, A.D., Georgiou, G., 2013. High-throughput sequencing of the paired human immunoglobulin heavy and light chain repertoire. Nat Biotechnol 31, 166–169. doi:10.1038/nbt.2492
Delgado, S., Erickson, B.R., Agudo, R., Blair, P.J., Vallejo, E., Albariño, C.G., Vargas, J., Comer, J.A., Rollin, P.E., Ksiazek, T.G., Olson, J.G., Nichol, S.T., 2008. Chapare Virus, a Newly Discovered Arenavirus Isolated from a Fatal Hemorrhagic Fever Case in Bolivia. PLoS Pathogens 4, e1000047. doi:10.1371/journal.ppat.1000047
Boder E.T., Wittrup K.D., 1997. Yeast surface display for screening combinatorial polypeptide libraries. Nat Biotechnol 15, 553–557. doi:10.1038/nbt0697-553
Geisbert, T.W., Daddario-DiCaprio, K.M., Lewis, M.G., Geisbert, J.B., Grolla, A., Leung, A., Paragas, J., Matthias, L., Smith, M.A., Jones, S.M., Hensley, L.E., Feldmann, H., Jahrling, P.B., 2008. Vesicular Stomatitis Virus-Based Ebola Vaccine Is Well-Tolerated and Protects Immunocompromised Nonhuman Primates. PLoS Pathogens 4, e1000225. doi:10.1371/journal.ppat.1000225
Hall, A.J., Vinjé, J., Lopman, B., Park, G.W., Yen, C., 2011. Updated norovirus outbreak management and disease prevention guidelines.
Johnson, K.M., Wiebenga, N.H., 1965. Virus isolations from human cases of hemorrhagic fever in Bolivia. Experimental Biology and Medicine 118, 113–118. doi:10.3181/00379727-118-29772
Karin Bok, K.Y.G., 2013. Norovirus Gastroenteritis in Immunocompromised Patients. The New England journal of medicine 368, 971–971. doi:10.1056/NEJMc1301022
LeDuc, J.W., 1989. Epidemiology of hemorrhagic fever viruses. Review of Infectious Diseases.
Leroy, E.M., Kumulungui, B., Pourrut, X., Rouquet, P., Hassanin, A., Yaba, P., Délicat, A., Paweska, J.T., Gonzalez, J.-P., Swanepoel, R., 2005. Fruit bats as reservoirs of Ebola virus. Nature 438, 575–576. doi:10.1038/438575a
Lindesmith, L.C., Beltramello, M., Donaldson, E.F., Corti, D., Swanstrom, J., Debbink, K., Lanzavecchia, A., Baric, R.S., 2012. Immunogenetic Mechanisms Driving Norovirus GII.4 Antigenic Variation. PLoS Pathogens 8, e1002705. doi:10.1371/journal.ppat.1002705

Lindesmith, L.C., Donaldson, E.F., Baric, R.S., 2011. Norovirus GII.4 strain antigenic variation. J. Virol. 85, 231–242. doi:10.1128/JVI.01364-10
Lipkin, W.I., 2010. Microbe hunting. Microbiol. Mol. Biol. Rev. 74, 363–377. doi:10.1128/MMBR.00007-10
Marsh, G.A., Haining, J., Robinson, R., Foord, A., Yamada, M., Barr, J.A., Payne, J., White, J., Yu, M., Bingham, J., Rollin, P.E., Nichol, S.T., Wang, L.-F., Middleton, D., 2011. Ebola Reston virus infection of pigs: clinical significance and transmission potential. J Infect Dis. 204 Suppl 3, S804–9. doi:10.1093/infdis/jir300
Mattison, K., Shukla, A., Cook, A., Pollari, F., 2007. Human noroviruses in swine and cattle. Emerging infectious Diseases Vol. 13, No. 8, August 2007
McDaniel, J.R., DeKosky, B.J., Tanno, H., Ellington, A.D., Georgiou, G., 2016. Ultra-high-throughput sequencing of the immune receptor repertoire from millions of lymphocytes. Nature Protocols 11, 429–442. doi:10.1038/nprot.2016.024
Meyerson, N.R., Sawyer, S.L., 2011. Two-stepping through time: mammals and viruses. Trends in Microbiology 19, 286–294. doi:10.1016/j.tim.2011.03.006
Nunberg, J.H., York, J., 2012. The Curious Case of Arenavirus Entry, and Its Inhibition. Viruses 4, 83–101. doi:10.3390/v4010083
Peters, C.J., 2002. Human infection with arenaviruses in the Americas. Arenaviruses I 65–74. doi:10.1007/978-3-642-56029-3_3
Peters, C.J., 1996. Emerging infections--Ebola and other filoviruses. West. J. Med. 164, 36–38.
Pirofski, L., Casadevall, A., Rodriguez, L., Zuckier, L.S., Scharff, M.D., 1990. Current state of the hybridoma technology. J Clin Immunol 10, 5S–14S. doi:10.1007/BF00918686
Radoshitzky, S.R., Abraham, J., Spiropoulou, C.F., Kuhn, J.H., Nguyen, D., Li, W., Nagel, J., Schmidt, P.J., Nunberg, J.H., Andrews, N.C., Farzan, M., Choe, H., 2007. Transferrin receptor 1 is a cellular receptor for New World haemorrhagic fever arenaviruses. Nature 446, 92–96. doi:10.1038/nature05539
Salas, R., Pacheco, M.E., Ramos, B., Taibo, M.E., Jaimes, E., Vasquez, C., Querales, J., de Manzione, N., Godoy, O., Betancourt, A., Araoz, F., Bruzual, R., Garcia, J., Tesh, R.B., Rico-Hesse, R., Shops, R.E., 1991. Venezuelan haemorrhagic fever. The Lancet 338, 1033–1036. doi:10.1016/0140-6736(91)91899-6
Sawyer, S.L., Elde, N.C., 2012. A cross-species view on viruses. Current Opinion in Virology 2, 561–568. doi:10.1016/j.coviro.2012.07.003
Smith, G.P., 1985. Filamentous fusion phage: novel expression vectors that display cloned antigens on the virion surface. Science 228, 1315–1317. doi:10.1126/science.4001944
Steinhauer, D.A., Holland, J.J., 1986. Direct method for quantitation of extreme polymerase error frequencies at selected single base sites in viral RNA. J. Virol. 57, 219–228.
Treanor, J.J., Atmar, R.L., Frey, S.E., Gormley, R., Chen, W.H., Ferreira, J., Goodwin, R., Borkowski, A., Clemens, R., Mendelman, P.M., 2014. A novel intramuscular

bivalent norovirus virus-like particle vaccine candidate--reactogenicity, safety, and immunogenicity in a phase 1 trial in healthy adults. J Infect Dis. 210, 1763–1771. doi:10.1093/infdis/jiu337

Wang, B., Kluwe, C.A., Lungu, O.I., DeKosky, B.J., Kerr, S.A., Johnson, E.L., Jung, J., Rezigh, A.B., Carroll, S.M., Reyes, A.N., Bentz, J.R., Villanueva, I., Altman, A.L., Davey, R.A., Ellington, A.D., Georgiou, G., 2015. Facile Discovery of a Diverse Panel of Anti-Ebola Virus Antibodies by Immune Repertoire Mining. Scientific Reports 5, 13926. doi:10.1038/srep13926

Weingartl, H.M., Embury-Hyatt, C., Nfon, C., Leung, A., Smith, G., Kobinger, G., 2012. Transmission of Ebola virus from pigs to non-human primates. Scientific Reports 2, 811. doi:10.1038/srep00811

Wolfe, N.D., 2011. The Viral Storm. doi:10.1016/0169-5347(93)90160–Q

Zack, D.J., Wong, A.L., Stempniak, M., Weisbart, R.H., 1995. Two kappa immunoglobulin light chains are secreted by an anti-DNA hybridoma: Implications for isotypic exclusion. Molecular Immunology 32, 1345–1353. doi:10.1016/0161-5890(95)00112-3

Chapter 2: Computational and functional analysis of the GP1–TfR1 interface reveals host range trade-offs in New World arenaviruses[1]

INTRODUCTION

Viruses need to enter cells of a host organism in order to make more copies of themselves. Many viruses interact with protein receptors found on the surface of host cells in order to gain entry into those cells. Like all proteins, these host receptors can vary in sequence from species to species. Viruses tend to be acutely adapted to use the receptor of one species, with the unintentional consequence of being poorly adapted to the receptor encoded by related species. For instance, HIV-1 can enter cells using the human CD4 receptor but not the CD4 of most other primate species (Humes et al., 2012), (Meyerson et al., 2015). A key event in the emergence of new diseases often involves evolution of the viral genome in a way that renders it compatible with the receptor ortholog encoded by a new host species (reviewed in (de Graaf and Fouchier, 2014), (Gerlier, 2011), (Graham and Baric, 2010), (Choe et al., 2011), (Parrish and Kawaoka, 2005), (Parrish et al., 2008). The identification of host genes that impact viral replication in a species-specific fashion is the foundation for understanding why viruses

[1] Scott A Kerr, Eleisha L Jackson, Oana I Lungu, Austin G Meyer, Ann Demogines, Andrew D Ellington, George Georgiou, Claus O Wilke, and Sara L Sawyer. 2015. "Computational and Functional Analysis of the Virus-Receptor Interface Reveals Host Range Trade-Offs in New World Arenaviruses." *Journal of Virology* 89 (22):11643–53. American Society for Microbiology doi:10.1128/JVI.01408-15. Scottdesigned and executed the experiments, processed and analyzed the data, wrote the initial draft and edited later drafts with the exception of the homology modeling and figure 5 was done by Eleisha Jackson with assistance from Oana Lungu, Austin Meyer, and Claus Wilke.

infect the species that they do, and essential for understanding the genetic changes that viruses must acquire to infiltrate new species.

The New World arenaviruses, which infect Central and South American rodent species, present an ongoing public health threat. Five different viruses in this family are zoonotic, meaning that they are transmitted from their rodent host species to humans (Figure 2.1) (Delgado et al., 2008), (Peters, 2002). Infection in humans can lead to hemorrhagic fever and individual outbreaks can have lethality rates as high as 30% (Borio et al., 2002) . The New World arenavirus phylogeny has four major clades: A, B, A/B recombinant, and C, with all zoonotic arenaviruses residing in clade B (Charrel et al., 2011). Transmission to humans likely occurs through direct contact with rodents and through inhalation of aerosolized virions excreted in rodent feces and urine (LeDuc, 1989). Currently, the geographic ranges of the rodent species that carry these viruses are constrained by specific habitat requirements. However, should arenaviruses ever spread to common species such as the house mouse (*Mus musculus*) or the brown rat (*Rattus norvegicus*), they could become a global threat of immense proportions.

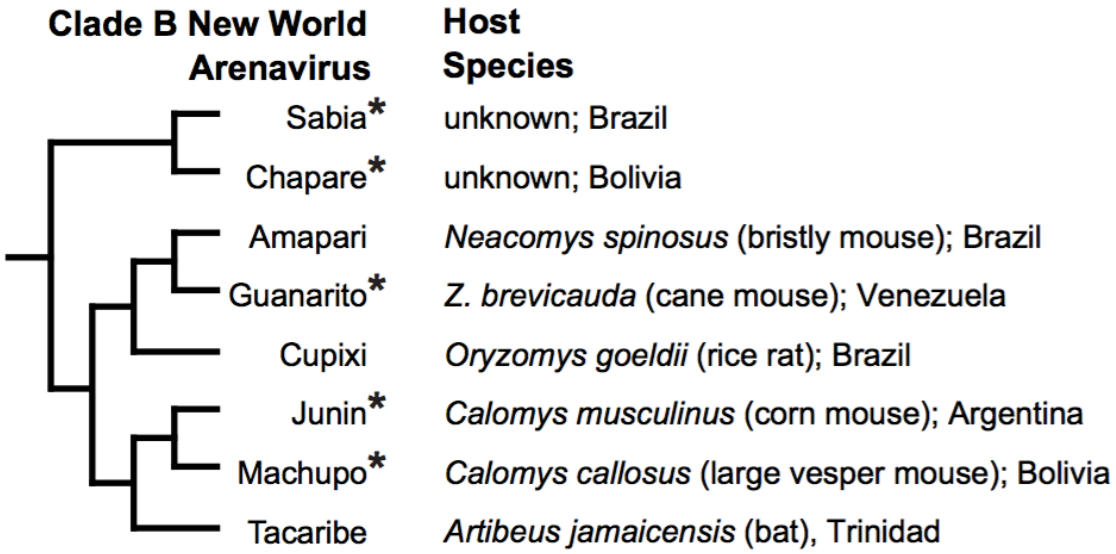

Figure 2.1. New World arenaviruses and the species that they infect.

A phylogeny of clade B New World arenaviruses is shown (adapted from (Charrel et al., 2011)). The rodent species that are known to be endemically infected with each virus are listed to the right, along with an indication of the country where the rodent/virus pair is found. Asterisks identify zoonotic viruses known to infect humans.

The clade B arenaviruses enter host cells via the host-encoded Transferrin Receptor 1 (TfR1) (Radoshitzky et al., 2007). The primary function of TfR1 is to mediate the uptake of iron-loaded transferrin, and to a lesser extent H-ferritin (Li et al., 2010), from the serum (reviewed in (Aisen, 2004)). The interaction of arenaviruses with TfR1 is mediated by the virus surface spike, or glycoprotein (GP). The viral spike consists of a trimer of GP1/GP2 dimers and interaction with TfR1 involves GP1 (reviewed in (Rojek and Kunz, 2008)). A co-crystal structure demonstrating the interaction between human TfR1 and the GP1 of one New World arenavirus, Machupo virus, has been solved

(Abraham et al., 2010). Each of the clade B arenaviruses have distinct patterns of compatibility with the TfR1s encoded by various mammalian species (Abraham et al., 2010), (Radoshitzky et al., 2008), (V. K. Martin et al., 2010), (Abraham et al., 2009), (Flanagan et al., 2008). For instance, Machupo virus enters cells through the TfR1 of its rodent host species, *Calomys callosus*, but not through the TfR1 of the closely-related Junin virus host species, *Calomys musculinus* (Radoshitzky et al., 2008). In addition, human TfR1 is a functional receptor only for the five zoonotic New World arenaviruses, but not other New World arenaviruses (Radoshitzky et al., 2007), (Flanagan et al., 2008), (Helguera et al., 2012). The TfR1 of brown rats and house mice have been found to be non-functional entry receptors for all clade B arenaviruses tested (Radoshitzky et al., 2008), (Abraham et al., 2009), (Flanagan et al., 2008), (Cuevas et al., 2011) in line with the observation that these species have never been found to harbor arenaviruses in nature. Two other families of animal viruses, carnivore parvoviruses and rodent MMTV-like retroviruses, also use TfR1 to enter cells (Ross et al., 2002), (Parker et al., 2001). For all of the virus families that use TfR1, existing evidence suggests that the ability to enter cells through the TfR1 ortholog of a particular species is a necessary criterion for infection in the wild, and that viral adaptation is often required to utilize the TfR1 of the new species, (Parrish and Kawaoka, 2005), (Stucker et al., 2012), (Demogines et al., 2013), (Kaelber et al., 2012).

Recently, we have demonstrated that much of the sequence variability in TfR1 between different rodent and carnivore species is the result of host-virus evolutionary arms races (Demogines et al., 2013), (Kaelber et al., 2012). Specifically, *TFR1* has experienced repeated rounds of natural selection for mutations that reduce its functionality as a virus entry receptor. In turn, the viruses that use TfR1 have been counter-selected in the gene encoding their surface spike for mutations that re-establish cellular entry through new receptor variants (Parrish and Kawaoka, 2005), (Stucker et al., 2012). In arms races such as this, codon positions where mutations most potently alter the virus-receptor physical interaction, without affecting protein folding or function, are subject to the strongest positive selection and thus evolve rapidly (Meyerson and Sawyer, 2011), (Daugherty and Malik, 2012). Arms race dynamics can be detected by identifying codons that have a significantly higher number of non-synonymous substitutions than would be expected under a model of neutral or purifying selection (Meyerson and Sawyer, 2011), (Daugherty and Malik, 2012), (Sironi et al., 2015). We previously performed positive selection analysis on an alignment of *TFR1* sequences from various rodent species, and found three codons (corresponding to human TfR1 residue positions 205, 209, and 215) near the Machupo binding region that have undergone recurrent positive selection during the speciation of rodents and are therefore evolving at an unusually high rate, (Demogines et al., 2013). However, the effect of mutations at these sites in TfR1 have not been tested. Recently, positive selection analysis has proven extraordinarily accurate in identifying the species-specific motifs in entry receptors that

govern interactions with viruses (Demogines et al., 2013), (Kaelber et al., 2012), (Demogines et al., 2012), (Meyerson et al., 2014), but it remains to be explored whether positive selection analysis could add value to our current understanding of the arenavirus-binding surface of TfR1 and the species-specificity of this interaction.

Here we show that TfR1 from the common brown rat functions as a receptor for Machupo virus if residues from the Machupo virus host species, *Calomys callosus*, are substituted into the small protein motif identified by positive selection analysis. We also show that the specific TfR1 residues that dictate Machupo entry are not the same residues that govern entry by Chapare and Sabia arenaviruses. Moreover, a human SNP in this region, L212V, which has previously been shown to make human TfR1 a worse receptor for Machupo virus entry (Demogines et al., 2013), makes it a better receptor for the Junin and Sabia arenaviruses. These findings suggest the potential for evolutionary trade-offs, where selection for resistance for one virus could make humans or rodents susceptible to other arenaviruses in nature. In all of these experiments, we show that the strength of binding affinity between the virus and TfR1 correlates to cellular entry of the virus. Based on this, we develop a structural model for assessing the relative energy of binding of Machupo GP1 to TfR1 variants. This model is based on homology modeling of TfR1 variants and subsequent rigid-body docking to Machupo GP1. Binding energies between modeled TfR1 variants and Machupo GP1 are calculated using the Rosetta interface scoring function (Leaver-Fay et al., 2011), (Chaudhury et al., 2011). We find that the

binding-energy predictions made by our model show good agreement with the functional results obtained in this study and others. Our results suggest that a combination of positive selection analysis, structural modeling, and experimental verification may provide an efficient approach for screening and assessing potential spillover risks of viruses circulating in animal populations.

MATERIALS AND METHODS

Cells and Plasmids.

Human embryonic kidney 293T cells (ATCC) and canine osteosarcoma D17 (ATCC) were maintained in Dulbecco modified Eagle's medium (Cellgro) supplemented with 10% fetal bovine serum (Gibco), 100 units ml^{-1} penicillin, 100 μg ml^{-1}streptomycin, and 2 mM L-glutamine (Cellgro). Human, *Calomys callosus*, and *Rattus norvegicus* TfR1 with a C-terminal FLAG tag were PCR amplified from pcDNA3.1+ vectors (Radoshitzky et al., 2008) and cloned into the Gateway entry vector pCR8 using the pCR8/GW/TOPO TA Cloning Kit (Invitrogen). The following primers were used to amplify TfR1 for TA cloning: 5′-TTAATACGACTCACTATAGGG-3′ and 5′-TAGAAGGCACAGTCGAGGC-3.′ Gateway LR recombination (Invitrogen) was performed to transfer *TFR1* genes from pCR8 into the entry site in a Gateway-converted LPCX retroviral vector. Site-directed mutagenesis of the Rat *TfR1* plasmid was performed to create the rat-short *TFR1* mutant using the QuikChange Site-Directed Mutagenesis kit (Stratagene) with the following primers: 5’-

GGTGACCATAAATTCAGGTAATGGCGTATACCTAGTGGAGGCTCCTGAGGGT TATGTGGC and 3'-CCTCAGGAGCCTCCACTAGGTATACGCCATTACCTGAATTTATGGTCACCAAG TTTTGAG, and rat-long *TfR1* mutant using primers: 5'-GGTGACCATAAATGCAAGTAATGGCGTATACCTATTGGAGAGTCCTGAGGGT TATGTGGC and 3'-CCTCAGGACTCTCCAATAGGTATACGCCATTACTTGCATTTATGGTCACCAAG TTTTGAG. Site-directed mutagenesis was also performed on human TfR1 to introduce the L212V mutation (Demogines et al., 2013). Plasmids encoding Machupo (Carvallo strain) and Junin (MC2 strain) GP have been described previously (Radoshitzky et al., 2007). Sabia and Chapare GP sequences, NCBI accession numbers YP_089665 and YP_001816782 respectively, in pCAGGS were a gift from Hyeryun Choe.

Generation of Stable Cell Lines

The LPCX:*TFR1* retroviral vectors described above were packaged into virions in 293T cells by co-transfecting them along with pC-VSV-G (a gift from Hyeryun Choe) and the NB-MLV gag-pol packaging plasmid pCS2-mGP (Yamashita and Emerman, 2004) using TransIT-293 (Mirus). Two days later, supernatants containing virions were collected, filtered through 0.22 μm filters, and used to infect D17 cells. 1 mL of D17 cells at a concentration of 50,000 cells/mL were plated in 12-well plates 24 hours prior to infection. On the day of infection, media was removed and cells were infected with 2 mL

of media containing 125-1000 μL of virus and polybrene at a final concentration of 5 μg/mL. Following infection cells were spinoculated at 1200g for 90 minutes at 30ºC. 24 hours after infection, media was removed and fresh media containing 1.0 μg/mL puromycin was added to select for transduced cells. All TfR1 receptors tested have a C-terminal FLAG tag that is extracellular when the receptor is at the cell surface (Abraham et al., 2009); expression of TfR1 proteins was detected in live cells by flow cytometry using a FLAG antibody conjugated with Allophycocyanin (Abcam).

Entry Assays

Pseudoviruses used for entry assays (arenavirus GP-pseudotyped MLV recombinant retroviruses) were packaged in 293T cells. TransIT-293 (Mirus) was used to co-transfect the GFP-encoding transfer vector pQCXIX (BD Biosciences) along with plasmids encoding MLV Gag-Pol and arenavirus GP. After 48 hours, supernatants containing viruses were harvested, filtered with 0.22 μm filters, aliquoted, and frozen at –80°C. For entry assays, cell lines stably expressing wildtype and mutant TfR1s were plated at a concentration of 1×10^5 cells per well in 24-well plates and, after 24 hours, infected with pseudotyped virus along with polybrene at a final concentration of 5 μg/mL. The plates were spinoculated with centrifugation at 1200g for 90 minutes at 30°C. Following spinoculation, cells were washed once with PBS and the media was

replaced. Two days post-infection, cells were trypsinized, treated with 1% paraformaldehyde for 1 hour and labeled using a FLAG antibody conjugated with Allophycocyanin (APC; Abcam, catalog ab72569) to ascertain TfR1 expression. Cells were analyzed by flow cytometry. Analysis of flow cytometry data was performed using FlowJo 8.8.6 (TreeStar Inc). Cells were gated for live populations and data for 10,000 cells was collected for analysis. For each experiment, cell populations were further gated to represent equivalent MFI for each cell line. This population of cells expressing equivalent amounts of TfR1 was scored for GFP expression (viral entry). Where TfR1 expression is reported, it is reported as the mean fluorescence intensity (MFI) in the analyzed population.

Soluble Protein Expression

Soluble TfR1s (amino acid positions 117-760 in the human TfR1 numbering scheme) were amplified with a 3' primer that introduces a histidine tag and cloned into pCR4 (Invitrogen); 5'-Human-GCCCATCTGTCCCGGCCCTGCAGCACGTCGCTTATATTGGGATGACCTGAAGAGAAAG, 5'-Rat-GCCCATCTGTCCCGGCCCTGCAGCACGTCGCTTATTTTGGGCAGACCTCAAAACAC, 3'-CTATTAATGGTGATGGTGATGGTGATGGTGATGGTGTGATCCACCTCCCTTGTCATCGTCGTCCTTGTAG. This plasmid was used as a template to amplify the TfR1

soluble portion which was then joined by PCR to a geneblock (IDT) containing the human preprolactin signal sequence (residues 1-34), CCGCCACCATGAACATCAAAGGATCGCCATGGAAAGGGTCCCTCCTGCTGCT GCTGGTGTCAAACCTGCTCCTGTGCCAGAGCGTGGCCCCCTTGCCCATCTGTC CCGGCCCTGCAGCACGTCGC, using the 5' primer – CCGCCACCATGAACATCAAAGGATCGCCATG, and the same 3' primer as listed above. The product of this reaction was TOPO-TA cloned into pCR8 (Invitrogen) and then Gateway cloned (Invitrogen) into the mammalian expression vector pLPCX. Plasmids were purified via Midi or Maxi Prep purification (Qiagen). For each TfR1, Expi293F cells (LifeTechnologies) were transfected and incubated for 7 days according to the manufacturer's protocol. A pCDM8 plasmid encoding Machupo virus GP1 fused to the Fc domain of human immunoglobulin (IgG1) protein was received from Dr. Sheli Radoshitzky (Radoshitzky et al., 2007). This fusion protein was expressed in Expi293F cells according to the manufacturer's protocol.

Soluble TfR1 and Machupo Virus GP Purification

Supernatant was collected following TfR1 production in Expi293F cells and centrifuged for 20 minutes at 4,000 rcf to clear cellular debris. Following centrifugation, the supernatant was passed through a 0.45 μm and then a 0.22 μm filter. An equivalent volume of binding buffer was added (10 mM imidazole, 50 mM NaH_2PO_4, 300 mM NaCl) and incubated with nickel coated beads for 3 hours at 4°C (Complete His-Tag

purification resin, Roche). After incubation the bead-supernatant slurry was passed through 5 mL gravity flow columns (Thermo) two times. The column was washed with 10 mL of wash buffer (20 mM imidazole, 50 mM NaH_2PO_4, 300 mM NaCl). TfR1 was eluted from the column with elution buffer (250 mM imidazole, 50 mM NaH_2PO_4, 300 mM NaCl). Elution fractions containing TfR1 were pooled, concentrated and buffer exchanged with TfR1 buffer (100 mM NaCl, 100 mM KCl, 5 mM KH_2P0_4, pH 6.7) using Amicon ultra 100 kilodalton (kDa) filter units (Millipore) to capture fully formed TfR1 dimer. Samples were flash frozen for storage. Purified protein was analyzed by boiling for 10 minutes in protein loading buffer with 5% beta mercaptoethanol and resolved on 4-20% SDS-PAGE gels (NuSep). Gel was stained with Gel-Code Blue (Life Technologies). For the soluble Machupo GP1-Fc, following transfection, the cellular supernatant containing expressed and secreted protein was centrifuged for 20 minutes at 3,000 rcf at 4°C to clear cellular debris. The supernatant was passed through 0.45 μm filters and then 0.22 μm filters. 1 mL of Protein A bead slurry (Thermo) was equilibrated by washing 3 times with 2 mL of PBS, pH 7.4. Filtered supernatant was incubated with equilibrated beads at 4°C on an overhead rotator overnight. Following binding, the bead-supernatant mix was passed through a 5 mL gravity flow column (Thermo). The column was washed with 15 mL wash buffer (PBS pH 7.4 + 0.5 M NaCl), and subsequently washed with 15 mL PBS pH7.4. Machupo GP1-Fc was eluted with elution buffer (PBS pH 7.4 + 3.0 MgCl) in 1 mL fractions. Fractions containing protein, as determined by absorbance readings at 280 nm wavelength via spectrophotometer (Nanodrop, ND-1000), were

pooled. Sample was buffer exchanged into PBS pH 7.4 to reduce MgCl concentration to 10 mM and flash frozen for storage. Purified protein was analyzed and stained as described above.

ELISAs

50 μL of TfR1 at 4 μg/mL per well was incubated in PBS overnight at 4ºC to bind the protein to the ELISA plate. Following binding, wells were washed and blocked with 5% milk in PBS for 2 hours at room temperature. Wells were incubated with Machupo GP1-Fc in PBS for 1 hour at room temperature. Wells were washed and incubated with 1:2000 HRP-conjugated goat antibody raised against Human Fc (Jackson ImmunoResearch). Wells were washed and 50 μL of 1-Step Ultra TMB-ELISA Substrate Solution (TMB; Thermo Scientific Pierce) was added to the wells and incubated for approximately 15 min. The reaction was quenched with 2M H_2SO_4 and the plate was read at 450 nm. Curves were fit using 4 parameter non-linear regression. For the human transferrin-TfR1 interaction, transferrin-HRP(Jackson ImmunoResearch) in PBS was incubated with 1 mM FeCl(III) for 1 hour at room temperature to load the transferrin with iron. The iron-loaded transferrin-HRP was added to the ELISA wells and incubated at room temp for 1-hour. Wells were washed and 50 μL of TMB substrate was added to the wells and incubated for approximately 15 min. The reaction was quenched with 2 M H_2SO_4 and the plate was read at 450 nm. Curves were fit using 4 parameter non-linear regression using the PRISM software suite. The 4 parameter equation used was: Y=Max

+ ((Min-Max)/(1+(X/EC50)^HillSlope)). To ensure accuracy, curves were also fit using the hyperbola equation: Y = Max + (min-max)/(1+X/Kd)

Structural Homology Modeling and Docking

We assessed binding affinity in the TfR1–Machupo virus GP1 interface computationally using a strategy of homology modeling and docking. In brief, we first generated homology models of the TfR1–GP1 complex, using the software MODELLER (Eswar et al., 2006), (Webb and Sali, 2014) and the published co-crystal structure for human TfR1–Machupo GP1 (Abraham et al., 2010). We then refined these models using RosettaDock (Chaudhury et al., 2011). We modeled the TfR1 of house mouse, brown rat, *Calomys callosus*, and human, as well as various mutants of these receptors: rat-short, rat-long, mouse-human, and human L212V. Our starting point for homology modeling was the crystal structure for the human TfR1–Machupo GP1 (PDB Code: 3KAS), (Abraham et al., 2010), which we cleaned by removing all atoms that did not belong to amino acids. We then made a multiple sequence alignment using the TfR1s of rat, mouse, human and *C. callosus* using the software MAFFT. We gave the aligned sequences of the target TfR1 and the human TfR1 to MODELLER as the input alignment for modeling. Next, we made 100 models, using the basic MODELLER homology-modeling protocol. We then used the loop modeling protocol to re-model the loops for each modeled mutant structure. We next took each of these 100 modeled complexes and re-docked them in RosettaDock using rigid-body moves (Chaudhury et al., 2011). The re-docking procedure

consisted of two steps: prepackaging of the side chains and the actual docking. Modeling parameters were as follows: For prepackaging, we used the docking prepack protocol in Rosetta with the following flags:-database /path/to/rosetta/database; -l pdb_list.txt #List of structures to prepack; -docking:partners A_B; -ex1; -ex2aro, -use_input_sc; -out:file:fullatom; -out:path:pdb ./output_pdbs/. For docking, we used the RosettaDock docking protocol with the following flags:-database /path/to/rosetta/database; -l pdb_list.txt #List of prepacked structures; -partners A_B; -dock_pert 3 8; -spin, -ex1; -ex2aro; -use_input_sc ; -nstruct 100; -out:file:scorefile human_MACV_GP1_docking.fasc #Name of the output scorefile; -out:path:pdb ./output_pdbs/ #Path to output directory for pdbs. Next, we performed a step to refine the docked orientation of the Machupo GP1 relative to the new TfR1. For each input structure obtained from MODELLER, we generated 100 docked complexes, for a total of 100*100 = 10,000 docked complexes for each modeled TfR1. We took the models with the best RosettaDock interface scores to be our representative structures for each modeled complex. Lower interface scores indicate tighter binding affinity. Our complete computational pipeline is available at: https://github.com/wilkelab/MACV_TfR1_modeling.

RESULTS

Signatures of positive selection in *TFR1* refine mapping of the species-specific determinants of Machupo virus entry.

A small motif on TfR1 responsible for species-specific interactions with Machupo virus was previously defined by genetic mapping studies. Radoshitzky and colleagues mapped this region using the *TFR1* from house mouse (*Mus musculus*), which does not encode a functional receptor for Machupo virus. They substituted into this gene motifs from the human *TFR1*, which does encode a receptor for Machupo virus, and showed that a 5 amino acid motif from human TfR1 (positions R208-L212; blue type in Figure 2A) conferred a partial increase in Machupo virus entry (Radoshitzky et al., 2008). (For simplicity, all TfR1 coordinates herein refer to the human TfR1 numbering.) The co-crystal structure between Machupo virus GP1 and human TfR1 shows that these residues lie predominantly on a beta strand of TfR1 (brown residues in Figure 2.2B) in a binding interface where multiple motifs contribute to inter-molecular interactions (Abraham et al., 2010). Of the three residue positions that we previously identified to be under positive selection, one (residue 209) falls in this region and two more lie just outside of this region (residues 205 and 215, yellow highlight in Figure 2.2A) (Demogines et al., 2013). Based on this, we hypothesized that the species-specificity of TfR1 for virus entry might be influenced by TfR1 residues slightly outside of the region previously defined.

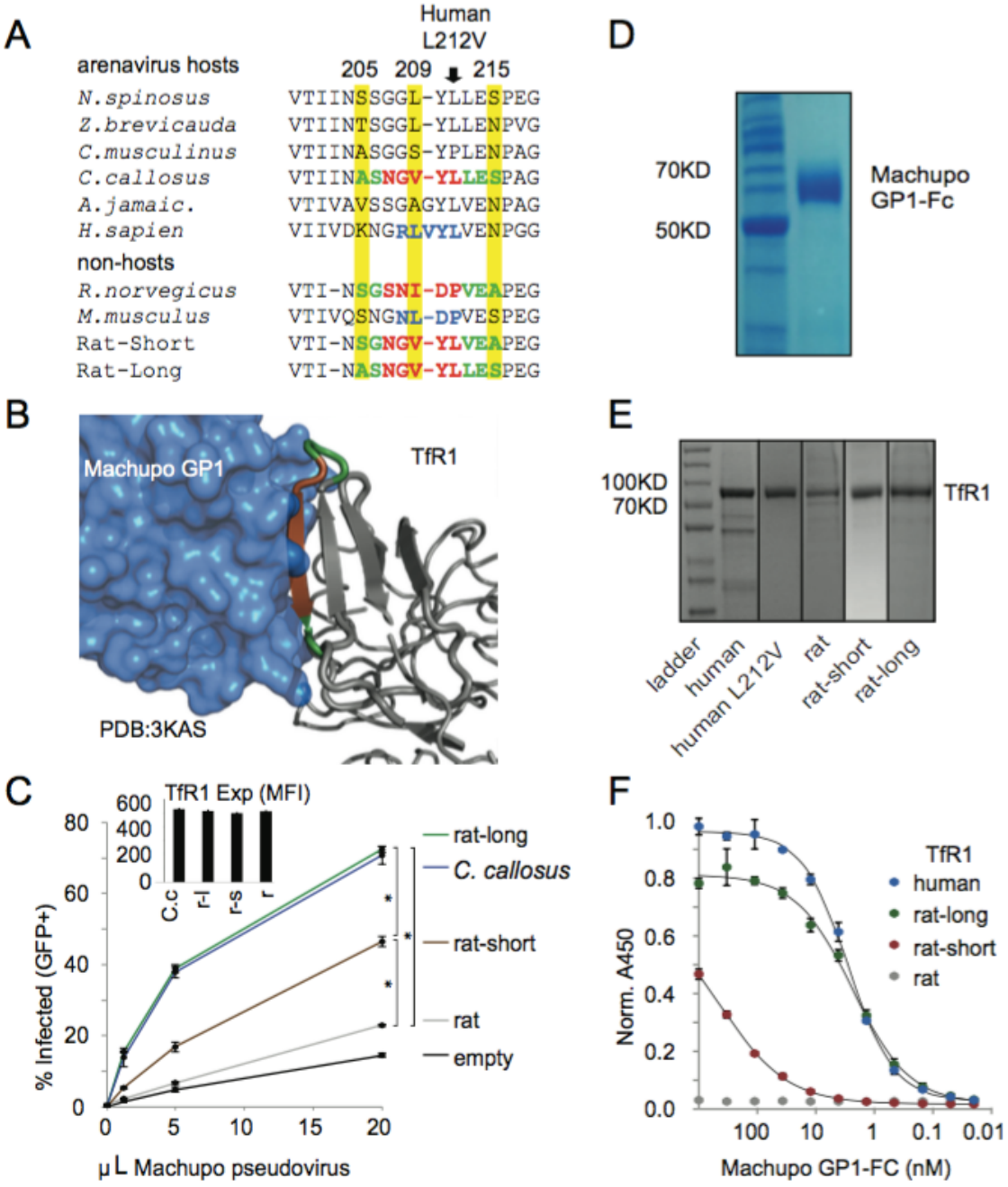

Figure 2.2. An extended region of TfR1 determines species-specificity of Machupo virus entry.

Figure 2.2. An extended region of TfR1 determines species-specificity of Machupo virus entry.

A. An alignment of one portion of the TfR1 apical domain is shown for host and non-host species. The amino acid numbering corresponds to human TfR1. The three residues experiencing recurrent positive selection, as previously defined (Demogines et al., 2013), are highlighted in yellow. These residue positions are in the arenavirus binding region of TfR1, and are not known to be important for the interaction between TfR1 and other viruses that use this receptor. In blue type, a strategy is summarized that was previously used to map the Machupo-binding interface on TfR1 (Radoshitzky et al., 2008). In that previous work, this region was swapped from the human TfR1 (RLVYL) into the house mouse (*M. musculus*) TfR1, replacing the corresponding 4-residues (NLDP). In the present work, residues in the *C. callosus* TfR1 were swapped into the rat TfR1 to create the rat-short (red type) and rat-long (red plus green type) chimeric TfR1 shown in the bottom two lines. **B.** The co-crystal structure shows the interaction between Machupo virus GP1 (blue) and the human TfR1 apical domain (grey) (PDB: 3KAS) (Abraham et al., 2010). The residue positions mutated in the rat-short TfR1 chimera are shown in brown. The residues positions mutated in the rat-long chimera are shown in green and brown. **C.** Canine D17 cells were transduced to stably express the wild type and chimeric TfR1s with C-terminal FLAG tags. Cells were infected with increasing volumes of Machupo pseudovirus (GFP-encoding retrovirus pseudotyped with Machupo virus glycoprotein (GP)). Cells were monitored for GFP expression to determine the percentage of infected cells. Error bars indicate standard deviation of three technical replicates. Experiment was performed 3 times with similar results seen in all experiments, graph represents data from one experiment. A t-test was performed to determine if differences between mean values were statistically significant, * <1e-8. Cell surface expression of TfR1 was monitored with a FLAG antibody via flow cytometry (inset) concurrently with measurement of GFP signal. Expression is given as mean fluorescent intensity (MFI). **D.** A Coomasie-stained SDS page gel shows purified Machupo virus GP1 fused to the human IgG1 Fc fragment. **E.** Coomasie-stained SDS page gels show the five purified TfR1 proteins. **F.** ELISA comparing the relative binding affinities of Machupo GP1 to each of the purified TfR1. Purified TfR1 was bound to wells, and then GP1 was incubated at decreasing concentrations to determine the relative binding affinities. Error bars indicate standard deviation of three technical replicates. Experiment was performed 2 times with similar results seen in both experiments, graph represents data from one experiment. Curves were fit using 4 parameter non-linear regression.

To test this hypothesis, we examined the TfR1 from the brown rat (*Rattus norvegicus*), which does not function as a receptor for Machupo virus. We focused on the brown rat instead of house mouse because house mouse TfR1 has a variant amino acid at position 348 that is not shared by most other rodent TfR1s, or by the human TfR1, but which has also been shown to participate in the interaction with Machupo virus (Abraham et al., 2010), (Radoshitzky et al., 2008). We used the TfR1 from the Machupo virus rodent host, *Calomys callosus*, as our permissive control TfR1. We created two chimeric TfR1's in which we swapped residues from the permissive *C. callosus* TfR1 into the non-permissive rat TfR1 background. In the first chimera, termed rat-short, we replaced five amino acid residues in rat TfR1 (SNIDP) to their respective *C. callosus* residues (NGVYL; red type in Figure 2.2A). This clone is structurally similar to the mouse-human TfR1 swap previously described, in that we swapped 5 amino acids including and upstream of the "L" or "P" at position 212. In the second chimera, termed rat-long, we mutated the rat amino acid residues (SGSNIDPVEA) corresponding to human positions 205-215 to their respective *C. callosus* TfR1 residues (ASNGVYLLES; red and green type in Figure 2.2A). This chimera thus contains the entire stretch of *C. callosus* TfR1 encompassing the three positions that have been targeted by positive selection. (This region is 11 amino acids long in human TfR1 and 10 amino acids long in rodent TfR1.) Stable cell lines expressing each TfR1 were established in canine osteosarcoma cells (D17) so that virus entry assays could be performed. D17 cells were used because the canine TfR1 is not a functional receptor for arenaviruses (Radoshitzky

et al., 2008), (Abraham et al., 2009), although modest amounts of background entry are observed for some viruses ((Flanagan et al., 2008) and demonstrated herein). All TfR1 receptors were fused to a C-terminal FLAG tag that is localized extracellularly when the receptor is embedded in the cellular membrane, allowing receptor expression at the cell surface to be detected in live cells by flow cytometry using a FLAG antibody (see methods) (Figure 2.2C, inset).

Pseudoviruses were used to test arenavirus entry into these cells. Specifically, Machupo virus glycoprotein (GP) was pseudotyped onto murine leukemia virus (MLV) particles carrying a green fluorescent protein (GFP) gene. Upon virus entry and infection of the cell, the retroviral machinery in the MLV virion drives integration of the GFP gene into the cellular (D17) genome. To assess entry via different versions of TfR1, the D17-TfR1 cell lines were infected with increasing amounts of Machupo pseudovirus and fluorescent cells expressing the GFP reporter were counted by flow cytometry two days post infection. As expected, the TfR1 of the natural Machupo host species, *C. callosus*, supported high levels of viral entry mediated by the Machupo GP (Figure 2.2C). As was seen in the mouse-human TfR1 chimera (Radoshitzky et al., 2008), the rat-short TfR1 chimera permitted a moderate amount of entry, much greater than rat TfR1, confirming that the five amino acid positions introduced from the *C. callosus* TfR1 were partially responsible for Machupo GP mediated entry. The rat-long mutant, whose design was influenced by the evolutionary signatures found in *TFR1*, had a similar entry phenotype

to the *C. callosus* TfR1, indicating that the species-identity of residues in this small 10 amino acid region more completely defines Machupo virus entry through the TfR1 of different species. However, in some contexts other amino acids such as position 348 may also play a role (Abraham et al., 2010), (Radoshitzky et al., 2008).

To determine whether or not these mutations alter binding affinity between the virus and rat TfR1, we purified a portion of the Machupo virus GP1 (residues 79–248) fused to the Fc domain of human IgG1 (Figure 2.2D), as was described previously (Radoshitzky et al., 2008). We also purified soluble TfR1 (see methods) representing rat as well as the rat-short and rat-long TfR1 variants (Figure 2.2E). Despite repeated attempts, we were unable to express and purify the *C. callosus* TfR1. Instead, we purified human TfR1 as a positive control, since Machupo virus can also use this receptor (Radoshitzky et al., 2007). Each TfR1 was coated onto an ELISA plate, and purified Machupo virus GP1-Fc was added at decreasing concentrations. Rat TfR1 did not bind GP1 at any concentrations tested (Figure 2.2F). The rat-short TfR1 showed moderate binding to GP1 with an EC_{50} value of 412 $\pm$ 33 nM, while both rat-long TfR1 and human TfR1 bound much tighter to GP1 with EC_{50} values of 2.37 $\pm$ 0.18 nM and 2.81 $\pm$ 0.12 nM, respectively. Therefore, protein-protein interaction affinities between arenavirus GP and TfR1 correlate with cellular entry, as shown here and previously (Abraham et al., 2010), (Radoshitzky et al., 2008), (Abraham et al., 2009), (Flanagan et al., 2008), (Radoshitzky et al., 2011).

Virus-specific effects on cellular entry through TfR1

Residues 205-215 in TfR1 interact, in part, with loop 10 in the Machupo virus GP1 (Abraham et al., 2010). As has been previously noted, that loop and surrounding sequence (colored light pink in Figure 2.3A) is substantially shorter in length in the GP1 of other arenaviruses (Abraham et al., 2010). Based on this observation, we hypothesized that other New World arenaviruses may have unique contact orientations on TfR1.

To analyze how these structurally different arenavirus GP1s interact with TfR1, we examined our rat-short and rat-long TfR1 for their ability to support entry of another arenavirus. We pseudotyped MLV-based virions with the GP from Sabia virus, a zoonotic virus that is highly diverged from Machupo, both phylogenetically (Figure 2.1) and in the sequence of loop 10 (Figure 2.3B). We again observed that these substitutions into rat TfR1 created a functional receptor for the arenavirus (Figure 2.3C). However, in contrast to what we observed with Machupo virus, we found that both rat-short and rat-long TfR1 supported equal levels of entry of Sabia virus. So, residues outside of the previously defined region of TfR1 matter for host species compatibility, but to different extents for different arenavirus strains.

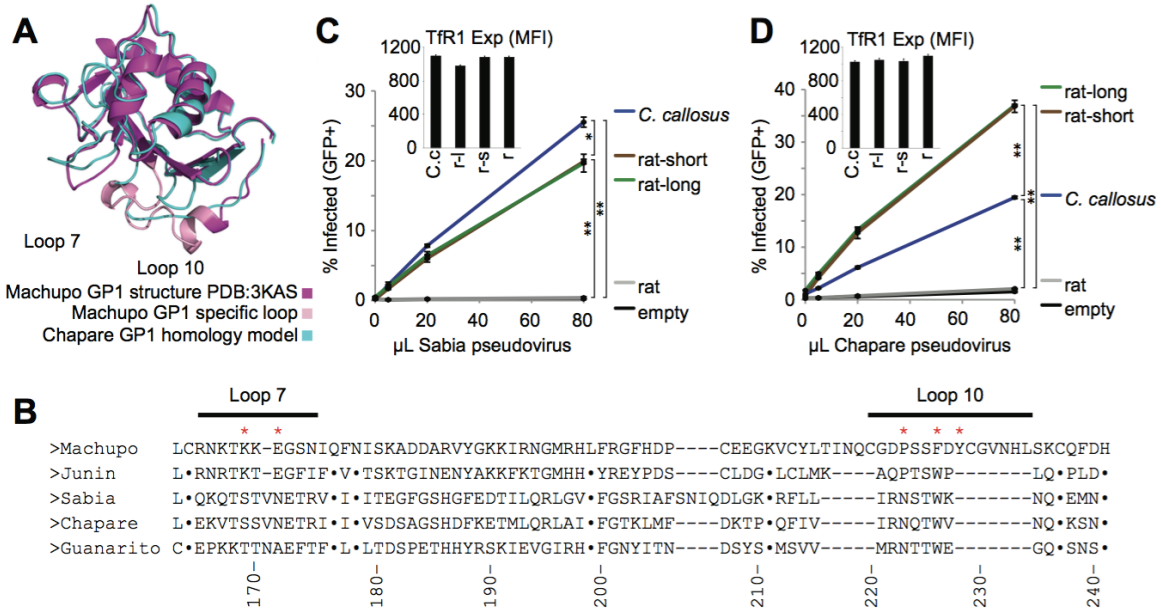

Figure 2.3. Virus-specific effects on entry through TfR1.

Figure 2.3. Virus-specific effects on entry through TfR1.

A. The Chapare virus GP1 (blue) was homology modeled on the Machupo virus GP1 crystal structure (magenta; PDB 3KAS). The Machupo virus GP1 loop 10 and surrounding residues are shown in light pink, and are absent in the Chapare virus GP1. Similar results were seen with Sabia and Junin models (not shown). **B.** An alignment illustrates the C-terminal region of GP1 from Machupo, Junin, Sabia, Chapare, and Guanarito arenaviruses. Identical residues to Machupo virus have been replaced with dots. Machupo virus GP1 sites that make contact with TfR1 (Abraham et al., 2010) are indicated with red asterisks. They fall in loop 7, loop 10, and in two upstream regions which are not shown. Loop 10 is longer in length in Machupo virus compared to all other viruses. The numbering scheme is based on the Machupo virus protein. Note that the alignment differs somewhat from a similar alignment shown in (Abraham et al., 2010). The differences in these alignments concern the exact placement of insertions and deletions, but are within the range to be expected from different alignment approaches. This alignment was generated using MAFFT (Katoh et al., 2002), (Katoh et al., 2005). **C, D.** Canine D17 cells were transduced to stably express the wild type and chimeric TfR1s with C-terminal FLAG tags. Cells were infected with increasing volumes of GFP-encoding retrovirus pseudotyped with C) Sabia, or D) Chapare virus glycoprotein (GP). Cells were monitored for GFP expression to determine the percentage of infected cells. Error bars indicate standard deviation of three technical replicates. Experiments were performed 2 times with similar results seen in both experiments, graph represents data from one experiment. A t-test was performed to determine if differences between mean values were statistically significant, * <1e-5, ** <1e-10. Cell surface expression of TfR1 was monitored with a FLAG antibody via flow cytometry (inset) concurrently with measurement of GFP signal. Expression is given as mean fluorescent intensity (MFI).

Sabia virus GP1 is four amino acids longer upstream of loop 10, compared to other viruses such as Junin, Chapare, and Guanarito (Figure 2.3B). To confirm that the unique pattern of entry through these modified rat TfR1 receptors was not a result of this elongated GP1 motif, we tested entry of Chapare virus, another zoonotic virus closely related to Sabia virus (Figure 2.1) but lacking the 4 amino acid insertion (Figure 2.3B). We saw the same result, where this virus entered cells equally through the rat-short and rat-long TfR1 (Figure 2.3D). Further, we saw additional virus-specific effects in that, for Sabia virus, rat-short and rat-long TfR1 permitted less viral entry than the *C. callosus* TfR1, while in the case of Chapare, they permitted more. This result demonstrates the complexities of predicting host-virus compatibility in nature, where both host and virus genetic variation have functional consequences.

Previously, a human SNP in the arenavirus-binding region of TfR1, L212V (Figure 2.4A), was found to reduce entry by Machupo virus (Figure 2.4B) (Demogines et al., 2013). It was not previously investigated whether this phenotype was due to reduced interaction affinity. We purified the SNP variant TfR1 L212V protein (Figure 2.2E) and again performed an ELISA to measure interaction with Machupo GP1. We found that TfR1 L212 bound much more tightly to Machupo virus GP1 than did TfR1 L212V (Figure 2.4C), in concordance with the entry phenotypes observed. The EC_{50} values of L212 and L212V TfR1 binding to GP1 were 2.1 $\pm$ 0.37 nM and >1μM, respectively. While the interaction between the virus GP1 and TfR1 L212V is very weak, this still

appears to result in a modest amount of virus entry (Figure 2.4B). This could be because the strength of the interaction is compounded through avidity effects, or because the ELISA results underestimate binding due to a high off-rate that may not be as relevant to entry. In contrast, TfR1 binding to iron-loaded human transferrin was not affected by this amino acid change (Figure 2.4D).

We next tested two other zoonotic New World arenaviruses for entry through the L212 or L212V allelic variants of human TfR1. We tested one arenavirus that is closely related to Machupo (Junin virus) and one that is distantly related (Sabia virus) (Figure 2.1). In contrast to what we found for Machupo virus, TfR1 L212V supported higher levels of entry than the more common TfR1 L212 allelic form, and this was true for both the Junin virus (Figure 2.4E) and the Sabia virus (Figure 2.4F). In sum, successful pairings between viruses and TfR1 depended on sequence determinants in both the host and virus. For this reason, we next investigated the prospects for quickly screening the effects of mutations via structure-based homology-modeling and docking.

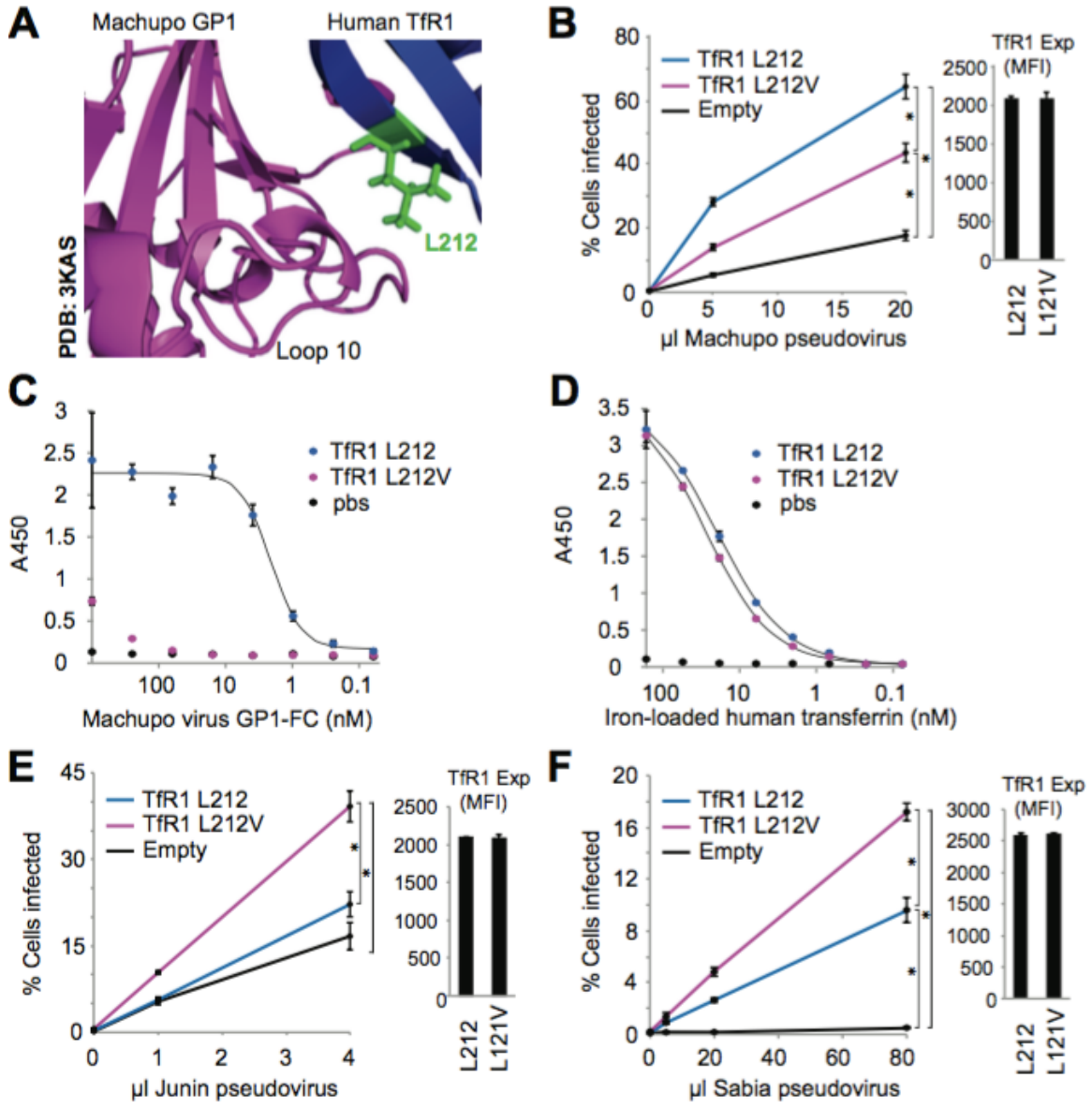

Figure 2.4. Human TfR1 L212V SNP has an opposite effect on the entry of related arenaviruses.

Figure 2.4. Human TfR1 L212V SNP has an opposite effect on the entry of related arenaviruses

A. The L212 residue in TfR1 contacts loop 10 in the Machupo virus GP1 (PDB Code: 3KAS)(Abraham et al., 2010). **B.** Canine D17 cells were transduced to stably express the human TfR1 with either L212 or bearing the human SNP mutation, L212V, both with a C-terminal FLAG tag. Cells were infected with increasing volumes of a GFP-encoding retrovirus psuedotyped with Machupo virus glycoprotein. Cells were monitored for GFP expression to determine the percentage of infected cells. Error bars indicate standard deviation of three technical replicates. Experiment was performed 2 times with similar results seen in both experiments, graph represents data from one experiment. A t-test was performed to determine if differences between mean values were statistically significant, * <1e-3. Cell surface expression of TfR1 was monitored with a FLAG antibody via flow cytometry (panel on right) concurrently with measurement of GFP signal. Expression is given as mean fluorescent intensity (MFI). **C.** ELISA comparing the relative binding affinities of the purified human L212 and L212V TfR1 to Machupo virus GP1. Purified TfR1 was bound to wells. GP1 was then incubated at decreasing concentrations to determine the relative binding affinities. Error bars indicate standard deviation of three technical replicates. Experiment was performed 2 times with similar results seen in both experiments, graph represents data from one experiment. Curves were fit using 4 parameter non-linear regression. **D.** ELISA comparing the relative binding affinities of the purified human L212 and L212V TfR1 to iron loaded human transferrin. For the ELISA, purified TfR1 was bound to wells. Iron-loaded TfR1 was incubated at decreasing concentrations to determine the relative binding affinities. Error bars indicate standard deviation of three technical replicates. Experiment was performed 2 times with similar results seen in both experiments, graph represents data from one experiment. Curves were fit using 4 parameter non-linear regression. **E, F.** The experiment is the same as in panel B. In this case, cells were infected over increasing volumes with a GFP-encoding retrovirus psuedotyped with E) Junin, or F) Sabia virus glycoprotein.

Structure-Based Prediction of Host-Virus Compatibility

It would be useful to be able to computationally predict whether a virus of one species is compatible with the receptor encoded by another species. Towards this goal, we developed a computational pipeline for assessing the effect of species-specific mutations in TfR1 on GP1 binding (Figure 2.5A). In brief, we used the Machupo virus GP1–human TfR1 co-crystal structure (PDB Code: 3KAS) and MODELLER (Eswar et al., 2006), (Webb and Sali, 2014) to build homology models of Machupo GP1–TfR1 complexes, with species-specific substitutions made in TfR1. The substitutions in TfR1 that we modeled were the same species variants, alleles, and chimeric constructs described in the experimental sections above. We then fine-tuned these models through re-docking with RosettaDock (Chaudhury et al., 2011). The docking procedure yields characteristic "binding funnels" with the best (i.e., most negative) scores falling into a narrow range of root-mean-square deviations (RMSDs) relative to the starting conformation (i.e., the models from MODELLER) (Figure 2.5A). We used the distribution of the top-10 best interface scores as our final measure of the predicted binding strength between the Machupo GP1 and the given TfR1.

We tested this method on the eight TfR1 variants discussed in this study: human, human L212V, mouse, the mouse-human chimera, rat, rat-short, rat-long, and *C. callosus* (Figure 2.5B). Our computational results showed broad agreement with the experimental

findings. TfR1s that functioned as partial or full receptors for Machupo virus in entry assays (colored yellow and green in Figure 2.5C) had systematically lower (i.e., better) interface scores than TfR1s that did not function as receptors for Machupo virus (colored red in Figure 2.5C). The model accurately predicted the better binding of Machupo GP1 to wild-type human TfR1 compared to the TfR1 L212V variant. Recapitulating the experimental work done previously (Radoshitzky et al., 2008), it also predicted the successively greater binding strength of Machupo virus GP1 to mouse TfR1, then mouse-human chimeric TfR1, followed by human TfR1. The model predicted that rat-short TfR1 bound to Machupo virus with affinity that is greater than rat TfR1 but less than *C. callosus* TfR1. One prediction was not completely in line with our experimental observations. Rat-long TfR1 was accurately predicted to bind Machupo virus with an affinity greater than rat TfR1, but was not predicted to bind differently than rat-short TfR1 as was our observation. Thus, we found that we could reasonably model Machupo GP1 binding to TfR1 in a way that is predictive of whether the virus would be able to enter cells through the TfR1 of different species. We attempted to apply this modeling approach to the other arenavirus strains that we had used in our entry assays, but we found that we were unable to obtain satisfactory homology models and docks due to low template-target sequence identity. Although our approach has this and other limitations, discussed further below, it provides a way to quantify a critical determinant of the cross-species transmission potential of a virus into a new species.

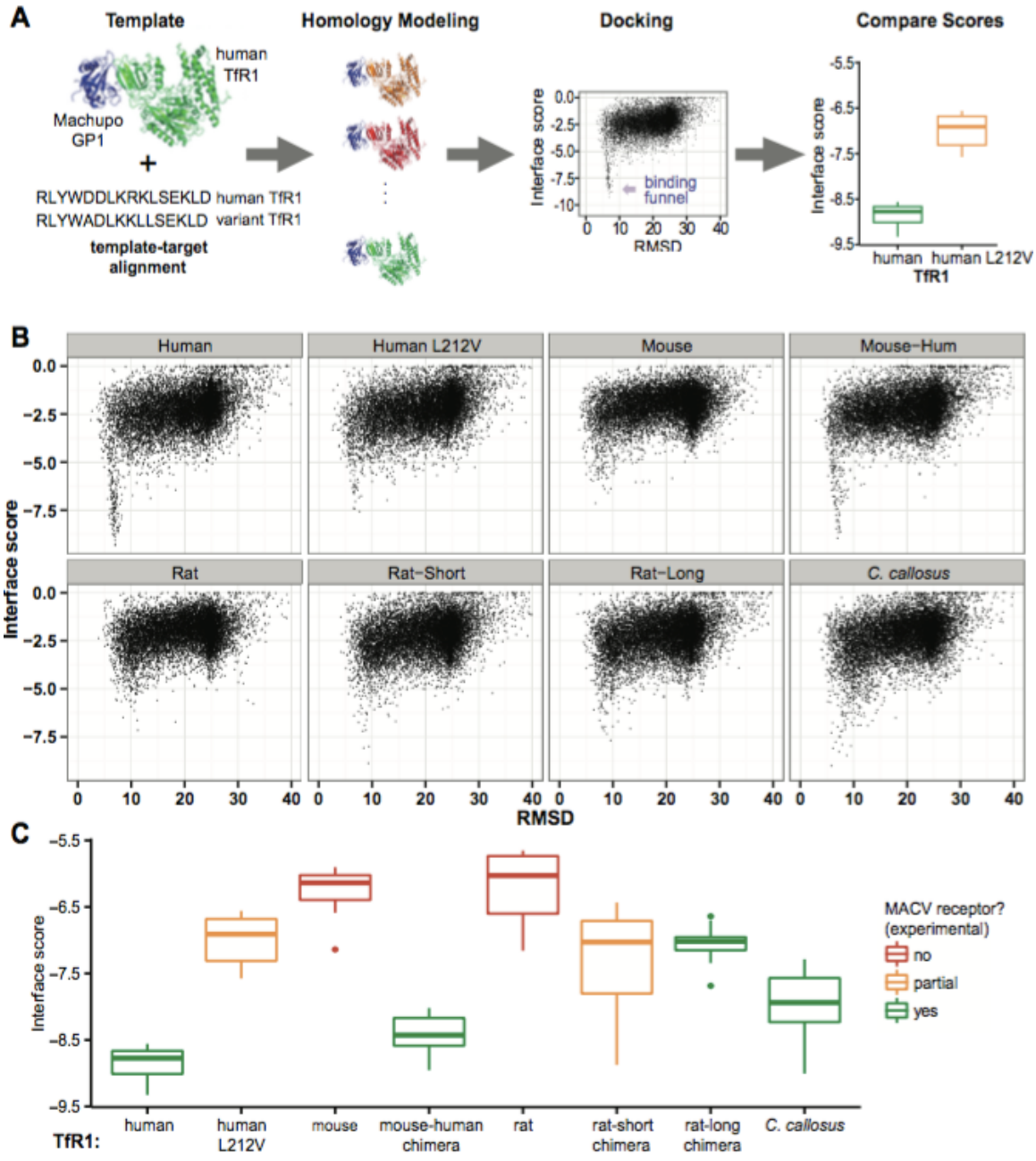

Figure 2.5. Computational modeling of Machupo virus GP1 binding to different TfR1 variants.

Figure 2.5. Computational modeling of Machupo virus GP1 binding to different TfR1 variants.

A. The computational pipeline consisted of homology modeling of variant TfR1 to the template co-crystal of the TfR1 – GP1 interaction, followed by structural refinement and re-docking. The re-docking procedure yields a characteristic "binding funnel" of low-energy conformations at around 8Å root-mean-square deviation (RMSD) relative to the starting position before docking. We use the top 10 best (i.e., lowest) scores to compare predicted binding strength, as shown in cartoon in the final panel. **B.** Binding funnels for the eight models we analyzed. Each dot shows the Rosetta interface score and RMSD from the un-docked configuration for one of the 10,000 docked models we generated. **C.** Comparison of the top-10 best scores across all models considered for each variant TfR1. Each boxplot shows the distribution of the interface scores for the 10 best docked conformations for each model. The red, yellow, and green color-coding refers to the ability of each TfR1 to act as a receptor for Machupo virus, based on experimental results presented herein, or elsewhere for mouse TfR1 (Radoshitzky et al., 2008), (Demogines et al., 2013), and the mouse-human TfR1 (Radoshitzky et al., 2008). (One note should be made regarding the color coding of mouse-human TfR1 as green. In the previously published work, the mouse-human TfR1 became fully functional for virus entry only when another mutation, K348N, was also included (Radoshitzky et al., 2008). On the other hand, K348N alone did not change the functionality of TfR1 for entry (Radoshitzky et al., 2008).)

DISCUSSION

Entry receptors are species-specific in their interactions with many viruses, so their characterization in wildlife populations is imperative. Understanding the role of receptors in defining the host range of viruses is important for understanding virus spillover to new animal hosts and to humans, and to the development of model organisms in which to study viral pathogenesis in the lab (Meyerson et al., 2015), (Sawyer and Elde, 2012). Here we propose a combination of computational and experimental approaches to map out the possible host space of a particular virus. Our approach is general and could be applied towards studying the potential spillover risk of many viruses, and their interactions with host factors beyond TfR1.

This work has uncovered potential evolutionary trade-offs in the TfR1-arenavirus system. We have shown that a human SNP in TfR1 offers resistance to one virus while making the receptor more vulnerable to other viruses. While this SNP is found in Asia, and not in regions of the world where New World arenaviruses are found (Demogines et al., 2013), one could imagine a situation where selection starts operating on a SNP due to a local infection by a virus to which it offers protection, causing its rise in frequency. This mechanism, however, would create a population that is potentially more vulnerable to the zoonotic transmission of other viruses. A similar trade-off was evident in the mutational analysis of rat TfR1. Here we saw that, for Sabia virus, rat-short and rat-long TfR1 were worse receptors than the *C. callosus* TfR1, while in the case of Chapare virus,

they were better. With receptors, then, a complex fitness landscape can arise where resistance to one pathogen may come at the expense of susceptibility to others.

In the experiments that were performed, a small number of amino acid substitutions in rat TfR1 (rat-short and rat-long) transformed it into a functional receptor for several arenaviruses. This would suggest that SNPs in this region of TfR1, potentially already circulating in rat populations, could lead to individuals that are more susceptible to some arenaviruses and hence might ultimately become carriers of these viruses. This could provide a conduit for host range expansion into a species that is found globally.

Signatures of positive selection can be a valuable guide to mapping species-specific determinants of virus-receptor compatibility. All that is required to test for positive selection is a sequence alignment of the receptor gene, specifically from species which have served as the long-term viral reservoir. As we have now illustrated with rodent arenaviruses and retroviruses (Demogines et al., 2013), canine parvoviruses (Kaelber et al., 2012), bat SARS-like coronaviruses (Demogines et al., 2012), and primate lentiviruses (Meyerson et al., 2014), the use of evolutionary analyses to finely map the viral interaction surfaces on entry receptors seems to be accurate in many contexts, and can guide the rapid characterization of the host protein receptors that govern species tropism of many emerging viruses. Similar phenomena have also been described for XPR1 gammaretrovirus receptors of rodents and birds (Yan et al., 2010),

(C. Martin et al., 2013). Reciprocally, positively selected sites in genes encoding viral glycoproteins can identify the host-receptor binding site (Demogines et al., 2013), (Meyer and Wilke, 2015).

Indels have accumulated in a region of arenavirus GP1 (loop 10) that contacts TfR1. These changes, combined with positive selection for non-synonymous mutations in portions of the GP1 that contact TfR1 (Demogines et al., 2013), have resulted in GP1 proteins of arenaviruses being highly divergent. As a consequence, the application of positive selection analysis, phylogenetic studies, and genetic mapping studies to this system becomes difficult, as all of these methods require quality alignments of viral sequences. To help solve this problem, more extensive surveillance of viruses could provide intermediate sequences that resolve the location of indels in viral alignments. Also, multiple co-crystal structures in this system, for instance the GP1 of several different arenaviruses in complex with the TfR1 of their relative host species, could help elucidate how well or poorly the binding architecture has been preserved.

The structural docking method described here can be used to evaluate the effects of mutations at the receptor–virus interface, similar to what was also done in a recent study with Middle East respiratory syndrome coronavirus (MERS-CoV) and its receptor DPP4 (van Doremalen et al., 2014). Relative to molecular dynamics methods used previously by us to predict the effect of mutations in the Machupo virus GP1–TfR1

system (Meyer et al., 2014), the docking method described here is much less computationally expensive. While we showed that our structural docking method works well in several contexts in this study, there are limitations. Most obvious is the fact that a co-crystal structure of the interacting proteins in complex is required. While co-crystals are not yet available for many host-virus systems, the number of such structures is quickly growing. It is possible to thread related proteins onto these structures, but we have found that this procedure was more accurate for the host protein, TfR1, than for the viral protein, GP1. Rodent and human TfR1s display only moderate divergence and thus can be reliably homology-modeled: all rodent TfR1s analyzed share greater than 70% identity with human TfR1. By contrast, GP1 sequences from different arenaviruses are too divergent to be modeled via homology, due to both the length differences found specifically in the loop 10 binding region and their low amino-acid conservation (Machupo GP1 residues 87-242 share only 25% to 46% identity with the corresponding GP1 residues of Junin, Guanarito, and Sabia) (Abraham et al., 2010). When we tried to model the GP1 of other arenaviruses, they would generally not dock reliably to any TfR1 variant considered (not shown).

There are several extended applications that can be envisioned for structural docking. First, the TfR1 of rodents with overlapping geographic ranges to *C. callosus* could be tested to see if there are other rodent species to which spillover of Machupo virus is likely. If these species have broader geographic range, this could represent

increased risk for humans in those areas. Second, mutations in viral surface glycoproteins could be tested in this model to see which would make the virus better at binding versions of the receptor encoded by new hosts, including humans or new rodent species. These would constitute virus mutations of interest to wildlife surveillance projects. Finally, the results with the L212V TfR1 SNP suggest that this model can be used to quickly predict the functional effects of human or rodent SNPs. Co-crystal structures describing relevant host-virus protein-protein interactions are the main limitation in this approach. This approach is in its infancy and will be refined by applying it to various problems and learning from its strengths and weaknesses. Investment in the generation of more co-crystal structures demonstrating interactions between host- virus interaction partners would be fruitful considering the success of the docking approach applied here for Machupo virus GP1 but the poor conservation between arenavirus GP1's.

ACKNOWLEDGEMENTS

This work was funded by grants from the Defense Threat Reduction Agency (HDTRA1-11-C-0061 to ADE, GG, SLS, COW) and from the National Institutes of Health (R01-GM-093086 to SLS). AD was supported by a fellowship from the American Cancer Society, and ELJ is supported by a National Science Foundation Graduate Research Fellowship.

We thank Dr. Nicholas Meyerson for critical discussions and comments on the manuscript. We thank Chhaya Das for assistance with protein expression. We thank Dr. Jonathan Abraham for advice on TfR1 purification, Dr. Sheli Radoshitzky for the GP1-Fc construct, and Dr. Hyeryun Choe for TfR1 and GP plasmids.

Eleisha Jackson, with assistance from Oana Lungu and Austin Meyer, is responsible for the computational work and all credit for that section is attributed to her. This work was adapted with permission from Scott A Kerr, Eleisha L Jackson, Oana I Lungu, Austin G Meyer, Ann Demogines, Andrew D Ellington, George Georgiou, Claus O Wilke, and Sara L Sawyer. 2015. "Computational and Functional Analysis of the Virus-Receptor Interface Reveals Host Range Trade-Offs in New World Arenaviruses." *Journal of Virology* 89 (22):11643–53. American Society for Microbiology doi:10.1128/JVI.01408-15.

REFERENCES

Abraham, J., Corbett, K.D., Farzan, M., Choe, H., Harrison, S.C., 2010. Structural basis for receptor recognition by New World hemorrhagic fever arenaviruses. Nature Publishing Group 17, 438–444. doi:10.1038/nsmb.1772

Abraham, J., Kwong, J.A., Albariño, C.G., Lu, J.G., Radoshitzky, S.R., Salazar-Bravo, J., Farzan, M., Spiropoulou, C.F., Choe, H., 2009. Host-Species Transferrin Receptor 1 Orthologs Are Cellular Receptors for Nonpathogenic New World Clade B Arenaviruses. PLoS Pathogens 5, e1000358. doi:10.1371/journal.ppat.1000358

Aisen, P., 2004. Transferrin receptor 1. The International Journal of Biochemistry & Cell Biology 36, 2137–2143. doi:10.1016/j.biocel.2004.02.007

Borio, L., Inglesby, T., Peters, C.J., Schmaljohn, A.L., Hughes, J.M., Jahrling, P.B., Ksiazek, T., Johnson, K.M., Meyerhoff, A., O'Toole, T., Ascher, M.S., Bartlett, J., Breman, J.G., Edward M Eitzen, J., Hamburg, M., Hauer, J., Henderson, D.A., Johnson, R.T., Kwik, G., Layton, M., Lillibridge, S., Nabel, G.J., Osterholm, M.T., Perl, T.M., Russell, P., Tonat, K., Biodefense, F.T.W.G.O.C., 2002. Hemorrhagic Fever Viruses as Biological Weapons: Medical and Public Health Management. JAMA 287, 2391–2405. doi:10.1001/jama.287.18.2391

Charrel, R.N., Coutard, B., Baronti, C., Canard, B., 2011. Arenaviruses and hantaviruses: from epidemiology and genomics to antivirals. Antiviral Research.

Chaudhury, S., Berrondo, M., Weitzner, B.D., Muthu, P., Bergman, H., Gray, J.J., 2011. Benchmarking and Analysis of Protein Docking Performance in Rosetta v3.2. PLoS ONE 6, e22477. doi:10.1371/journal.pone.0022477

Choe, H., Jemielity, S., Abraham, J., Radoshitzky, S.R., Farzan, M., 2011. Transferrin receptor 1 in the zoonosis and pathogenesis of New World hemorrhagic fever arenaviruses. Current opinion in microbiology 14, 476–82. doi:10.1016/j.mib.2011.07.014

Cuevas, C.D., Lavanya, M., Wang, E., Ross, S.R., 2011. Junin virus infects mouse cells and induces innate immune responses. J. Virol.

Daugherty, M.D., Malik, H.S., 2012. Rules of Engagement: Molecular Insights from Host-Virus Arms Races. http://dx.doi.org/10.1146/annurev-genet-110711-155522 46, 677–700. doi:10.1146/annurev-genet-110711-155522

de Graaf, M., Fouchier, R.A.M., 2014. Role of receptor binding specificity in influenza A virus transmission and pathogenesis. The EMBO Journal 33, 823–841. doi:10.1002/embj.201387442

Delgado, S., Erickson, B.R., Agudo, R., Blair, P.J., Vallejo, E., Albariño, C.G., Vargas, J., Comer, J.A., Rollin, P.E., Ksiazek, T.G., Olson, J.G., Nichol, S.T., 2008. Chapare Virus, a Newly Discovered Arenavirus Isolated from a Fatal Hemorrhagic Fever Case in Bolivia. PLoS Pathogens 4, e1000047. doi:10.1371/journal.ppat.1000047

Demogines, A., Abraham, J., Choe, H., Farzan, M., 2013. Dual host-virus arms races shape an essential housekeeping protein. PLoS biology.
Demogines, A., Farzan, M., Sawyer, S.L., 2012. Evidence for ACE2-utilizing coronaviruses (CoVs) related to severe acute respiratory syndrome CoV in bats. J. Virol.
Eswar, N., Webb, B., Marti-Renom, M.A., Madhusudhan, M.S., 2006. Curr Protoc Bioinformatics Chapter 5. doi:10.1016/j.febslet.2010.04.028/full
Flanagan, M.L., Oldenburg, J., Reignier, T., Holt, N., Hamilton, G.A., Martin, V.K., Cannon, P.M., 2008. New World Clade B Arenaviruses Can Use Transferrin Receptor 1 (TfR1)-Dependent and -Independent Entry Pathways, and Glycoproteins from Human Pathogenic Strains Are Associated with the Use of TfR1. J. Virol. 82, 938–948. doi:10.1128/JVI.01397-07
Gerlier, D., 2011. Emerging zoonotic viruses: new lessons on receptor and entry mechanisms. Current Opinion in Virology 1, 27–34. doi:10.1016/j.coviro.2011.05.014
Graham, R.L., Baric, R.S., 2010. Recombination, reservoirs, and the modular spike: mechanisms of coronavirus cross-species transmission. J. Virol. 84, 3134–3146. doi:10.1128/JVI.01394-09
Helguera, G., Jemielity, S., Abraham, J., Cordo, S.M., Martinez, M.G., Rodríguez, J.A., Bregni, C., Wang, J.J., Farzan, M., Penichet, M.L., Candurra, N.A., Choe, H., 2012. An antibody recognizing the apical domain of human transferrin receptor 1 efficiently inhibits the entry of all new world hemorrhagic Fever arenaviruses. Journal of virology 86, 4024–8. doi:10.1128/JVI.06397-11
Humes, D., Emery, S., Laws, E., Overbaugh, J., 2012. A species-specific amino acid difference in the macaque CD4 receptor restricts replication by global circulating HIV-1 variants representing viruses from recent infection. J. Virol. 86, 12472–12483. doi:10.1128/JVI.02176-12
Kaelber, J.T., Demogines, A., Harbison, C.E., Allison, A.B., Goodman, L.B., Ortega, A.N., Sawyer, S.L., Parrish, C.R., 2012. Evolutionary Reconstructions of the Transferrin Receptor of Caniforms Supports Canine Parvovirus Being a Re-emerged and Not a Novel Pathogen in Dogs. PLoS Pathogens 8, e1002666. doi:10.1371/journal.ppat.1002666
Katoh, K., Kuma, K.I., Toh, H., Miyata, T., 2005. MAFFT version 5: improvement in accuracy of multiple sequence alignment. Nucl. Acids Res. 33, 511–518. doi:10.1093/nar/gki198
Katoh, K., Misawa, K., Kuma, K.I., Miyata, T., 2002. MAFFT: a novel method for rapid multiple sequence alignment based on fast Fourier transform. Nucl. Acids Res. 30, 3059–3066. doi:10.1093/nar/gkf436
Leaver-Fay, A., Tyka, M., Lewis, S.M., Lange, O.F., Thompson, J., Jacak, R., Kaufman, K., Renfrew, P.D., Smith, C.A., Sheffler, W., Davis, I.W., Cooper, S., Treuille, A., Mandell, D.J., Richter, F., Ban, Y.-E.A., Fleishman, S.J., Corn, J.E., Kim, D.E., Lyskov, S., Berrondo, M., Mentzer, S., Popović, Z., Havranek, J.J., Karanicolas, J.,

Das, R., Meiler, J., Kortemme, T., Gray, J.J., Kuhlman, B., Baker, D., Bradley, P., 2011. Rosetta3: An Object-Oriented Software Suite for the Simulation and Design of Macromolecules. Methods in enzymology 487, 545–574. doi:10.1016/B978-0-12-381270-4.00019-6

LeDuc, J.W., 1989. Epidemiology of hemorrhagic fever viruses. Review of Infectious Diseases.

Li, L., Fang, C.J., Ryan, J.C., Niemi, E.C., 2010. Binding and uptake of H-ferritin are mediated by human transferrin receptor-1. Proceedings of the ….

Martin, C., Buckler-White, A., Wollenberg, K., Kozak, C.A., 2013. The avian XPR1 gammaretrovirus receptor is under positive selection and is disabled in bird species in contact with virus-infected wild mice. J. Virol. 87, 10094–10104. doi:10.1128/JVI.01327-13

Martin, V.K., Droniou-Bonzom, M.E., Reignier, T., Oldenburg, J.E., Cox, A.U., Cannon, P.M., 2010. Investigation of Clade B New World Arenavirus Tropism by Using Chimeric GP1 Proteins. J. Virol. 84, 1176–1182. doi:10.1128/JVI.01625-09

Meyer, A.G., Sawyer, S.L., Ellington, A.D., Wilke, C.O., 2014. Analyzing machupo virus-receptor binding by molecular dynamics simulations. PeerJ 2, e266. doi:10.7717/peerj.266

Meyer, A.G., Wilke, C.O., 2015. Geometric Constraints Dominate the Antigenic Evolution of Influenza H3N2 Hemagglutinin. PLoS Pathogens 11, e1004940. doi:10.1371/journal.ppat.1004940

Meyerson, N.R., Rowley, P.A., Swan, C.H., Le, D.T., Wilkerson, G.K., Sawyer, S.L., 2014. Positive selection of primate genes that promote HIV-1 replication. Virology 454-455, 291–298. doi:10.1016/j.virol.2014.02.029

Meyerson, N.R., Sawyer, S.L., 2011. Two-stepping through time: mammals and viruses. Trends in Microbiology 19, 286–294. doi:10.1016/j.tim.2011.03.006

Meyerson, N.R., Sharma, A., Wilkerson, G.K., Overbaugh, J., Sawyer, S.L., 2015. Identification of Owl Monkey CD4 Receptors Broadly Compatible with Early-Stage HIV-1 Isolates. J. Virol. 89, 8611–8622. doi:10.1128/JVI.00890-15

Parker, J., Murphy, W.J., Wang, D., O'Brien, S.J., 2001. Canine and feline parvoviruses can use human or feline transferrin receptors to bind, enter, and infect cells. Journal of ….

Parrish, C.R., Holmes, E.C., Morens, D.M., Park, E.-C., Burke, D.S., Calisher, C.H., Laughlin, C.A., Saif, L.J., Daszak, P., 2008. Cross-species virus transmission and the emergence of new epidemic diseases. Microbiol. Mol. Biol. Rev. 72, 457–470. doi:10.1128/MMBR.00004-08

Parrish, C.R., Kawaoka, Y., 2005. THE ORIGINS OF NEW PANDEMIC VIRUSES: The Acquisition of New Host Ranges by Canine Parvovirus and Influenza A Viruses. http://dx.doi.org/10.1146/annurev.micro.59.030804.121059 59, 553–586. doi:10.1146/annurev.micro.59.030804.121059

Peters, C.J., 2002. Human infection with arenaviruses in the Americas. Arenaviruses I 65–74. doi:10.1007/978-3-642-56029-3_3

Radoshitzky, S.R., Abraham, J., Spiropoulou, C.F., Kuhn, J.H., Nguyen, D., Li, W., Nagel, J., Schmidt, P.J., Nunberg, J.H., Andrews, N.C., Farzan, M., Choe, H., 2007. Transferrin receptor 1 is a cellular receptor for New World haemorrhagic fever arenaviruses. Nature 446, 92–96. doi:10.1038/nature05539

Radoshitzky, S.R., Kuhn, J.H., Spiropoulou, C.F., Albariño, C.G., Nguyen, D.P., Salazar-Bravo, J., Dorfman, T., Lee, A.S., Wang, E., Ross, S.R., Choe, H., Farzan, M., 2008. Receptor determinants of zoonotic transmission of New World hemorrhagic fever arenaviruses. PNAS 105, 2664–2669. doi:10.1073/pnas.0709254105

Radoshitzky, S.R., Longobardi, L.E., Kuhn, J.H., Retterer, C., Dong, L., Clester, J.C., Kota, K., Carra, J., Bavari, S., 2011. Machupo Virus Glycoprotein Determinants for Human Transferrin Receptor 1 Binding and Cell Entry. PLoS ONE 6, e21398. doi:10.1371/journal.pone.0021398

Rojek, J.M., Kunz, S., 2008. Cell entry by human pathogenic arenaviruses. Cellular Microbiology 10, 828–835. doi:10.1111/j.1462-5822.2007.01113.x

Ross, S.R., Schofield, J.J., Farr, C.J., 2002. Mouse transferrin receptor 1 is the cell entry receptor for mouse mammary tumor virus. Proceedings of the ….

Sawyer, S.L., Elde, N.C., 2012. A cross-species view on viruses. Current Opinion in Virology 2, 561–568. doi:10.1016/j.coviro.2012.07.003

Sironi, M., Cagliani, R., Forni, D., Clerici, M., 2015. Evolutionary insights into host-pathogen interactions from mammalian sequence data. Nature Reviews Genetics 16, 224–236. doi:10.1038/nrg3905

Stucker, K.M., Pagan, I., Cifuente, J.O., Kaelber, J.T., 2012. The role of evolutionary intermediates in the host adaptation of canine parvovirus. Journal of ….

van Doremalen, N., Miazgowicz, K.L., Milne-Price, S., Bushmaker, T., Robertson, S., Scott, D., Kinne, J., McLellan, J.S., Zhu, J., Munster, V.J., 2014. Host species restriction of Middle East respiratory syndrome coronavirus through its receptor, dipeptidyl peptidase 4. J. Virol. 88, 9220–9232. doi:10.1128/JVI.00676-14

Webb, B., Sali, A., 2014. Comparative Protein Structure Modeling Using MODELLER. John Wiley & Sons, Inc., Hoboken, NJ, USA. doi:10.1002/0471250953.bi0506s47

Yamashita, M., Emerman, M., 2004. Capsid is a dominant determinant of retrovirus infectivity in nondividing cells. J. Virol. 78, 5670–5678. doi:10.1128/JVI.78.11.5670-5678.2004

Yan, Y., Liu, Q., Wollenberg, K., Martin, C., Buckler-White, A., Kozak, C.A., 2010. Evolution of functional and sequence variants of the mammalian XPR1 receptor for mouse xenotropic gammaretroviruses and the human-derived retrovirus XMRV. J. Virol. 84, 11970–11980. doi:10.1128/JVI.01549-10

Chapter 3 Discovery of a Panel of Anti-Ebola Virus Antibodies by Immune Repertoire Mining[2]

INTRODUCTION

Ebolaviruses are negative-sense RNA filamentous viruses that cause very high morbidity and mortality (Bowen et al., 1977). Host cell entry is mediated first by the attachment of the heavily glycosylated glycoprotein (GP) on the viral envelope to the host cell encoded T-cell immunoglobulin and mucin domain 1 (TIM-1) (Kondratowicz et al., 2011). Following cathepsin cleavage in the lysosome, GP mediates cellular entry by binding the host cell encoded Niemann-Pick C1 (NPC1) (Carette et al., 2011). Five antigenically distinct ebolaviruses exhibiting 35-45% genome sequence divergence have been discovered (Towner et al., 2008): Ebola virus (abbreviated as EBOV, formerly designated as Zaire ebolavirus); Sudan virus (SUDV); Bundibugyo virus (BDBV); Reston virus (RESTV, for which no zoonotic infections have been reported to date) (M. E. G. Miranda and N. L. J. Miranda, 2011); and Taï Forest virus (TAFV, one incident of human infection) (Le Guenno et al., 1995). The recent EBOV outbreak in West Africa,

[2] This work was adapted with permission from Wang B, Kluwe CA, Lungu OI, DeKosky BJ, Kerr SA, Johnson EL, Jung J, Rezigh AB, Carroll SM, Reyes AN, Bentz JR, Villanueva I, Altmam AL, Davey RA, Ellington AD & Georgiou G. Facile Discovery of a Diverse Panel of Anti-Ebola Virus Antibodies by Immune Repertoire Mining. Scientific Reports. Nature Publishing Group; 2015;5: 13926. doi:10.1038/srep13926. Scott designed and executed the experiments presented here with cloning and ELISA assistance from Jiwon Jung and Bo Wang. Scott processed and analyzed the data under the guidance of Oana Lungu. Scott assisted in the writing of and edited several drafts of the published paper.

centered in Guinea, Sierra Leone, and Liberia with isolated outbreaks in Nigeria and Mali, was the largest ever with a mortality rate estimated at 70% of recorded definitive clinical outcomes (http://www.cdc.gov/vhf/ebola/outbreaks/2014-west-africa/index.html) (Team, 2014). Phylogenetic comparison of isolates from the recent outbreak (Baize et al., 2014) with 20 Ebolavirus genomes from earlier outbreaks suggested that the 2014 West African virus likely spread from central Africa within the past decade, having diverged from a common ancestor around 2004 (Gire et al., 2014). The five Ebolavirus species have varying rates of molecular evolution, with the highest of $8.21x10^{-4}$ nucleotide substitutions/site/year for Reston virus (Carroll et al., 2013). The ongoing evolution of Ebolaviruses poses significant challenges to the development of immunodiagnostics. Specifically, there is a critical need for the discovery of panels of monoclonal antibodies with distinct affinities and specificities for different Ebolaviruses. Of particular importance is the Reston Virus, to date there are no reported antibodies that can bind the glycoprotein of the Reston Virus

Antibodies to EBOV and SUDV have been produced from hybridomas (Dias et al., 2011), (Qaiu et al., 2011); by *in vitro* screening of synthetic scFv libraries (Koellhoffer et al., 2012), (Chen et al., 2014), and from human immune antibody libraries constructed from infected individuals (Maruyama et al., 1999). However additional monoclonal antibodies to Ebolaviruses are urgently needed both for diagnostic purposes and as therapeutics (Parren et al., 2002), (Qiu et al., 2014). Specifically, the generation of diagnostic antibodies to Ebolaviruses is complicated by the structural complexity of the

GP, which is heavily glycosylated in a host cell-specific manner (Feldmann et al., 1994), (Lin et al., 2003) and subjected to proteolytic cleavage during entry (Hood et al., 2010), as well as by the sequence diversity of the Ebolaviruses. Finally, characterization of useful antibodies to Ebolaviruses is limited by the safety concerns associated with handling the live virus.

Antibody discovery has relied either on the immortalization (Köhler and Milstein, 1975) or cloning of antibodies isolated from individual B cells obtained from an antigen-challenged host (Reddy et al., 2010), (Saggy et al., 2012), (Lane and Koprowski, 1982), (Ghosh and Campbell, 1986), (Wu et al., 2010), (Corti et al., 2011) or, alternatively, on the *in vitro* isolation from combinatorial libraries using a variety of screening techniques (Bradbury et al., 2011). The current collection of antibody technologies is predicated on the isolation of clones that display high antigen binding. However, animal immunization induces the stimulation and expansion of a highly diverse population of B cells encoding an antibody repertoire with a wide range of antibody affinities (Reddy et al., 2010), (Saggy et al., 2012). Antibodies with low affinity nonetheless may exhibit other highly desirable properties, including broad cross-reactivity or heteroclitic specificity, i.e. stronger binding reaction to a different antigen other than the one used for immunization (Lane and Koprowski, 1982), (Ghosh and Campbell, 1986), (Van Regenmortel, 2014). Unfortunately, there is no straightforward way to identify such interesting antibodies. For example, while the isolation of antibodies that bind to multiple antigens (e.g. to different flu hemagglutinins) or that neutralize

rapidly evolving pathogens such as HIV-1 or flu has been accomplished by B cell cloning, the process typically requires the screening of many thousands of B cells and therefore is very laborious and expensive (Wu et al., 2010), (Corti et al., 2011), (Walker et al., 2011), (Walker et al., 2009).

In order to satisfy the need for a wider variety of antibodies to Ebolaviruses, we developed a novel approach to comprehensively mine the full suite of antibody diversity, shaped by *in vivo* selective mechanisms and generated within the boundary of reactive secondary lymphoid tissues in immunized animals. We reasoned that antibodies encoded by antigen-stimulated B cells that had undergone the greatest degree of expansion within the confinement of a secondary lymphoid organ are most likely to display desirable antigen recognition properties including heteroclite recognition of diverse Ebolaviruses. Briefly, mice were first immunized in the footpad with Ebola virus-like particles (VLPs). Footpad immunization triggers a strong and highly-focused immune reaction in the PLN, especially for particles <40 nm such as VLPs (Reddy et al., 2006). Antigen experienced, $CD138^+$ B cells (plasmablasts) from the PLN were isolated and the natively paired V_H:V_L repertoire encoded by these cells was determined by NextGen sequencing (DeKosky et al., 2013). Antibodies corresponding to the highest frequency V_H:V_L pairs, and thus likely arising from the most clonally expanded and highly-transcribing $CD138^+$ B cells within the PLN, were expressed recombinantly and their binding properties were characterized. We employed this technique to generate the first Reston Ebola Virus GP-specific

antibodies. (RESTV, Reston, 1996, NCBI Accession number AB050936), an Ebolavirus for which no anti-GP monoclonal antibodies are available.

RESULTS

Immunization of the PLN yields antigen-specific antibodies

Fig. 3.1 summarizes our approach for mining the antibody repertoire encoded by the most highly expanded, antigen-experienced B cells following antigen stimulation. Footpad immunization leads to a strong inflammatory response in the draining popliteal lymph node (**Fig. 3.1a**). Unlike lymph nodes that drain sites of frequent extracorporeal interaction (e.g. the oral cavity or lungs), the germinal centers of the popliteal lymph node are normally relatively unstimulated (Kamala, 2007). Footpad immunization results in a marked increase in cellularity in the ipsilateral popliteal lymph node relative to the unstimulated contralateral lymph node (Gleichmann, 1981), (Ravel and Descotes, 2005), and a large fraction of the constituent antibody-secreting B cells were expected to be antigen-specific.

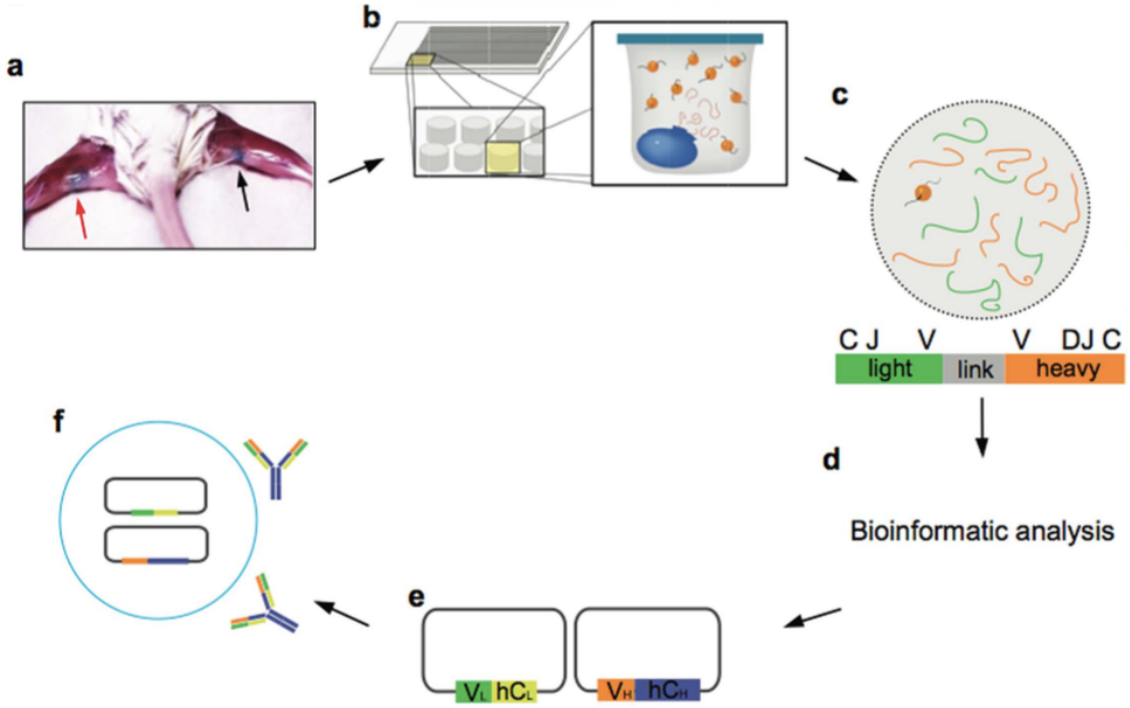

Figure 3.1: Isolation of antibodies by mining the paired V_H:V_L repertoire of draining popliteal lymph node (PLN) antibody-secreting B cells.

(a) Footpad immunization leads to a marked increase in cellularity within the ipsilateral popliteal lymph node (PLN) relative to the contralateral lymph node (red and black arrows respectively). (b) PLN $CD138^+$ cells isolated by magnetic sorting are deposited into 125 pL wells on PDMS slides that also contain poly(dT) beads. Cells are lysed *in situ* and mRNA is captured on the poly(dT) beads (DeKosky et al., 2013). (c) The poly(dT) beads are emulsified and V_H:V_L amplicons are generated following reverse transcription and overlap extension PCR. (d) V_H:V_L amplicons are sequenced using Illumina 2x250 MiSeq and the highest frequency V_H:V_L pairs are identified via bioinformatics analysis. (e) Highest frequency V_H (orange) and V_L (green) genes are synthesized and cloned into IgH and IgL expression vectors containing human IgG1 (blue) and human kappa (yellow) constant regions, respectively. (f) Following co-transfection into Expi293 cells, recombinant IgG antibodies are expressed and purified.

Ebola VLPs were produced by co-transfection of HEK293FT cells with plasmids encoding the three major virus structural proteins: nucleoprotein (NP), VP40 and GP of the RESTV strain and were purified by sucrose density centrifugation. Electron microscopy and gel staining confirmed that the other ebola VLPs created with the same process displayed a morphology and consistency characteristic of EBOV virions (**Fig. 3.2.**). Three mice were immunized with Ebola VLPs in emulsified adjuvant in the left hind footpad, followed by boost immunization in the lateral hock to minimize pain and discomfort. After the second boost, a strong anti-VLP titer was observed in all three mice and a weaker anti-GP was observed indicating that a portion of the immune response was against other, non-GP elements of the VLP (**Figure 3.3**). A final boost was administered and 6 days later the popliteal lymph nodes were extracted.

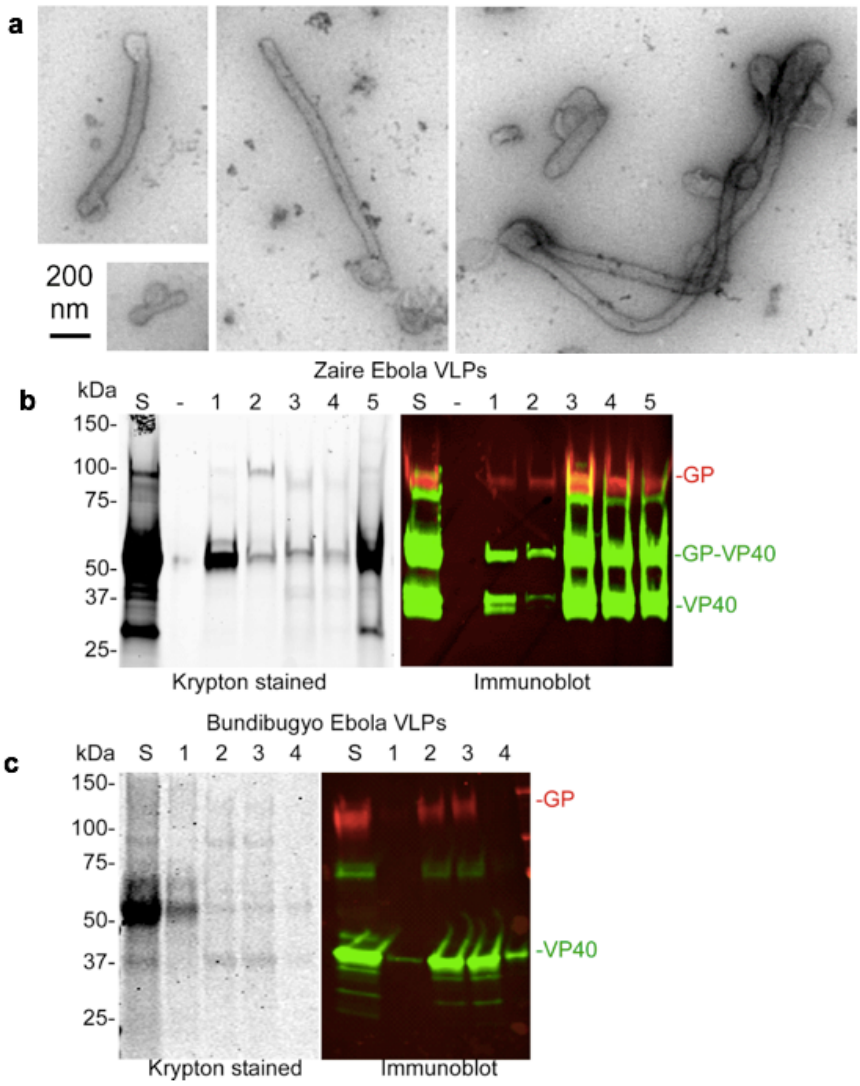

Figure 3.2: VLP production and characterization.

Figure 3.2: VLP production and characterization.

(a) Transmission electron microscopy images of EBOV VLPs. VLPs were purified by sucrose gradient and imaged using transmission electron microscopy. Particles of heterogeneous size were visible and examples are shown**. (b,c)** Total protein (left panel) and immunoblot (right panel) analysis of Ebola **(b)** and Bundibugyo **(c)** virus VLPs. VLPs were generated by transfecting plasmids encoding NP, VP40 and GP into 293FT cells. VLPs from culture supernatants were pelleted through sucrose and then applied to a sucrose gradient (S). Fractions were then collected from top (1-4) and material pelleting also collected (5). Gels were either stained with krypton total protein stain (left panels) or with VP40 (green) and GP (red) specific antibodies (right panels). Bundibugyo VLP pellet from the gradient was not analyzed.

CD45R$^-$CD19$^-$CD138$^+$ antibody secreting B cells were enriched by magnetic sorting and the paired V_H:V_L repertoire from single cells was determined following sequestration of the cells into 125 pL wells on PDMS slides (DeKosky et al., 2013) (**Fig. 3.1b).** Approximately 1x10^5 CD45R$^-$CD19$^-$CD138$^+$ plasmablasts were isolated by magnetic sorting, of which 2.5-3.5x10^4 cells were processed to create natively paired V_H:V_L amplicons. Linked V_H:V_L amplicons of approximately 850 bp were generated and then sequenced using Illumina MiSeq technology (**Fig. 3.1c**). High quality reads were clustered based on the CDRH3:CDRL3 sequences (**Fig. 3.1d**).

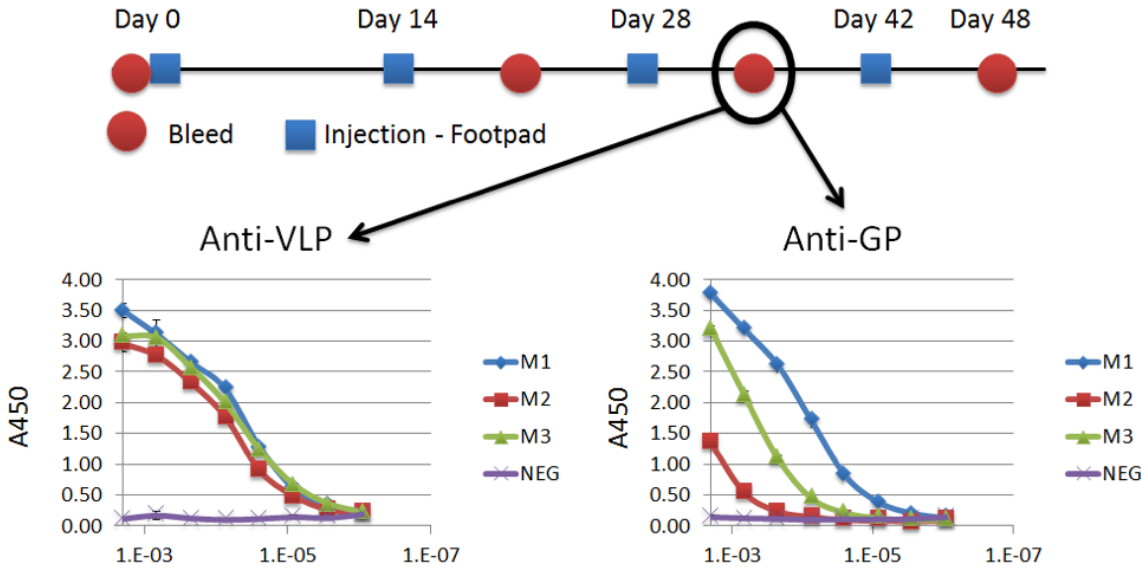

Figure 3.3 – Bleed/Injection Schedule and Bleed 3 Titers

Mice were injected every two weeks with Reston-Ebola VLPs. Serum was collected prior to injection and ~one week after the 2nd, 3rd and 4th injection. Mice were sacked 6 days after the final injection. Titers were determined using serum from the bleed following the 3rd VLP injection. Titers were measure against VLPs that were used to immunize and against recombinant soluble Reston-Ebola Glycoprotein (GP).

THE PLN PLASMABLAST IGG REPERTOIRE ELICITED BY IMMUNIZATION WITH EBOV

641, 572, and 546 unique V_H:V_L pairs (represented by ≥2 sequence reads per pair each), comprising the PLN plasmablast repertoires were identified in mouse 1 (M1), mouse 2 (M2) and mouse 3 (M3), respectively. The repertoires from both Ebola VLPs immunized mice investigated were skewed, with the top ten most abundant V_H:V_L pairs representing 52%, 33% and 31% of the total sequence counts in each mouse, respectively (**Table 3.1**).

Mouse 1 - 641 Clonotypes				
Rank	Sequence Reads	% of Total Reads	CDRH3	CDRL3
RM1.1	27714	17%	CARGAITTGFAYW	CQNDHSYPLTF
RM1.2	11534	7%	CARQGYRYGLYAMDYW	CQQWSSYPTF
RM1.3	10054	6%	CVGGDYW	CQQWSSYPLTF
RM1.4	7433	5%	CTRAIGRAMDYW	CQQSNEDPYTF
RM1.5	6978	4%	CTRGDDGAWFATW	CQQWSSNPFTF
RM1.6	5625	3%	CARSKFITTSMDYW	CHQHYNTPRTF
RM1.7	5475	3%	CTRGWDGIAYW	CQQDYSSPRTF
RM1.8	4428	3%	CARQGVLTIDYW	CHQWTSYPWTF
RM1.9	4220	3%	CARGVWSPYFDYW	CSQSTHVPYTF
RM1.10	3527	2%	CARHYYGSRDYFDYW	CQQHYSTPWTF
Mouse 2 - 572 Clonotypes				
Rank	Sequence Reads	% of Total Reads	CDRH3	CDRL3
RM2.1	2273	7%	CARYRYAMDYW	CHQWSSYRTF
RM2.2	1477	4%	CARPYYGMDYW	CQQSNEDPWTF
RM2.3	1316	4%	CARRDGYYWYFDVW	CQQGNTLPWTF
RM2.4	972	3%	CARWGWVGAMDYW	CQQSNSWPLTF
RM2.5	934	3%	CARGGYGSPFAYW	CFQGSHVPFTF
RM2.6	855	3%	CARSYYDYDEGLGYYAMDYW	CHQYHRSPYTF
RM2.7	832	3%	CARQGRSYFYALDYW	CAQNLELPYTF
RM2.8	814	2%	CARQTNSFDYW	CQQWSSNPYTF
RM2.9	682	2%	CARDGEVRRRYYAMDYW	CQHSWEIPLTF
RM2.10	663	2%	CARQPFDYW	CFQGSHVPYMF
Mouse 3 - 546 Clonotypes				
Rank	Sequence Reads	% of Total Reads	CDRH3	CDRL3
RM3.1	1897	5%	CARGGDGSYVRAMDYW	CHQRSSFPLTF
RM3.2	1518	4%	CARSGGTNW	CWQGTHFPLTF
RM3.3	1380	4%	CARHSPSYGNFAWFAYW	CQQWSNPPWTF
RM3.4	1093	3%	CVLEAFDYW	CQQRSSYPFTF
RM3.5	1031	3%	CASQIYYGYDEGFDYW	CHQRSSYHTF
RM3.6	1003	3%	CARRRNYFAMDYW	CQQGNTLPWTF
RM3.7	985	3%	CARGIGGGFAYW	CQQNNEGPYTF
RM3.8	902	2%	CARDWDVAYW	CQQRSSYPPTF
RM3.9	873	2%	CARETGRNYGYSYVMDYW	CQQRTSYPLTF
RM3.10	727	2%	CASDYDGAMDYW	CHQYHRSPWTF

Table 3.1: Top ten VH:VL pairs.

The top ten VH:VL pairs as ranked by total number of sequence reads from sequencing run. The % of the total sequencing reads for each pair was calculated. The CRDH3 and CDRL3 for each pair is listed in the final two columns.

Construction and characterization of anti-EBOV VLP antibodies

The 7 highest frequency V_H:V_L clonotypes from each mouse were selected for characterization. Antibody genes for these 21 most prevalent V_H:V_L antibody clonotypes were synthesized and cloned as mouse V region-human constant domain chimeric antibodies, expressed in HEK293 cells, and characterized for antigen binding. We identified three antibodies designated RM2.4, RM3.2, and RM3.3 that bound to both RESTV VLPs as well as to RESTV recombinant GP (**Fig. 3.4**).

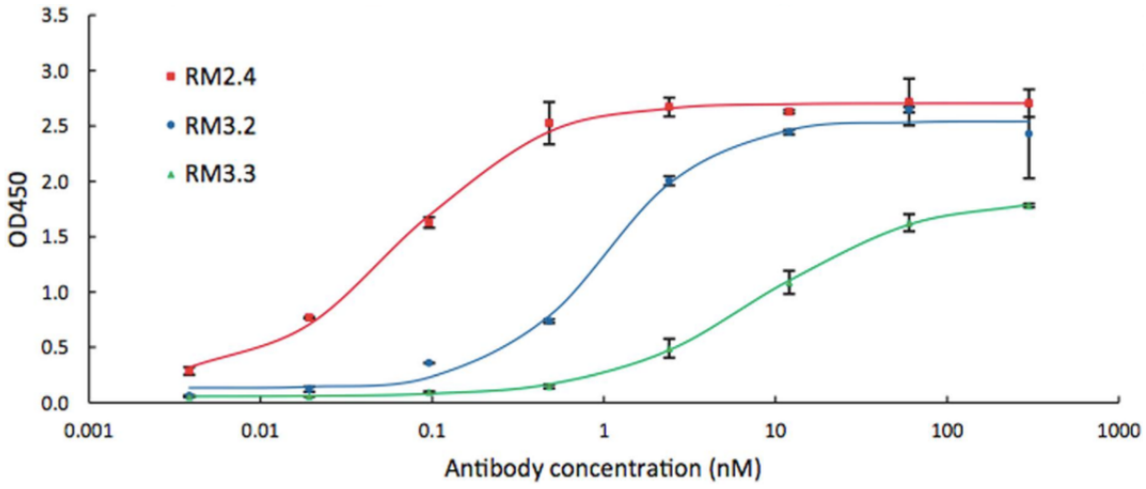

Figure 3.4: Functional characterization of IgG antibodies isolated via mining of RESTV immunized PLN CD138$^+$ B cell repertoire.

Binding to RESTV GP for select antibodies as determined by ELISA. Curves were fitted using 4-parameter non-linear regression. Error bars represent the standard deviation for three technical replicates.

DISCUSSION

Here we report an approach for generating a panel of distinct monoclonal antibodies that bind RESTV GP. We found that in multiple animals immunized with RESTV VLPs, the repertoire of $CD138^+$ plasmablasts in the draining PLN contained highly expanded, antigen-specific, antibody sequences. We find that these highly expanded sequences include antibodies that display affinity to GP. These results demonstrate the power of mining the antibody repertoire of highly expanded B cells after immunization for discovery of antibodies with interesting properties.

The ability to isolate distinct antibodies with very different CDR3 sequences per animal as well as a much larger number of somatic variants whose sequences are also available in the V_H:V_L sequence database provides a rich source of antibodies for practical purposes. Undoubtedly, many PLN B cells encoding antigen-specific antibodies are likely to have been subject to more limited expansion and thus are present at a lower abundance within the repertoire. However, such medium or low abundance antibody sequences within the repertoire are present at comparable levels to those elicited by environmental stimuli and thus recognizing unrelated antigens. Therefore the low abundance antigen-specific antibody sequences in the repertoire cannot be identified directly without significant additional effort.

In case of rapidly spreading emerging diseases such as Ebola, rapid and robust diagnostics are critical for treatment and disease control. For Ebola in particular, validated PCR based assays suitable for field work in third world countries are not

available. Highly sensitive antibody based immunodiagnostics are extremely important and easy to implement (Towner et al., 2008). However, a dearth of monoclonal antibodies for emergent Ebolaviruses limits the ability to use antigen-capture technologies for viral identification of early-stage infections. The panel of antibodies identified and characterized here should be useful for diagnostic applications that aim to identify Reston Ebola. By using multiplex immunoassay platforms such as the Luminex MagPlex® technology, it should be possible to multiplex up to 50 different antibodies with varying specificities for a broad range of epitopes, thus ensuring wide coverage of Ebolaviruses variants. Studies to incorporate the antibodies we have described here onto the Luminex MagPlex® diagnostic platform for field applications are on-going.

METHODS

VLP Production and Characterization

VLPs were produced by co-transfection of HEK293FT (Invitrogen) cells with plasmids encoding the three major virus structural proteins, NP, VP40 and GP. All open reading frames for virus structural proteins were obtained from NCBI and were codon optimized for mammalian cell expression using Gene Designer (DNA 2.0), synthesized (Epoch Life Science) and inserted into either pcDNA3 (for Ebola GP) or pCAGGS (all other genes) mammalian expression plasmids. Cells were transfected with each of 5 ug NP, 5 ug VP40 and 1 ug GP encoding plasmids by the calcium chloride/BES transfection method. After 24 h cells were washed with DMEM, which was replaced with DMEM

containing 10% (v/v) FBS. After an additional 24 h, the culture supernatant was collected and clarified by centrifugation at 3750 rpm for 30 min at 4ºC to remove cell debris. The supernatants were then overlaid onto a 5 mL 20% (w/v) sucrose cushion in 20 mM NaCl, 20 mM HEPES, pH 7.4 in an SW28 ultracentrifuge tube (Beckman). The VLPs were then pelleted by centrifugation at 28,000 rpm for 2 h at 4ºC in an SW28 rotor. To further purify VLPs, the pellet was resuspended in PBS and overlaid onto a 20 to 60% sucrose step gradient (5% increments) in 20 mM NaCl, 20 mM HEPES, pH 7.4 in a SW55 rotor tube (Beckman). The gradient was centrifuged at 38,000 rpm for 2 h at 4ºC after which an opaque band corresponding to VLPs was visible. Fractions were collected corresponding to the band as well as directly above and below it and analyzed by SDS-PAGE, staining for total protein with Krypton stain (Thermo Scientific) as well as immunoblotting. The middle fraction containing the peak of the VLPs was stored at -80°C until required. For immunoblotting, proteins were transferred to nitrocellulose membranes and stained using broadly reactive polyclonal antibodies against GP (gift from Dr. Andrew Hayhurst, Texas Biomedical Research Inst.), VP40 (gift from Dr. Ricardo Carrion, Texas Biomedical Research Inst.) or NP (IBT Bioservices). A specific monoclonal antibody against Zaire Ebolavirus GP was also used (4F3, IBT Bioservices). Appropriate secondary antibodies were purchased from LiCor Biosciences. Blots were imaged using a LiCor Odyssey SA imager. Electron microscopy of VLPs was performed at the University of Texas Health Sciences Center, San Antionio, Department of Pathology electron microscopy facility. VLPs were adhered to copper grids. The samples

were fixed in glutaraldehyde and osmium tetroxide was used as contrast agent. Images were captured on a Philips 208S digital imaging electron transmission microscope.

Immunizations and Serum Titer Determination

The study was approved by the University of Texas Institutional Animal Care and Use Committee (AUP-2013-00015). All animal experiments were carried out in accordance with the approved protocol. VLPs in PBS pH 7.4 were emulsified in a 1:1 ratio with TiterMax Gold adjuvant (Sigma). For footpad immunizations, 20 μL (containing a total of 5 g VLPs) antigen/adjuvant mixture was injected into the subcutaneous space of three BALB/c mice; for lateral hock injections, up to 50 μL was injected into the subcutaneous space just proximal to the lateral aspect of the ankle. Mice were immunized at footpad on day 0 for primary immunizations, and in the lateral hock on days 21, 35, and 77 for secondary immunizations. At days 10, 28, and 42 mice were bled for titration of the antigen-specific response. In order to determine serum antibody titer, mice were restrained in a tube restrainer, the tail wiped with isopropyl alcohol, and small incisions made with a fresh scalpel blade to nick the tail vein. 20-50 μL blood was obtained and allowed to coagulate at room temperature (RT) for 30 min, followed by centrifugation at 13,000 g for 15 min to pellet the clot. The serum was then used for ELISA assays. High binding ELISA plates (Corning) were coated overnight (O/N) at 4°C with 50 μL of 4 μg/mL Zaire Ebolavirus VLPs in PBS pH 7.4. Antigen solution was decanted and plates were then blocked at RT for 2 h in 2% milk (w/v) in PBS. Blocking

solution was then decanted and plates were then incubated with 50 μL of serum diluted three-fold from 1:100 to 1:218,700 in 2% milk (w/v) in PBS for 1 h. Plates were then aspirated and washed 3 times with PBS containing 0.05% tween-20 (PBST), then incubated with 50 μL of 1:5000 diluted goat anti-mouse HRP secondary antibody (Jackson ImmunoResearch) for 1 h. Plates were washed 3 times with PBST, and incubated with 50 μL TMB-Ultra (Thermo Scientific) for 15 min. The reaction was quenched with 50 μL 2 M H_2SO_4 and absorbance was read at 450 nm on a Tecan M200 plate reader.

Tissue Collection, Cell Isolation, and Subtype Purification

After determination of significant titer for Ebolavirus VLPs (signal evident above background at dilution > 1:10,000), mice were administered a final boost at day 77, and lymph nodes were collected 6 days later. For lymph nodes collection, mice were injected with 5-10 μL of 2% Evans Blue (Sigma) in PBS into the footpad. 30 min post-injection, mice were sacrificed by carbon dioxide asphyxiation followed by cervical dislocation. The skin and fur around the leg was removed to reveal the blue-stained popliteal lymph node (**Fig. 3.1a**), located just behind the knee. The lymph node was isolated and and stored in PBS pH 7.4 supplemented with 0.1% (w/v) BSA, 2 mM EDTA in a 6-well plate (Corning). Lymph node was homogenized by mechanical disruption using two 18G needles. The cells were then passed through a 70 μm cell strainer (Corning), with additional disruption using the plunger from a 3 mL syringe to aid passage of single cells.

Cells were then spun down at 500 g for 10 min in a swinging bucket rotor. The cell pellets were then resuspended in 2 mL red blood cell lysis buffer (155 mM NH_4Cl, 12 mM $NaHCO_3$, 0.1 mM EDTA) and incubated at room temperature for 3.5 min. The lysis reaction was quenched by adding 20 mL PBS buffer followed by centrifugation at 500 g for 10 min at RT. Cells were washed again with 5 mL PBS buffer and resuspended in a final volume of 1 mL buffer. Plasma cells were then isolated using the Miltenyi Plasma Cell Isolation kit (Miltenyi Biotec). Briefly, non-plasma cells were depleted by magnetic labeling of CD49b and CD45R followed by enrichment of magnetically-labeled $CD138^+$ cells. CD45R is a pan-B cell marker expressed on naïve and activated B lymphocytes, but not on antibody-secreting cells. Conversely, CD138 is expressed on pre-B and immature B-lymphocytes in the bone marrow, lost upon emigration into secondary lymphoid tissues, and re-expressed upon differentiation into plasma cells.

Single Cell V_H:V_L Sequencing

Sorted cells were analyzed by single B cell V_H:V_L sequencing as previously described (DeKosky et al., 2013). Briefly, single cells were isolated into 125 pL wells printed in PDMS along with poly(dT) conjugated magnetic beads. Cell lysis and capture of mRNA was performed *in situ*, and beads were collected and emulsified to serve as template for emulsion overlap extension RT-PCR. A follow-up nested PCR resulted in 850 bp amplicons containing linked genetic information for V_H and V_L genes. 850 bp amplicons were analyzed using the Illumina MiSeq 2x250 platform. V_H and V_L genes

were amplified separately for full-length V_H and V_L analysis using the Illumina MiSeq platform as previously described (DeKosky et al., 2013).

Sequence Analysis

Raw MiSeq data was analyzed as previously described (DeKosky et al., 2013). Briefly, raw data were filtered for a minimum Phred quality score of 20 over 50% of nucleotides to ensure high read quality in the CDR3 regions of heavy and light genes. Sequence data were submitted to the IMGT information system for V-D-J germline gene mapping. Sequences were filtered for in-frame V-D-J junctions and V_H:V_L pairs were compiled by exact CDRH3:CDRL3 nucleotide match. CDRH3 junction nucleotide sequences were clustered to 96% identity and resulting clusters with >=2 V_H:V_L reads were ranked by MiSeq read counts (DeKosky et al., 2013). Due to read length limitations of current next-generation sequencing technology, the complete V_H and V_L genes were also sequenced and analyzed separately. Full-length V_H and V_L genes were filtered for a minimum Phred quality score of 20 over 50% of nucleotides and were compiled by CDRH3 and CDRL3 exact nucleotide match. Consensus sequences of V_H and V_L genes (i.e. from all reads passing quality filters and that contained exact matches to the CDRH3:CDRL3 pair of interest) were used for antibody gene synthesis, expression, and *in vitro* analysis (DeKosky et al., 2013).

IgG Synthesis, Expression, and Purification

Consensus V_H and V_L genes were designed and purchased as gBlocks (Integrated DNA Technologies) and cloned into the pcDNA3.4 vector (Invitrogen) containing *Oryctolagus cuniculus* IgG leader peptide as fusions to human IgG1 and kappa constant regions, respectively. Sequences of both the heavy and the light chain for each antibody variant were confirmed by Sanger sequencing. Plasmids for each antibody variant were transfected into Expi293 cells (Invitrogen) at a 1:3 heavy:light ratio. After incubating at 37°C with 8% CO_2 at 125 rpm for 6 days, the supernatant containing secreted antibodies was collected by centrifugation at 500 g for 15 min at 25°C. Supernatant was passed over a column of 0.5 mL Protein A agarose resin (Thermo Scientific) three times to ensure efficient binding. After washing with 20 column volumes of PBS, antibodies were eluted with 3 mL 100 mM citric acid pH 3.0 and immediately neutralized with 500 μL 1M Tris pH 8.0. Antibodies were buffer exchanged into PBS, pH 7.4 utilizing Amicon Ultra-30 centrifugal spin columns (Millipore) for storage and subsequent use.

ELISA

Costar 96-well ELISA plates (Corning) were coated with 50 μL of 4 μg/mL recombinant Ebola Glycoprotein (a gift from Dr. Erica O. Saphire, The Scripps Research Institute) or Ebola virus VLPs. The coated plates were incubated at 4°C O/N, after which

they were decanted and blocked with 2% milk in PBS for 2 h at RT. After blocking, 1:5 serially diluted antibodies were applied to the plates for 1h, after which 1:5000 diluted donkey anti-human IgG HRP-conjuated secondary antibodies were applied (Jackson ImmunoResearch) for 1 h. For detection, 50 μL TMB-Ultra substrate was applied for 15 min before quenching with 50 μL 2 M H_2SO_4. Absorbance was measured at 450 nm using a Tecan M200 plate reader. Data were analyzed and fitted for EC_{50} using a 4-parameter logistic nonlinear regression model in the Prism software. The 4-parameter equation used was: Y=Max + ((Min-Max)/(1+(X/EC50)^HillSlope)). To ensure accuracy, curves were also fit using the hyperbola equation: Y = Max + (min-max)/(1+X/Kd)

ACKNOWLEDGEMENTS

We would like to thank C. Das for aid in antibody expression, Dr. G. Ippolito for insightful advice and critical reading of the manuscript, and Dr. C. Lee for help with SPR experiments. We also thank Dr. E. O. Saphire for providing recombinant Ebola virus GP. This study was supported by the National Institute of Allergy and Infectious Diseases of the National Institutes of Health under Award Number R01AI096228 (A.L.A.) and by the Defense Threat Reduction Agency grant HDTRA1-12-C-0105 and HDTRA1-12-C-007. O.I.L. was funded by NIH CORE funding NIH 1K12GM102745.

Robert Davey's group build and contributed the VLP's used in the immunizations for this study. This work was adapted with permission from Wang B, Kluwe CA, Lungu OI, DeKosky BJ, Kerr SA, Johnson EL, Jung J, Rezigh AB, Carroll SM, Reyes AN, Bentz JR, Villanueva I, Altmam AL, Davey RA, Ellington AD & Georgiou G. Facile Discovery of a Diverse Panel of Anti-Ebola Virus Antibodies by Immune Repertoire Mining. Scientific Reports. Nature Publishing Group; 2015;5: 13926. doi:10.1038/srep13926

REFERENCES

Baize, S., Pannetier, D., Oestereich, L., Rieger, T., Koivogui, L., Magassouba, N., Soropogui, B., Sow, M.S., Keïta, S., De Clerck, H., Tiffany, A., Dominguez, G., Loua, M., Traoré, A., Kolié, M., Malano, E.R., Heleze, E., Bocquin, A., Mély, S., Raoul, H., Caro, V., Cadar, D., Gabriel, M., Pahlmann, M., Tappe, D., Schmidt-Chanasit, J., Impouma, B., Diallo, A.K., Formenty, P., Van Herp, M., Günther, S., 2014. Emergence of Zaire Ebola Virus Disease in Guinea. http://dx.doi.org/10.1056/NEJMoa1404505 371, 1418–1425. doi:10.1056/NEJMoa1404505

Bowen, E., Lloyd, G., Harris, W.J., Platt, G.S., 1977. Viral haemorrhagic fever in southern Sudan and northern Zaire: preliminary studies on the aetiological agent. The Lancet.

Bradbury, A.R.M., Sidhu, S., Dübel, S., McCafferty, J., 2011. Beyond natural antibodies: the power of in vitro display technologies. Nat Biotechnol 29, 245–254. doi:10.1038/nbt.1791

Carette, J.E., Raaben, M., Wong, A.C., Herbert, A.S., Obernosterer, G., Mulherkar, N., Kuehne, A.I., Kranzusch, P.J., Griffin, A.M., Ruthel, G., Cin, P.D., Dye, J.M., Whelan, S.P., Chandran, K., Brummelkamp, T.R., 2011. Ebola virus entry requires the cholesterol transporter Niemann-Pick C1. Nature 477, 340–343. doi:10.1038/nature10348

Carroll, S.A., Towner, J.S., Sealy, T.K., McMullan, L.K., Khristova, M.L., Burt, F.J., Swanepoel, R., Rollin, P.E., Nichol, S.T., 2013. Molecular evolution of viruses of the family Filoviridae based on 97 whole-genome sequences. J. Virol. 87, 2608–2616.

doi:10.1128/JVI.03118-12
Chen, G., Koellhoffer, J.F., Zak, S.E., Frei, J.C., Liu, N., Long, H., Ye, W., Nagar, K., Pan, G., Chandran, K., Dye, J.M., Sidhu, S.S., Lai, J.R., 2014. Synthetic Antibodies with a Human Framework That Protect Mice from Lethal Sudan Ebolavirus Challenge. ACS Chem. Biol. 9, 2263–2273. doi:10.1021/cb5006454
Corti, D., Voss, J., Gamblin, S.J., Codoni, G., Macagno, A., Jarrossay, D., Vachieri, S.G., Pinna, D., Minola, A., Vanzetta, F., Silacci, C., Fernandez-Rodriguez, B.M., Agatic, G., Bianchi, S., Giacchetto-Sasselli, I., Calder, L., Sallusto, F., Collins, P., Haire, L.F., Temperton, N., Langedijk, J.P.M., Skehel, J.J., Lanzavecchia, A., 2011. A neutralizing antibody selected from plasma cells that binds to group 1 and group 2 influenza A hemagglutinins. Science 333, 850–856. doi:10.1126/science.1205669
DeKosky, B.J., Ippolito, G.C., Deschner, R.P., Lavinder, J.J., Wine, Y., Rawlings, B.M., Varadarajan, N., Giesecke, C., Dörner, T., Andrews, S.F., Wilson, P.C., Hunicke-Smith, S.P., Willson, C.G., Ellington, A.D., Georgiou, G., 2013. High-throughput sequencing of the paired human immunoglobulin heavy and light chain repertoire. Nat Biotechnol 31, 166–169. doi:10.1038/nbt.2492
Dias, J.M., Kuehne, A.I., Abelson, D.M., Bale, S., Wong, A.C., Halfmann, P., Muhammad, M.A., Fusco, M.L., Zak, S.E., Kang, E., Kawaoka, Y., Chandran, K., Dye, J.M., Saphire, E.O., 2011. A shared structural solution for neutralizing ebolaviruses. Nature Structural & Molecular Biology 18, 1424–1427. doi:10.1038/nsmb.2150
Feldmann, H., Nichol, S.T., Klenk, H.-D., Peters, C.J., Sanchez, A., 1994. Characterization of Filoviruses Based on Differences in Structure and Antigenicity of the Virion Glycoprotein. Virology 199, 469–473. doi:10.1006/viro.1994.1147
Ghosh, S., Campbell, A.M., 1986. Multispecific monoclonal antibodies. Immunology Today 7, 217–222. doi:10.1016/0167-5699(86)90108-8
Gire, S.K., Goba, A., Andersen, K.G., Sealfon, R.S.G., Park, D.J., Kanneh, L., Jalloh, S., Momoh, M., Fullah, M., Dudas, G., Wohl, S., Moses, L.M., Yozwiak, N.L., Winnicki, S., Matranga, C.B., Malboeuf, C.M., Qu, J., Gladden, A.D., Schaffner, S.F., Yang, X., Jiang, P.-P., Nekoui, M., Colubri, A., Coomber, M.R., Fonnie, M., Moigboi, A., Gbakie, M., Kamara, F.K., Tucker, V., Konuwa, E., Saffa, S., Sellu, J., Jalloh, A.A., Kovoma, A., Koninga, J., Mustapha, I., Kargbo, K., Foday, M., Yillah, M., Kanneh, F., Robert, W., Massally, J.L.B., Chapman, S.B., Bochicchio, J., Murphy, C., Nusbaum, C., Young, S., Birren, B.W., Grant, D.S., Scheiffelin, J.S., Lander, E.S., Happi, C., Gevao, S.M., Gnirke, A., Rambaut, A., Garry, R.F., Khan, S.H., Sabeti, P.C., 2014. Genomic surveillance elucidates Ebola virus origin and transmission during the 2014 outbreak. Science 345, 1369–1372. doi:10.1126/science.1259657
Gleichmann, H., 1981. Studies on the mechanism of drug sensitization: T-cell-dependent popliteal lymph node reaction to diphenylhydantoin. Clin. Immunol. Immunopathol. 18, 203–211.
Hood, C.L., Abraham, J., Boyington, J.C., Leung, K., Kwong, P.D., Nabel, G.J., 2010.

Biochemical and structural characterization of cathepsin L-processed Ebola virus glycoprotein: implications for viral entry and immunogenicity. Journal of virology 84, 2972–82. doi:10.1128/JVI.02151-09

Kamala, T., 2007. Hock immunization: a humane alternative to mouse footpad injections. J. Immunol. Methods 328, 204–214. doi:10.1016/j.jim.2007.08.004

Koellhoffer, J.F., Chen, G., Sandesara, R.G., Bale, S., Ollmann Saphire, E., Chandran, K., Sidhu, S.S., Lai, J.R., 2012. Two Synthetic Antibodies that Recognize and Neutralize Distinct Proteolytic Forms of the Ebola Virus Envelope Glycoprotein. ChemBioChem 13, 2549–2557. doi:10.1002/cbic.201200493

Kondratowicz, A.S., Lennemann, N.J., Sinn, P.L., Davey, R.A., Hunt, C.L., Moller-Tank, S., Meyerholz, D.K., Rennert, P., Mullins, R.F., Brindley, M., Sandersfeld, L.M., Quinn, K., Weller, M., McCray, P.B., Chiorini, J., Maury, W., 2011. T-cell immunoglobulin and mucin domain 1 (TIM-1) is a receptor for Zaire Ebolavirus and Lake Victoria Marburgvirus. Proc. Natl. Acad. Sci. U.S.A. 108, 8426–8431. doi:10.1073/pnas.1019030108

Köhler, G., Milstein, C., 1975. Continuous cultures of fused cells secreting antibody of predefined specificity. Nature 256, 495–497. doi:10.1038/256495a0

Lane, D., Koprowski, H., 1982. Molecular recognition and the future of monoclonal antibodies. Nature 296, 200–202. doi:10.1038/296200a0

Le Guenno, B., Formenty, P., Wyers, M., Gounon, P., Walker, F., Boesch, C., 1995. Isolation and partial characterisation of a new strain of Ebola virus. The Lancet 345, 1271–1274. doi:10.1016/S0140-6736(95)90925-7

Lin, G., Simmons, G., Pöhlmann, S., Baribaud, F., Ni, H., Leslie, G.J., Haggarty, B.S., Bates, P., Weissman, D., Hoxie, J.A., Doms, R.W., 2003. Differential N-linked glycosylation of human immunodeficiency virus and Ebola virus envelope glycoproteins modulates interactions with DC-SIGN and DC-SIGNR. J. Virol. 77, 1337–1346. doi:10.1128/JVI.77.2.1337-1346.2003

Maruyama, T., Rodriguez, L.L., Jahrling, P.B., Sánchez, A., Khan, A.S., Nichol, S.T., Peters, C.J., Parren, P.W., Burton, D.R., 1999. Ebola virus can be effectively neutralized by antibody produced in natural human infection. J. Virol. 73, 6024–6030.

Miranda, M.E.G., Miranda, N.L.J., 2011. Reston ebolavirus in humans and animals in the Philippines: a review. J Infect Dis. 204 Suppl 3, S757–60. doi:10.1093/infdis/jir296

Parren, P.W.H.I., Geisbert, T.W., Maruyama, T., Jahrling, P.B., Burton, D.R., 2002. Pre- and postexposure prophylaxis of Ebola virus infection in an animal model by passive transfer of a neutralizing human antibody. J. Virol. 76, 6408–6412. doi:10.1128/JVI.76.12.6408-6412.2002

Qiu, X., Alimonti, J.B., Melito, P.L., Fernando, L., Ströher, U., Jones, S.M., 2011. Characterization of Zaire ebolavirus glycoprotein-specific monoclonal antibodies. Clinical Immunology 141, 218–227. doi:10.1016/j.clim.2011.08.008

Qiu, X., Wong, G., Audet, J., Bello, A., Fernando, L., Alimonti, J.B., Fausther-Bovendo, H., Wei, H., Aviles, J., Hiatt, E., Johnson, A., Morton, J., Swope, K., Bohorov, O.,

Bohorova, N., Goodman, C., Do Kim, Pauly, M.H., Velasco, J., Pettitt, J., Olinger, G.G., Whaley, K., Xu, B., Strong, J.E., Zeitlin, L., Kobinger, G.P., 2014. Reversion of advanced Ebola virus disease in nonhuman primates with ZMapp. Nature. doi:10.1038/nature13777

Ravel, G., Descotes, J., 2005. Popliteal lymph node assay: facts and perspectives. J Appl Toxicol 25, 451–458. doi:10.1002/jat.1072

Reddy, S.T., Ge, X., Miklos, A.E., Hughes, R.A., Kang, S.H., 2010. Monoclonal antibodies isolated without screening by analyzing the variable-gene repertoire of plasma cells. Nature.

Reddy, S.T., Swartz, M.A., Hubbell, J.A., 2006. Targeting dendritic cells with biomaterials: developing the next generation of vaccines. Trends in Immunology 27, 573–579. doi:10.1016/j.it.2006.10.005

Saggy, I., Wine, Y., Shefet-Carasso, L., Nahary, L., Georgiou, G., Benhar, I., 2012. Antibody isolation from immunized animals: comparison of phage display and antibody discovery via V gene repertoire mining. Protein Eng. Des. Sel. 25, 539–549. doi:10.1093/protein/gzs060

Team, W.E.R., 2014. Ebola Virus Disease in West Africa — The First 9 Months of the Epidemic and Forward Projections. http://dx.doi.org/10.1056/NEJMoa1411100 371, 1481–1495. doi:10.1056/NEJMoa1411100

Towner, J.S., Sealy, T.K., Khristova, M.L., Albariño, C.G., Conlan, S., Reeder, S.A., Quan, P.-L., Lipkin, W.I., Downing, R., Tappero, J.W., Okware, S., Lutwama, J., Bakamutumaho, B., Kayiwa, J., Comer, J.A., Rollin, P.E., Ksiazek, T.G., Nichol, S.T., 2008. Newly Discovered Ebola Virus Associated with Hemorrhagic Fever Outbreak in Uganda. PLoS Pathogens 4, e1000212. doi:10.1371/journal.ppat.1000212

Van Regenmortel, M.H.V., 2014. Specificity, polyspecificity, and heterospecificity of antibody-antigen recognition. J. Mol. Recognit. 27, 627–639. doi:10.1002/jmr.2394

Walker, L.M., Huber, M., Doores, K.J., Falkowska, E., Pejchal, R., Julien, J.-P., Wang, S.-K., Ramos, A., Chan-Hui, P.-Y., Moyle, M., Mitcham, J.L., Hammond, P.W., Olsen, O.A., Phung, P., Fling, S., Wong, C.-H., Phogat, S., Wrin, T., Simek, M.D., Protocol G Principal Investigators, Koff, W.C., Wilson, I.A., Burton, D.R., Poignard, P., 2011. Broad neutralization coverage of HIV by multiple highly potent antibodies. Nature 477, 466–470. doi:10.1038/nature10373

Walker, L.M., Phogat, S.K., Chan-Hui, P.-Y., Wagner, D., Phung, P., Goss, J.L., Wrin, T., Simek, M.D., Fling, S., Mitcham, J.L., Lehrman, J.K., Priddy, F.H., Olsen, O.A., Frey, S.M., Hammond, P.W., Protocol G Principal Investigators, Kaminsky, S., Zamb, T., Moyle, M., Koff, W.C., Poignard, P., Burton, D.R., 2009. Broad and potent neutralizing antibodies from an African donor reveal a new HIV-1 vaccine target. Science 326, 285–289. doi:10.1126/science.1178746

Wu, X., Yang, Z.-Y., Li, Y., Hogerkorp, C.-M., Schief, W.R., Seaman, M.S., Zhou, T., Schmidt, S.D., Wu, L., Xu, L., Longo, N.S., McKee, K., O'Dell, S., Louder, M.K., Wycuff, D.L., Feng, Y., Nason, M., Doria-Rose, N., Connors, M., Kwong, P.D.,

Roederer, M., Wyatt, R.T., Nabel, G.J., Mascola, J.R., 2010. Rational Design of Envelope Identifies Broadly Neutralizing Human Monoclonal Antibodies to HIV-1. Science 329, 856–861. doi:10.1126/science.1187659

Chapter 4: Identification of Norovirus Vaccine Specific CDR3s

INTRODUCTION

Vaccine development is an empirical process, governed by response rates, efficacy studies, side effects, the duration of protection, and data gleaned experimentally from large, longitudinal clinical studies. However, the current paradigm provides limited insights into the molecular mechanism(s) governing protective immunity and is inadequate for responding to newly emerging or rapidly evolving pathogens. A major goal in vaccinology is to develop molecular metrics of vaccine responsiveness and efficacy. This in turn requires precise knowledge of the identity, functionality and persistence of the antigen-specific circulating antibodies and B-cells induced by vaccination.

Human Noroviruses (HuNoVs) cause ~85-96% of acute non-bacterial gastroenteritis, worldwide. Outbreaks occur in communities, family homes, recreational facilities, elderly care facilites, day care centers, schools, cruise ships, hospitals and in the military (Farkas et al., 2002), (Glass et al., 2000), (Ho et al., 1989), (Koopmans et al., 2000), (Koopmans, 2008). HuNoVs are transmitted via ingestion of fecally contaminated food and water, exposure to contaminated fomites, vomitus and direct person-to-person contact. It has also been recently reported that airborne transmission of the virus may be possible (Bonifait et al., 2015). HuNoVs cause ~23,000,000 infections, 50,000

hospitalizations, and 700^{+} fatal cases per year in the US (Mead et al., 1999). About 13% of infections result in post-infectious irritable bowel syndrome (Zanini et al., 2012). Worldwide, HuNoV infections cause ~200,000 deaths/yr, mostly in infants (Patel et al., 2009), (Patel et al., 2008) and are an important cause of severe gastroenteritis in the elderly (van Asten et al., 2011). HuNoV infections also cause about ~30-50% of travelers' diarrhea, persist for months in immunosuppressed people, and are Category B biodefense pathogens.

The HuNoV ~7.6 Kb single-stranded, plus-sensed RNA genome encodes 3 open reading frames (ORF): a 1738 amino acid (AA) replicase (ORF1), a major capsid protein of ~530 AA (ORF2: VP1), and a 212 AA minor capsid protein (ORF3: VP2) (Clarke et al., 2015), (Jiang et al., 1993). The Norovirus phylogeny is subdivided into five genogroups (GI-GV), the HuNoV GI and GII strains are ~50% different at the amino acid level (Zheng et al., 2006). The GI and GII strains are the only two genogroups that infect humans and they cause ~15% and ~85% of the recent outbreaks, respectively (Zheng et al., 2010). GI and GII are further subdivided into ~8 and ~19 genotypes, respectively, that differ at the amino acid level by at least ~30% in VP1(Donaldson et al., 2010), (Green et al., 2000). Highly epidemic GII.4 strains have caused six pandemics since 1997(Desai et al., 2012) and that genotype alone accounts for over 70% of infections (Vega et al., 2014).

Norovirus infection requires viral interactions with histoblood group antigens (HBGA), typically A, B, O, and lewis antigens that are either expressed on host mucosal

cells (Donaldson et al., 2010) or bacterial cells that are hypothesized be shuttling the virus into cells (Jones et al., 2014), (Karst and Wobus, 2015). Infection is specifically mediated by interactions between the viral VP1 surface epitope and the host HBGAs. Antibodies that bind VP1 and block HBGA interactions are associated with protective immune responses in mice, swine, chimpanzees and humans (Bok et al., 2011), (Chachu et al., 2008b), (Chachu et al., 2008a). Therefore a goal in HuNov vaccine development is to construct a vaccine that successfully induces the lasting production of antibodies that bind VP1 and prevent interactions between the virus and it's congnate HBGA.

A major goal in vaccinology is to develop molecular metrics of vaccine responsiveness and efficacy. This in turn requires precise knowledge of the identity, functionality, and persistence of the antigen-specific circulating antibodies and B-cells induced by vaccine. Information on the V gene repertoire encoded by antigen-specific B-cells is also necessary. Of particular importance is the complementary determining region of the antibody heavy chain (CDRH3). The CDRH3 lies at the center of the antigen binding site, is the most divergent in terms of sequence, and is usually the primary determinant of antibody specificity. Recent advances in high throughput DNA sequencing have enabled the in-depth determination of the V gene repertoire of B cell subsets in humans and animals (Ippolito et al., 2012), (Reddy et al., 2010), (Wang et al., 2015), (DeKosky et al., 2013) (McDaniel et al., 2016). We and others have developed a number of bioinformatics tools for the analysis of the V gene repertoire including germline gene assignment, somatic hypermutation (SHM) frequency, characterization of

the hypervariable complementarity-determining region 3 (CDR3) length in the BCR, and aa usage, etc.

Recently, a biotech company Ligocyte (acquired by Takada), conducted a prime/boost (Day 0, Day 28) dose escalation study in human volunteers to test a norovirus candidate vaccine (Treanor et al., 2014). Here we mine both the B-cell antibody sequence repertoire and the antibodies in serum from a trial volunteer to elucidate the composition of antigen-specific antibodies to the norovirus candidate vaccine.

Using serum and cell samples from a study donor we sought to identify the antigen specific antibodies elicited following vaccination. The goal was to determine the repertoire and relative level of circulating antibodies specific to HuNoV arose in response to the vaccine. The vaccine consisted of equal amounts of two types of HuNoV VLPs, GI.1 and GII.4C. GI.1 is derived from a naturally occurring strain of HuNoV GI.1. GII.4C is a chimera derived from 3 strains of HuNoV GII.4. The donor was vaccinated on Day 0 and boosted on Day 28 of the trial. Each injection consisted of a dose consisting of 5ug of each component VLP. Takeda provided us with three serum time points for this particular donor, Day 0, 7, and 21. Over those time points it was observed that that donor's serum was reactive to both vaccine strains and the polyclonal serum response rose after vaccination (Table 1, dataset from Takeda). Three separate serum tests, performed by Takeda and their collaborators, Pan-Ig, IgA, and IgG, show that the serum titers rose over time. Additionally, a carbohydrate blocking assay demonstrates that the

polyclonal response blocks GI.1 and GII.4 interactions with their cognate HBGAs at roughly the same titer levels as the IgA and IgG response. The carbohydrate assay is a proxy for the serums ability to neutralize viral infection as it establishes the serums ability to prevent of HuNoV VP1 interactions with HBGA (Reeck et al., 2010). From these assays it is clear that there are antibody species in the polyclonal response that both bind and neutralize HuNoV GI.1 and GII.4. A major goal of this research is to identify and characterize these antibodies.

	GI.1							
	Pan-Ig		IgA		IgG		Carbohydrate blocking	
Day	Titer	Fold Rise	Titer	Fold Rise	Titer	Fold Rise	Titer	Fold Rise
0	1280	1.0	3.133	1.0	4.232	1.0	12.5	1.0
7	163840	128.0	165.324	52.8	190.921	45.1	589	47.1
21	655360	512.0	108.143	34.5	368.354	87	638	51.0

	GII.4							
	Pan-Ig		IgA		IgG		Carbohydrate blocking	
Day	Titer	Fold Rise	Titer	Fold Rise	Titer	Fold Rise	Titer	Fold Rise
0	5120	1.0	10.410	1.0	16.255	1.0	12.5	1.0
7	40960	8	130.290	12.5	149.295	9.2	82.1	6.6
21	163840	32	116.114	11.2	364.4	22.4	180.3	14.4

Table 4.1 – Takeda Data from Donor 04NUR001.

Table 4.1 – Takeda Data from Donor 04NUR001.

Takeda performed assays to detect ELISAs to detect Pan-Ig by ELISA, assay describe here (Graham et al., 1994), and IgA and IgG by dissociation-enhanced lanthanide fluorescent immunoassay (DELFIA), assay described (Kavanagh et al., 2011). Carbohydrate blocking assays were done to determine neutralization efficiency (Reeck et al., 2010). A comprehensive analysis of all donors and time points was described (Treanor et al., 2014) . Data is shown from the 3 serum time points processed in this work, Day 0, 7, and 21.

We use a sequencing and proteomics approach (Figure 4.1) to identify the serum monoclonal antibodies that specifically interact with the vaccine and their relative abundance over time points. These approaches allow for the molecular deconvolution of the immune response. PBMC samples from the donor (Day 0, 7, 28, and 56) are used to determine the both the VH sequences of the cell repertoire present in circulating B-Cells as well as construct a VH:VL paired library that allows use to determine the complete variable region composition for an antibody of interest. Serum samples are processed over an antigen column to isolate the antigen specific antibodies. These antibodies are trypsinized and processed by LC-MS/MS. Peptide spectra are mapped against the VH sequences to determine which sequences code for the antigen specific peptides. (Lavinder et al., 2015), (Lavinder et al., 2014) (Wine et al., 2015), (Wine et al., 2013)

We find that a single antibody makes ups the majority of the response and over 100 antibodies are present that are specific to the GII.4C portion of the vaccine. In addition we see that approximately half of the GII.4C specific antibodies are present before vaccination and half arose in response to vaccination. Furthermore, amongst the top 10 VH sequences of interest, we find 8 of them present in the VH:VL paired data set and are able to identify their cognate light chain.

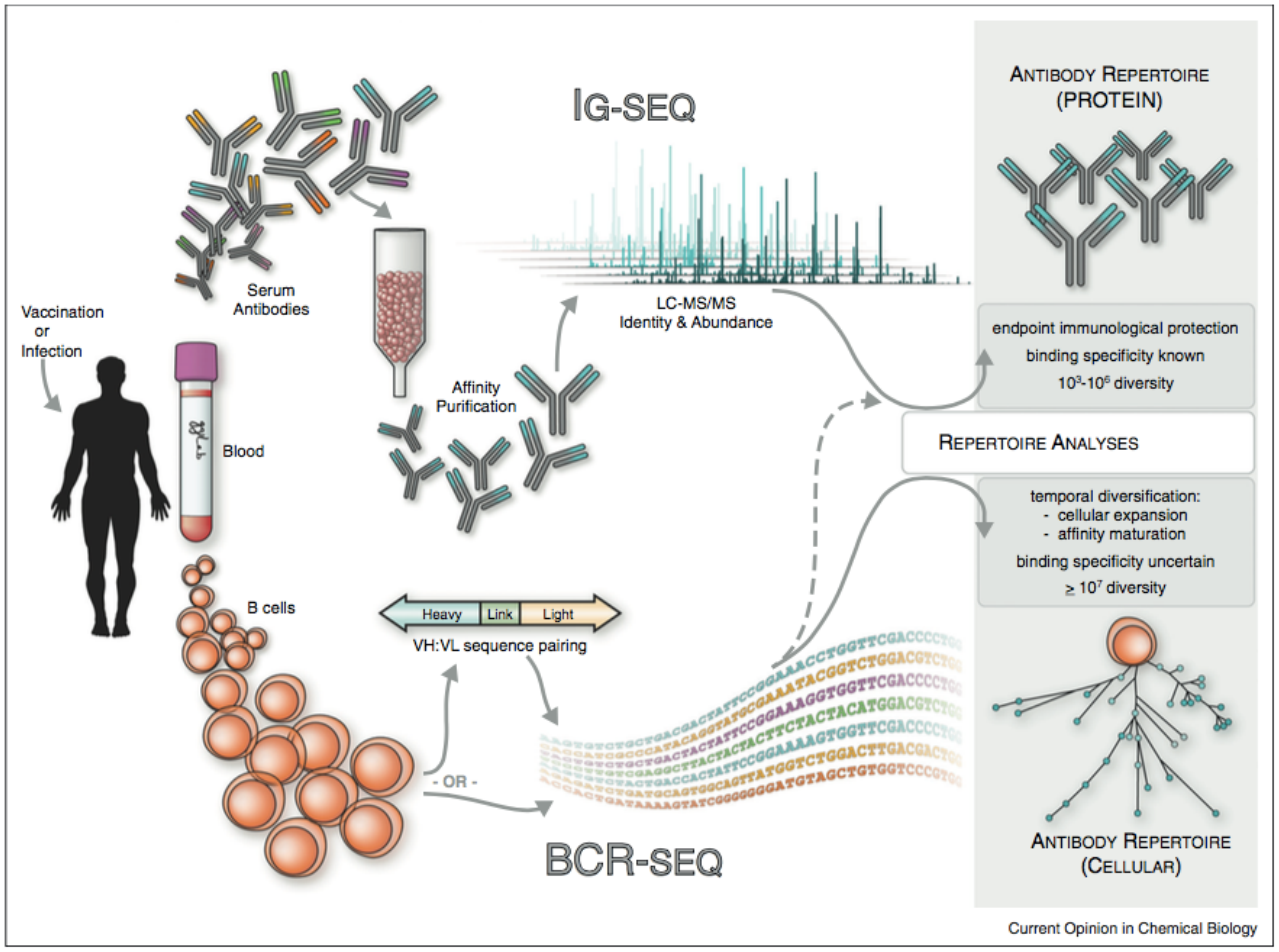

Figure 4.1 – Serum and B-Cell Pipeline

Antigen specific antibodies are isolated from serum and processed for mass spec. PBMC samples are split in half and processed for VH sequencing and VH:VL sequence pairing. The VH libraries are used to build the mass spec libraries and match sequences to unique antigen specific peptides. VH hits from the mass spec analysis are searched against the VH:VL databases to determine the full VH and VL sequences of antigen specific antibodies. Image adapted from (Lavinder et al., 2015)

METHODS

VH Sequencing

Prior to thawing cells, cell culture media and cell culture media with DNAse was pre-warmed in a 37°C water bath. Cell culture media is RPMI-1640 (Fisher) and 10% Fetal Bovine Serum (FBS). Cell culture media with DNAse is RPMI-1640-10% FBS and 20 U/ml of DNAse (Roche). Cells were thawed by gently swirly tube by hand in a 37°C water bath. Following thawing, cells were gently transferred to a 50 mL conical. While swirling the conical by hand, 1mL of cell culture media with DNAse was added dropwise. Cell culture media with DNAse was continually added and swirled until final suspension was 50 mL. Suspension was centrifuged at 300 G for 15 min. at room temperature (RT). Supernatant was removed until only cell pellet and ~500 uL remained. 3 mL of cell culture media (without DNAse) was added, cells were gently re-suspended, and were then incubated in a 37°C water bath for 30 min. Following incubation, 10 mLs of pre-chilled (4°C) FACS buffer (PBS ph7.2, 0.5% BSA, and 2mM EDTA, filter sterilized with 0.2 uM filter) was added to cells. Cell suspension was centrifuged at 300 G for 5 min at 4°C. Supernatant was removed and cells were suspended with FACS buffer to a final volume of 4 mLs. ½ of the cell sample was used to amplify the VH sequences and the other half was processed in order to determine VH:VL repertoire as described below. For the former, a portion of PBMCs (~5% of cells) were isolated and put into Triazol (Fisher) and stored at -80°C. The rest of the cell sample was used for

Fluorescently Activated Cell Sorting (FACS). For FACS, cells were spun down at 300 G for 5 min. and labeled. Labeling consisted of re-suspending cells in 100 uL of FACS buffer and adding: 40 uL of anti-CD20-FITC (BD Biosciences), 25 uL of anti-CD38-PE (BD Biosciences), 10 uL anti-CD3-PerCP-Cy5.5 (Biolegend), 40 uL anti-CD27-APC (BD Biosciences), and 20ul anti-CD19-V450 (BD Biosciences). Following addition of fluorophores, cells were incubated at RT in the dark for at least 20 min. with occasional agitation. Following labeling, cells were spun at 300 G for 5 min. and re-suspended in 1 mL of FACS buffer. Cells were sorted using an Aria FACS machine (BD-Biosciences). $CD3^-$, $CD19^+$, $CD27^+$, $CD20^+$, and $CD38^-$ memory B-cells and $CD3^-$, $CD19^+$, $CD27^+$, CD20-, and $CD38^+$ Plasma Blast B-cells were isolated. Isolated cells were sorted directly into Trizol (Fisher) and stored at -80°C.

RNA was extracted from the three cell populations (PBMC, Memory and Plasma Blasts) using an RNA-easy isolation kit, (Qiagen) and stored in at final volume of 25 uL at -80°C. 1^{st} strand cDNA was created according to manufactures protocol using Superscript II (Invitrogen), oligo dT primers and 8 uL of RNA. The VH portion of IgM and IgG sequences were amplified by PCR with the Faststart High Fidelity PCR system (Roche) in seperate PCR reactions. The primer set used was described in (Ippolito et al., 2012). Each reaction was 500 uL in total volume, 50 uL was used for a negative control reaction. 10 uL of cDNA was added to the remaining PCR mixture and the reaction was split over 8 PCR tubes. Thermal cycler conditions were as follows: 1 cycle of 95°C for 2 min.; 4 cycles of 92°C for 1 min, 50°C for 1 min, 72°C for 1 min; 4 cycles of 92°C for 1

min., 55°C for 1 min., 72°C for 1 min.; 26 cycles of 92°C for 1 min., 63 °C for 1 min., 72 °C for 1 min; and 1 cycle of 72°C for 7 min., followed by a final hold step at 4°C. PCR reactions were run on a 1% agarose gel and the proper bands (~400 bp) were cut out and gel purified (Zymo). For each sample, 100 ng was submitted for Illumina Mi-Seq sequencing.

VH:VL Pairing

Cells were thawed as described above and ½ were used for VH:VL processing. B-Cells were isolated from the PBMC population as follows. 15 mL of pre-chilled FACS buffer was added to the 2 mL PBMC suspension. Cell suspension was centrifuge at 300 G for 15 min at 4°C. Supernatant was removed and cells were gently re-suspended in 400 uL of pre-chilled FACS buffer. 100 uL Memory B-Cell Biotin-Antibody Cocktail (Miltenyi) was added to the cells and incubated at 4°C for 10 min. 300 uL of pre-chilled FACS buffer was added and then 200 uL of Anti-Biotin Microbeads (Miltenyi) were added. Suspension was incubated at 4°C for 15 min. Following incubation, 10 mLs of pre-chilled FACS buffer was added to the cell suspension. Cells were then centrifuged at 300 G for 10 min. at 4°C. Supernatant was cleared and cells were re-suspended in 500 uL of pre-chilled FACS buffer. Cells were then passed through a 70 uM strainer (Fisher). After straining, cells were passed through a magnetized LD column (Miltenyi) to remove non-B cells from the suspension. 1 mL of pre-chilled FACS buffer was flowed through the LD column 3x to insure collection of all the B-cells. B-cells were centrifuged at 300

G for 10 min. at 4°C. Supernatant was removed and cells were re-suspended in 1 mL of PBS. B-cells were then run through the flow focusing device as described (McDaniel et al., 2016). Briefly, emulsions were created that contain: a single B-cell, reagents to lyse the cell, and beads for capturing mRNA. Following mRNA bead capture, beads were isolated and re-emulsified with pairing primer sets, and the reagents for the RT-PCR amplification. The primer sets amplify and link VH sequences and VL sequences pairs such the the VH and VL from a single B-cell are linked together on the PCR product. DNA was purified and paired sequences were amplified by nested PCR to produce enough product for Illumina Mi-Seq sequencing. VH and VL only sequences were also amplified from the paired amplicons and submitted for each paired reaction in addition to the VH:VL paired amplification. Following sequencing, antibody sequences are processed for quality. VH:VL pairs are bio-informatically identified from the data sets wherein sequences with ≥90% CDRH3 sequence identity are binned into clusters (McDaniel et al., 2016).

Isolation of HuNoV specific antibodies from serum and sample processing for LC-MS/MS

An antigen column was set up at each serum time point. HuNoV VLP was added to 15 mLs of PBS and buffer exchanged using VivaSpin Turbo 15 10K molecular weight cut-off spin tubes (Sartorious), tube were centrifuged at 4000 G at 4°C for ~ 20 min. until volume was ~500uL. The process was repeated 2 more times for a total of 3 rounds of

buffer exchange. Following buffer exchange, 1 mg of VLPs were added to 250 mg of N-hydroxysuccinimide (NHS)-agarose beads (Thermo). Prior to VLP addition, NHS-agarose beads were hydrated with 2.5 mLs of PBS. The bead suspension was rotated end-over-end at 4°C overnight and then the beads were spun down and washed 2x with PBS. Unreacted NHS groups were blocked with 1M ethanolamine, pH 8.3, for 20 min at RT, washed with PBS, and packed into a 5 mL column (Thermo). Following column packing, conjugated VLPs were washed with 10 column volumes (CV) of 4M Urea in PBS. Column was then washed with 20 CVs of PBS. Serum underwent melon gel purification according to the manufactures standard protocol (Thermofisher) to isolate serum antibodies and remove albumin. Following melon gel purification, serum was run through the GII.4C column 5x by gravity flow to capture antigen specific antibodies. The column was washed with PBS 2x then washed with water 1x. Antigen specific antibodies were eluted from column with 1 mL of 5% formic acid. Elution was repeated 11x for a total of 12 elution fractions. 10 uL of each elution fraction was neutralized with 100ul of 25x PBS in 2% milk and used in the ELISA step described below to detect which fractions contained GII.4C specific antibodies. Elution fractions containing GII.4C specific fractions were combined, speed vacuumed to remove formic acid. Samples were suspended with 50 ul of water and re-speed vacuumed, this process was repeated 2-3x until pH was ~5.5. Following final speed vacuuming, samples were re-suspended into 50uL of 100mM Tris-pH 8.

The concentrated elution and 50ul from the flow through were processed for mass spec. 50 uL of trifluoroethanol was added to each sample. Samples were then reduced by adding 5 uL of 110 mM TCEP and incubated in the dark at 55° for 45 min. Then 3 uL of 550 mM idoacetamide was added and samples incubated for in the dark for 30 min. at RT to alkylate the cysteines. 892 uL of 50 mM Tris pH 8 with 2mM CaCl was added to each sample. Samples were then digested with 2 ug of trypsin for 5 hours at 37 degrees to produce peptide fragments. The reaction was quenched with 10 uL of 100% formic acid. Peptides were then bound to a C18 Hypersep SpinTip (Thermo), washed 3x with 0.1% formic acid, eluted with 60% acetonitrile, 0.1% formic acid, and submitted for LC-MS/MS mass spectrometry processing.

ELISA

ELISA was performed on all elutions, washes, and pre-flow through serum samples and confirmed that the column captured all GII.4C specific antibodies for each sample processed. Wells of the ELISA plate (Costar) were coated with 50 uL of GII.4C VLP at 4mg/ml overnight at 4°C. The next day the plate was washed 3x with 0.05% Tween-PBS. Wells were blocked with 5% Milk-PBS for at least 1 hr. at RT and washed again. Samples (elutions, flow through, washes, flow through, and melon gel purified serum) were incubated for at least 1 hour at RT and then wells were washed. 50ul 1:2000 Goat anti-human-IgG-HRP (Jackson Immune) was used as the secondary and was incubated in the well for at least 20 min. After a final wash, 50 ul of TMB Substrate

(Thermo) was added to each well and allowed to develop for 10-20 min. Reactions were then quenched with 50 uL of 2M H2SO4 and A450 readings were taken.

MS/MS Analysis

Samples were analyzed by liquid chromatography-tandem mass spectrometry on a Dionex Ultimate 3000 RSLCnano uHPLC system (Thermo Scientific) coupled to an LTQ Orbitrap Velos Pro mass spectrometer (Thermo Scientific). Peptides were first loaded onto an Acclaim PepMap RSLC NanoTrap column (Dionex; Thermo Scientific) prior to separation on a 75 μm×15 cm Acclaim PepMap RSLC C18 column (Dionex; Thermo Scientific) using a 5–40% (v/v) acetonitrile gradient over 250 min at 300 nl/min. Eluting peptides were injected directly into the mass spectrometer using a nano-electrospray source. The LTQ Orbitrap Velos Pro was operated in data-dependent mode with parent ion scans (MS1) collected at 60,000 resolutions. Monoisotopic precursor selection and charge state screening were enabled. Ions with charge ≥+2 were selected for collision-induced dissociation fragmentation spectrum acquisition (MS2) in the ion trap, with a maximum of 20 MS2 scans per MS1. Dynamic exclusion was active with a 45-s exclusion time for ions selected more than twice in a 30-s window. Each sample was run three times to generate technical replicate datasets.

Mass Spec Data Analysis

A database was created using quality processed VH sequences that had ≥2 reads. All cell types; PBMC, memory, plasma blast, and all time points; Day 0, Day 7, Day 28, and Day 56, were added to the database. The database was concatenated to a database of background proteins comprising of non-donor derived VL sequences (HD1 (Lavinder et al., 2014)), a consensus human protein database (Ensemble 73, longest sequence/gene), and a list of common protein contaminants (MaxQuant). Donor-specific spectra were searched against the corresponding donor-specific database using SEQUEST (Proteome Discoverer 1.4, Thermo). Searches considered fully-tryptic peptides only, allowing up to two missed cleavages. A precursor mass tolerance of 5 ppm and fragment mass tolerance of 0.5 Da were used. Modifications of carbamidomethyl cysteine (static) and oxidized methionine (dynamic) were selected. High-confidence peptide-spectrum matches (PSMs) were filtered at a false discovery rate of <1% as calculated by Percolator (q-value <0.01, Proteome Discoverer 1.4; Thermo Scientific).

Iso/Leu sequence variants were collapsed into single peptide groups. For each scan, PSMs were ranked first by posterior error probability (PEP), then q-value, and finally XCorr. Only unambiguous top-ranked PSMs were kept; scans with multiple top-ranked PSMs (equivalent PEP, q-value, and XCorr) were designated ambiguous identifications and removed. Observed precursor masses were recalibrated according to

the previous method (Cox et al., 2011), and the average mass deviation (AMD) for each peptide was calculated as described (Boutz et al., 2014) using data from elutions only. Peptides with an AMD >1.5 ppm were removed. Additionally, only peptides identified in all 3 replicate injections for at least one elution sample were kept as high-confidence identifications.

Peptide abundance was calculated from the extracted-ion chromatogram (XIC) peak area, as described (Lavinder et al., 2014), using peak area values generated by the Precursor Ions Area Detector node in Proteome Discoverer. For each peptide, a total XIC area was calculated as the sum of all unique XIC areas of associated precursor ions and the average XIC area across replicate injections was calculated for each sample. For each serum time point, peptides were only considered to be antigen specific if they were present in all three elution technical replicates and present in none of the three flow-through technical replicates.

Clonotype indexing and peptide-to-clonotype mapping

Full-length VH sequences were grouped into clonotypes based on single-linkage hierarchical clustering as described(Lavinder et al., 2014). Cluster membership required ≥90% identity across the CDR-H3 amino sequence as measured by edit distance. High-confidence peptides identified by MS/MS analysis were mapped to clonotype clusters, and peptides uniquely mapping to a single clonotype were considered “informative”.

Clonotype abundance was calculated using only informative peptides mapping to ≥4 amino acids of the CDR-H3 region, as a sum of XIC areas.

Quantitating abundances of serum antibodies

Relative abundance of each clonotype was calculated as the sum of XIC areas for the clonotype divided by the sum of all XIC areas in that sample. Fraction of serological repertoire refers to this relative abundance based on XIC. The amount of each clonotype is determined by multiplying its fraction of serological repertoire by the serum titer for the same sample.

Bioinformatics Analysis

CDRH3s from VH clonotypes identified as antigen specific in the serum analysis were used to search for CDRH3s in the VH:VL database by exact match. VH clonotypes and VH:VL sequences were isotyped using an in-house algorithm that searched the nucleotide sequence using isotype specific sequences and allowing for up to one mis-match. The search sequences used were: IgG-CCTCCACCAAGGGCCCATCGCAG; IgM- CCTCCACCAAGGGCCCATCGCAG; and IgA-CCTCCACCAAGGGCCCATCGCAG. IgG sequences for somatic hypermutation (SHM), CDRH3 length and CDRH3 hydrophobicity measurements were isotyoped from their respective time point databases using MiXCR (Bolotin et al., 2015). SHM was calculated by identifying the germline and counting the number of mismatches divided by the length of the VH gene. Hydrophobicity scores were calculated using the Kyte-

Doolittle hydrophobicity index. Box and whisker plots were built using the tool described here (Spitzer et al., 2014).

RESULTS

Identification of GII.4C specific clonotypes

A major limitation for developing the specific protocols to this experiment was the low volume of serum available from the clinical trial. For the donor analyzed, we processed serum samples from Day 0, Day 7, and Day 21 for which we had 2ml, 2ml, and 750ul of serum available respectively. As there was so little serum available we sought to focus our efforts on developing optimized processes for the purification of anti-HuNoV vaccine antibodies from small amounts of serum. We decided to use the limited serum available to determine the repertoire against GII.4C since the GII genogroup is so much more prevalent in terms of human infection.

Tryptic peptides from the 3 serum time points, Day 0, Day 7, and Day 21, were mapped against the VH clonotype data base. VH clonotypes consist of clusters of VH sequences that have 90% amino acid sequence in their CDRH3. A peptide is considered clonotype specific if it is unique to that clonotype and covers at least 4 amino acids of the CDR3 sequence in the MS/MS analysis. The number of unique GII.4C specific clonotypes identified rose in each time point; Day 0 had 57, Day 7 had 72, and Day has 90. Overall, when all serum time points are combined, 123 unique GII.4C clonotypes were identified. The fact that only 90 clonotypes of the 123 total clonotypes are present at

Day 21 suggests that 33 clonotypes seen at earlier points are not being induced by the vaccine and/or have fallen below the limit of detection (~4 ng/mL, (Wine et al., 2015)). The 57 clonotypes identified at Day 0 are considered to be pre-vaccine elicited and likely arose from prior natural infections, the rest arose in response to the vaccine.

The LC peak area (XIC) associated with each clonotype specific peptide was used to determine its abundance (Boutz et al., 2014). The XIC for each clonotype was calculated by adding the XIC from all of the peptides that map specifically to that clonotype. The relative abundance of each clonotype was calculated as the fraction of the clonotype XIC over the sum of all of the clonotypes XIC's in a given time point. The relative abundances of each clonotype at each time point are shown in Figure 4.2. Clonotypes that account for at least 1% of the overall response are shown in the figure 4.2 inset. A single clonotype, Clonotype 379, accounted for ~43% of the total response and was the dominant clonotype thorough out all 3 time points.

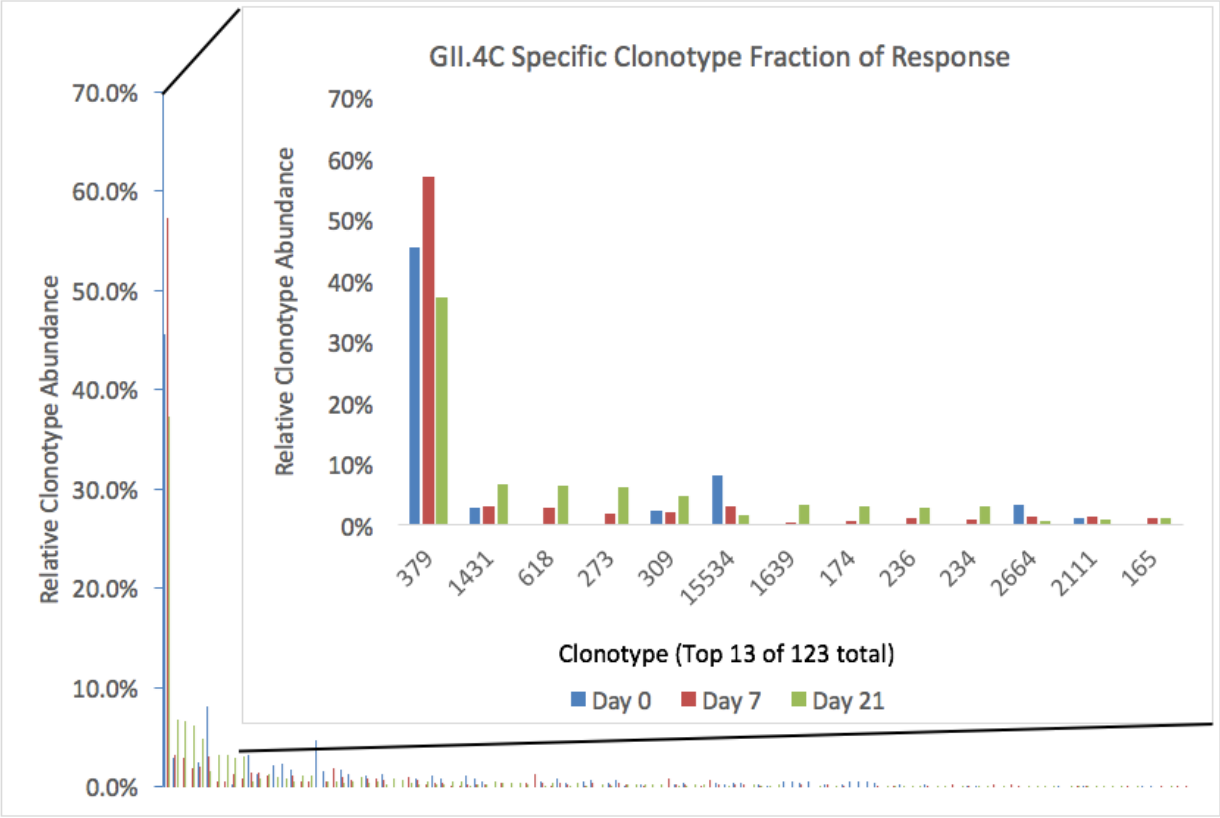

Figure 4.2- Relative Clonotype Abundance of GII.4C Specific Antibodies.

123 clonotypes were identified exclusively in the GII.4C column elution fractions. Relative clonotype abundance was calculated by dividing the mass spec peak area (XIC) for clonotype specific peptides by the overall sum of mass spec area (XIC) for the entire samples. Clonotypes are ranked according to their combined abundance over 3 time points. Clonotypes with >1% of total response are shown in the inset. ~50% of clonotypes are present in the Day 0 serum indicating that they were present prior to vaccination including clonotypes 379, 1431, 309, 15534, 236, 2664, and 2111 in the inset. ~50% of clonotypes arose in response to vaccination including clonotypes 618, 273, 1639, 174, 234, and 165 in the inset.

The polyclonal response in the donor's serum showed an ~20-fold increase in Day 21 titers compared to Day 0 in both the GII.4C IgG ELISA and Carbohydrate binding assays (Table 4.1). In order to determine if the results from the LC-MS/MS analysis correspond to the polyclonal result we calculated the abundance of the each clonotype to determine how much each one was represented in the response. Abundance for each clonotype at each time point was calculated by multiplying the relative abundance (calculated above) by the IgG serum titer for the corresponding time point found in Table 4.1. The results from this analysis are show in Figure 4.3. Many of the clonotypes identified have abundances that correspond to the serum IgG titer and carbohydrate blocking increases both at Day 7 and at Day 21. However, the abundance of the dominant clonotype at Day 21 is far greater, ~135-fold over Day 0, than the polyclonal serum data. This discrepancy suggests that the dominate clonotype may be over representative in the LC-MS/MS data or perhaps it is not specific to GII.4C and may have bound to some other element of the antigen column such as the agarose beads.

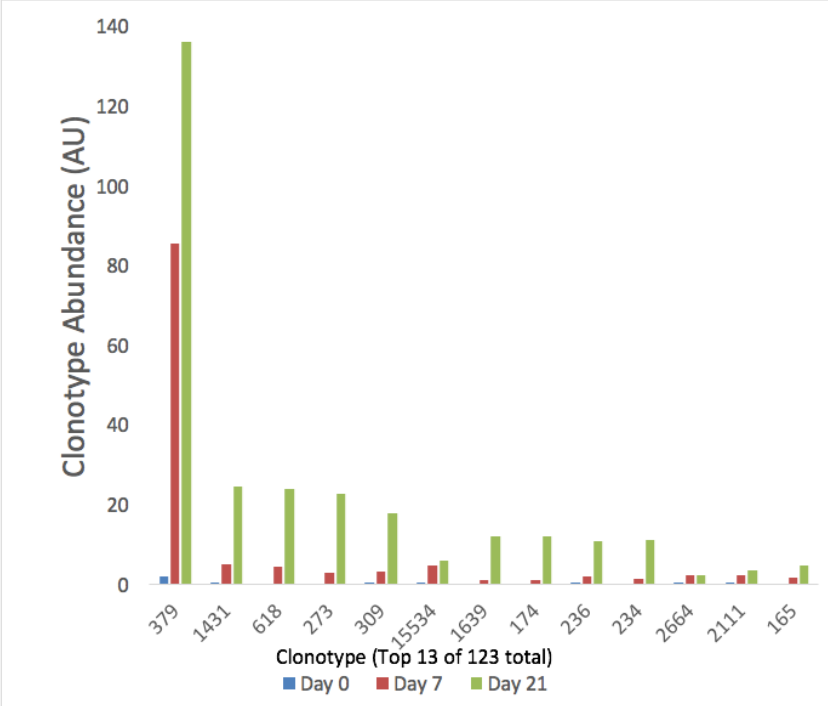

Figure 4.3 - Clonotype abundance of GII.4C Specific Antibodies

Clonotype abundance was calculated by multiplying the relative abundance, shown in figure 4.2, by the IgG serum titer at the corresponding time point from Table 4.1. The top 13 clonotypes are shown.

VH Repertoire

The VH sequence databases were analyzed to determine aspects related to diversity, gene usage and composition. The number of cells input for each time point considered, Day 0, Day 7, Day 28, and Day 56, was relatively consistent over time for each time point. The Table 4.2 shows the number of sequences, number of cells, and clonotypes derived from the VH data sets for each cell time point. The number of

clonotypes for the PBMC from Day 7 is considerably lower than the PBMC clonotypes found in the other time points, potentially due to a large expansion of vaccine specific B-cells that occurs around Day 7 following immune stimulation. Very few Plasma Blasts were recovered from the FACs analysis and interestingly the number of clonotypes identified exceeds the number of cells that were collect. This is likely due to over-sampling of the sequencing reads which increases the likelihood of a clonotype being called due to sequencing errors and PCR errors resulting from relatively low amounts of starting material.

VH Sequencing						
	Cell Type	Productive Sequences	# of Cells	Clonotypes		
				Total	IgG	IgM
Day 0	PBMC	1504013	250000	8590	263	6821
	Memory	220234	26109	5586	140	3230
	Plasma Blast	31428	114	1022	39	561
Day 7	PBMC	1350653	250000	1552	307	758
	Memory	232367	22140	5040	184	2790
	Plasma Blast	45472	389	743	64	270
Day 28	PBMC	522314	22000	3049	110	2705
	Memory	152326	26557	4627	133	3566
	Plasma Blast	62883	225	353	59	164
Day 56	PBMC	605972	250000	3169	80	2507
	Memory	181695	16104	2272	ND	1681

Table 4.2 – VH Sequencing and Clonotypes.

3 cell types were collected from each time point and VH's were processed for deep sequencing. A productive sequence has undergone quality processing, contains an antibody sequences, has no stop codons, and has an identifiable CDRH3. Clonotypes consist of sequences that have 90% CDRH3 sequence identity to one another. IgG and IgM were identified by searching for a constant region specific nucleotide sequence and allowing for one mismatch. ND = Not determined due to primer error.

The IgG clusters from the VH libraries from each time point (Day 0, Day 7, Day 28, and Day 56) as well as the GII.4C specific clonotypes were analyzed for different characteristics related to gene usage and their CDR3 regions. The time point data sets contain the VH data from all three cell types analyzed, PBMC, Memory, and Plasma Blasts. V-gene usage was calculated for each V-Gene family (Figure 4.4). V-Gene usage is fairly consistent over the 4 time points as well. In the GII.4C specific clonotypes, the V-gene usage mirrors the time point usage in the majority of V-genes. However, there are 6 V-genes in which the fraction of GII.4C specific clonotypes ≥3x the amount seen in the time point data sets. This suggests that V-genes; IGHV1-17, IGHV1-45, IGHV3-38, IGHV3-43, IGHV3-66, and IGHV4-4, code for antibody germlines predisposed to recognizing HuNorV GII.4C.

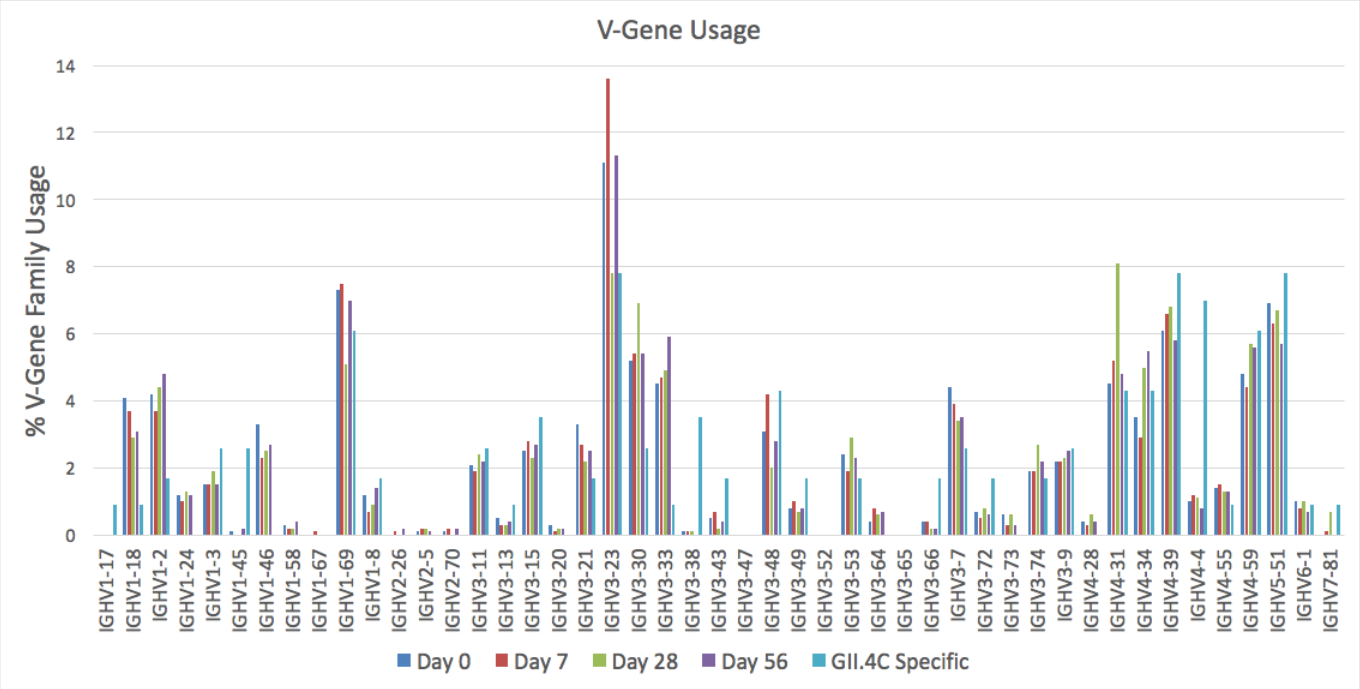

Figure 4.4 V-gene usage of IgG sequences time point and GII.4C specific clonotype data sets

V gene usage was calculated for each V-gene family. Each time point data set analyzed was composed of IgG isotypes from the VH sequence database from all three cell type processed at that time point. The GII.4C specific data set contains the clonotypes identified in the serum analysis.

CDRH3 composition can be informative as the CDRH3 peptide is usually found in the middle of the antigen binding site and typically contributes to the majority of the antigen binding. CDRH3 lengths for IgG clusters from each of the VH time point libraries and the GII.4C specific clonotypes were analyzed. We found that the CDRH3

length of the IgG coding cells does not vary over time and the GII.4C specific CDRH3 lengths are also consistent with the time point specific data (Figure 4.5). CDRH3 hydrophobicity was also determined, it was calculated using the Kyte-Doolittle hydrophobicity index. Average CDRH3 Hydrophobicity score was ~ -0.5 over all time points and the GII.4C specific clonotypes (Figure 4.6).

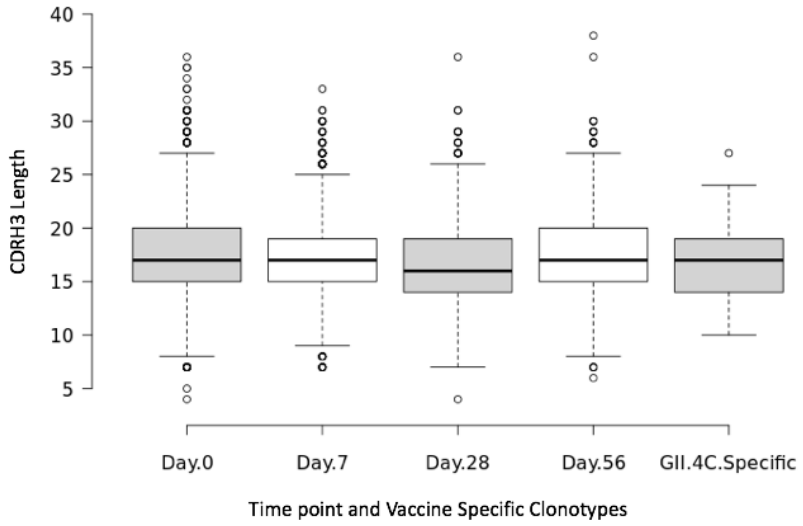

Figure 4.5 - CDR3 Length across time points and GII.4C specific clonotypes

CDR3 lengths were calculated for each time point and for GII.4C specific clonotypes. Time point data sets include all identified IgG clusters from all cell types (PBMCs, Memory, and Plasma Blasts). The GII.4C specific clonotypes include all of the clonotypes identified in the elution specific fraction identified over the three serum timepoints, Day 0, 7, and 21.

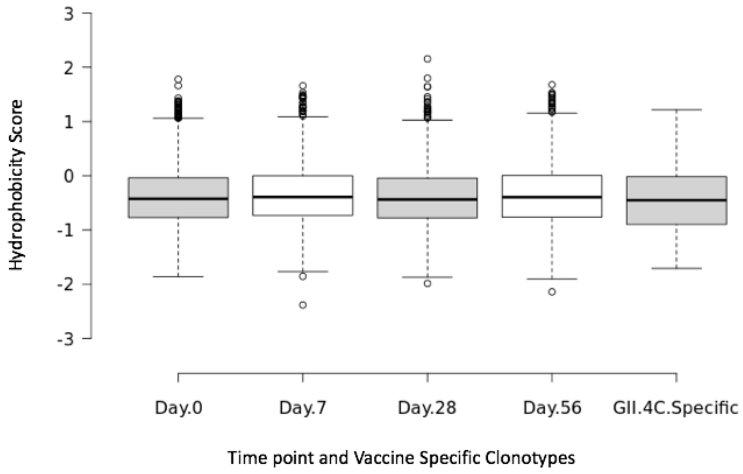

Figure 4.6 - CDR3 Hydrophobicity across time points and GII.4C specific clonotypes

CDR3 Hydrophobicity was calculated for each time point and for GII.4C specific clonotypes. Time point data sets include all identified IgG clusters from all cell types (PBMCs, Memory, and Plasma Blasts.) The GII.4C specific clonotypes include all of the clonotypes identified in the elution specific fraction identified over the three serum timepoints, Day 0, 7, and 21.

The somatic hypermuation (SHM) rate was calculated for the VH IgG sequence time points and the GII.4C specific clonotypes (Figure 4.7). SHM measures how many mutations have been made to a VH germ line sequence and are a measure of how much affinity maturation an antibody has undergone. When comparing the 4 different time points, Day 7 has the highest SHM rate, the media SHM rate is 8 amino acid changes per VH. The SHM rate decreases over the final two time points (Day 28 and Day 56). The GII.4C has a median SHM rate of 9.4 amino acid changes per VH as would be expected by a set of antibody sequences that bind antigen and have been selected by the immune system of affinity maturation.

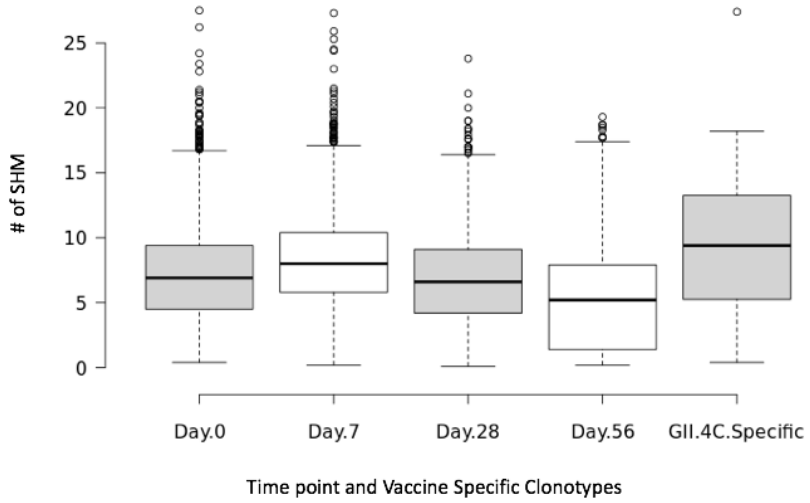

Figure 2.7 – Somatic hypermutation across time points and GII.4C specific clonotypes

Time point data sets include all identified IgG clusters from all cell types (PBMCs, Memory, and Plasma Blasts. The GII.4C specific clonotypes include all of the clonotypes identified in the elution specific fraction identified over the three serum timepoints, Day 0, 7, and 21. Somatic hypermutation was calculated as the number of mutations divided by the length of the germline sequence.

VH:VL Pairing Results

VH:VL paired sequences were clustered and isotyped. Table 4.3 shows the number of sequences, number of cells, and clonotypes derived from the VH:VL data sets for each cell time point. The number of clusters and isotypes is considerably lower than what was identified in the VH only database as the pairing process in inherently less efficient that VH only sequencing.

VH:VL paired sequencing						
	Productive VH:VL sequence pair	# of Cells	Clusters			
			Total	IgG	IgA	IgM
Day 0	1058236	115000	570	55	49	379
Day 7	945782	95000	1080	169	278	515
Day 28	389032	222000	910	32	55	753
Day 56	433663	120000	408	11	17	361

Table 4.3 – VH:VL Sequencing and clonotypes.

B-Cells were isolated from each time point and processed for VH:VL pairing. A productive VH:VL sequence pair is one that has undergone quality processing, contains a pair of identifiable antibody sequences that each contain a CDR3, and the pair consists of a VH and VL. To identify a cluster, sequences were sorted by most frequent CDRH3, the most abundant was seeded as the first cluster, if the following sequences had a 90% identical CDRH3 they were added to the cluster, if not they became the seed for the new cluster. IgG, IgA, and IgM were identified by searching for a constant region specific nucleotide sequence and allowing for one mismatch.

The CDRH3 amino acid sequences from the top GII.4C specific clonotypes identified in the LC-MS/MS analysis were searched against the CDRH3s identified VH:VL pairing databases from Days 0, 7, 28, and 56. CDRH3s from 8 of the top 10 clonotypes identified in the mass spec data were also identified by exact match to CDR3s in the paired databases (Table 4.4). The efficiency quickly dropped off as only 13 of the top 60 GII.4C clonotypes were identified in the paired databases. Nearly all of the corresponding VH:VL pairs were identified in the Day 7 paired data set. The top GII.4C specific CDR3s that were identified in the paired data bases are highly ranked within the VH:VL paired data when sorted by total number of sequencing reads for each cluster

with nearly all of them in the top 20% of paired clusters, indicating that the most abundant antibodies tend to be expressed by the most abundant transcripts.

Serum Clonotype	CDRH3	CDRL3	VH:VL Database Time-point Identified In
379	ARDYWNYHIRGWYPDY	QQSDSTPYT	Day 7
1431	ARDGPRPDGTGYAGPSNDY	QHRSSWPALT	Day 7
618	TRDQCGGDCSDF	QQSHSAPLT	Day 7
273	ARAVPLLGELSIRLSTFDN	AAWDDSLGAW V	Day 7
309	ARSPRTVAIKPYYFDY	QQYEDLPPT	Day 0
174	AGRASGSSPPH	QVYGSSQT	Day 7
236	AGHRGYSSGWPLDY	QQRTNWPPGVT	Day 7
234	ARDRPLASGWDRDDYYGMDV	QQANGPNGPLT	Day 7, 56
165	ARAGIIHAINGFDI	NSYTGGGALV	Day 7
3423	ARGTIYDFLAGDRGLGF	QQYYSSPPD	Day 7, 56
1227	AKDKTRTLRLGYSGMDV	QQSFSTPRT	Day 7, 56
178	ATGRVSSSWYRHEYIHH	HQYYTTPYT	Day 7
5855	AKDINFGGDTEVIKMGWFDL	QQYASSPPLT	Day 7
131	ARFPSAGYGMDV	LQSYGAPSFT	Day 7

Table 4.4 – GII.4C specific clonotypes identified in paired datasets.

14 clonotypes from the GII.4C specific data set were identified in the paired data sets. The top 8 in this table were found in the top 10 most abundant clonotypes as determined by LC-MS/MS (see inset in Figure 4.2). Heavy chain and light chain CDR3 pairs are listed. The time point identified in refers to the paired dataset time point the VH:VL CDR3 pairs were identified in. Underlined sequences have been selected for monoclonal expression and characterization.

ONGOING WORK AND DISCUSSION

Currently we are working on expressing, purifying and characterizing 8 of the paired data sequences identified (underlined in Table 4.4). In addition to exact CDR3 matches, the selected sequences had the best mass spec coverage when analyzing for non-CDRH3 peptides (CDR1, CDR2, SHMs). Monoclonals will be screened for binding activity to both HuNoV GI.1 and GII.4C VLPs as well as VLPs from other Norovirus strains. Monoclonals will also be screened in the carbohydrate assay for their ability to block viral interactions with their cognate HBGA sugar groups. Epitope mapping will be performed to identify which portion of the virus and the vaccine are eliciting the immune response. Samples from two additional donors have been processed and analysis is underway.

Prior to this study it was clear that this donor had a modest polyclonal response that contains antibodies that both bind and block HuNorV. However, composition and make-up of the poly clonal response was unclear. Using two pipelines to analyze both the serum antibody repertoire and the B-Cell VH sequences we have identified antibody sequences that are specific to the GII.4C VLP portion of a candidate Norovirus vaccine. We have identified over 100 clonotypes that are specific to the GII.4C VLP. Nearly half of the clonotypes that interact with the vaccine were present in the donor prior to vaccination including the dominate clonotype that makes up over 40% of the GII.4C response.

Time course data on the molecular composition and cellular response gleaned from this donor and others inform the vaccine development process. CDRH3 analysis and V-gene usage highlights aspects of the immune system that contribute to combating HuNoV. Monoclonal antibodies identified by this approach can be characterized with respect to binding affinity, ability to block infection, and which epitopes on the virus the bind too. Furthermore, analysis of additional donors will shed light on how universal the response mechanisms to the virus is.

ACKNOWLEDGEMENTS

Dr. Dan Boutz, Dr. John Blazek, Dr. Greg Ippolito, and Dr. Jon McDaniel contributed to the experimental design and thought process. Dr. Dan Boutz performed the LC-MS/MS runs, processed the data, and help with the final sequence analysis and selection. Dr. Jon McDaniel assisted in training on how to do the VH:VL pairing protocol and assisted with the VH sequence analysis. Dr. Constantine Chrysostomou build most of the computational programs used in this study. Dr. Sebastian Schaetzle, Dr. Jason Lavinder, and Jiwon Lee were very helpful and made great intellectual contributions to this project. Richard Salinas assisted with the FACS processing. The staff at UT's genome sequencing core (GSAF) processed and ran all of the MiSeq runs.

REFERENCES

Bok, K., Parra, G.I., Mitra, T., Abente, E., Shaver, C.K., Boon, D., Engle, R., Yu, C., Kapikian, A.Z., Sosnovtsev, S.V., Purcell, R.H., Green, K.Y., 2011. Chimpanzees as an animal model for human norovirus infection and vaccine development. Proc. Natl. Acad. Sci. U.S.A. 108, 325–330. doi:10.1073/pnas.1014577107

Bolotin, D.A., Poslavsky, S., Mitrophanov, I., Shugay, M., 2015. MiXCR: software for comprehensive adaptive immunity profiling. Nature.

Bonifait, L., Charlebois, R., Vimont, A., 2015. Detection and quantification of airborne norovirus during outbreaks in healthcare facilities. Clinical Infectious ….

Boutz, D.R., Horton, A.P., Wine, Y., Lavinder, J.J., Georgiou, G., Marcotte, E.M., 2014. Proteomic Identification of Monoclonal Antibodies from Serum. Anal. Chem. 86, 4758–4766. doi:10.1021/ac4037679

Chachu, K.A., LoBue, A.D., Strong, D.W., Baric, R.S., Virgin, H.W., 2008a. Immune Mechanisms Responsible for Vaccination against and Clearance of Mucosal and Lymphatic Norovirus Infection. PLoS Pathogens 4, e1000236. doi:10.1371/journal.ppat.1000236

Chachu, K.A., Strong, D.W., LoBue, A.D., Wobus, C.E., Baric, R.S., Virgin, H.W., 2008b. Antibody is critical for the clearance of murine norovirus infection. J. Virol. 82, 6610–6617. doi:10.1128/JVI.00141-08

Clarke, L.E., Warf, B.M., Flake, D.D., Hartman, A.-R., Tahan, S., Shea, C.R., Gerami, P., Messina, J., Florell, S.R., Wenstrup, R.J., Rushton, K., Roundy, K.M., Rock, C., Roa, B., Kolquist, K.A., Gutin, A., Billings, S., Leachman, S., 2015. Clinical validation of a gene expression signature that differentiates benign nevi from malignant melanoma. J. Cutan. Pathol. 42, 244–252. doi:10.1111/cup.12475

Cox, J., Michalski, A., Mann, M., 2011. Software Lock Mass by Two-Dimensional Minimization of Peptide Mass Errors. J. Am. Soc. Mass Spectrom. 22, 1373–1380. doi:10.1007/s13361-011-0142-8

DeKosky, B.J., Ippolito, G.C., Deschner, R.P., Lavinder, J.J., Wine, Y., Rawlings, B.M., Varadarajan, N., Giesecke, C., Dörner, T., Andrews, S.F., Wilson, P.C., Hunicke-Smith, S.P., Willson, C.G., Ellington, A.D., Georgiou, G., 2013. High-throughput sequencing of the paired human immunoglobulin heavy and light chain repertoire. Nat Biotechnol 31, 166–169. doi:10.1038/nbt.2492

Desai, R., Hembree, C.D., Handel, A., Matthews, J.E., Dickey, B.W., McDonald, S., Hall, A.J., Parashar, U.D., Leon, J.S., Lopman, B., 2012. Severe outcomes are associated with genogroup 2 genotype 4 norovirus outbreaks: a systematic literature review. Clin Infect Dis. 55, 189–193. doi:10.1093/cid/cis372

Donaldson, E.F., Lindesmith, L.C., LoBue, A.D., Baric, R.S., 2010. Viral shape-shifting: norovirus evasion of the human immune system. Nature Reviews Microbiology 8, 231–241. doi:10.1038/nrmicro2296

Farkas, T., Berke, T., Reuter, G., Szucs, G., Matson, D.O., Jiang, X., 2002. Molecular detection and sequence analysis of human caliciviruses from acute gastroenteritis outbreaks in Hungary. Journal of Medical Virology 67, 567–573. doi:10.1002/jmv.10140

Glass, R.I., Noel, J., Ando, T., Fankhauser, R., Belliot, G., Mounts, A., Parashar, U.D., Bresee, J.S., Monroe, S.S., 2000. The epidemiology of enteric caliciviruses from humans: a reassessment using new diagnostics. J Infect Dis. 181 Suppl 2, S254–61. doi:10.1086/315588

Graham, D.Y., Jiang, X., Tanaka, T., Opekun, A.R., Madore, H.P., Estes, M.K., 1994. Norwalk Virus Infection of Volunteers: New Insights Based on Improved Assays. J Infect Dis. 170, 34–43. doi:10.1093/infdis/170.1.34

Green, J., Vinjé, J., Gallimore, C.I., Koopmans, M., Hale, A., Brown, D.W.G., 2000. Capsid Protein Diversity among Norwalk-like Viruses. Virus Genes 20, 227–236. doi:10.1023/A:1008140611929

Ho, M.-S., Monroe, S., Stine, S., Cubitt, D., Glass, R., Madore, H.P., Pinsky, P., Ashley, C., Caul, E.O., 1989. VIRAL GASTROENTERITIS ABOARD A CRUISE SHIP. The Lancet 334, 961–965. doi:10.1016/S0140-6736(89)90964-1

Ippolito, G.C., Hoi, K.H., Reddy, S.T., Carroll, S.M., Ge, X., Rogosch, T., Zemlin, M., Shultz, L.D., Ellington, A.D., VanDenBerg, C.L., Georgiou, G., 2012. Antibody Repertoires in Humanized NOD-scid-IL2Rγnull Mice and Human B Cells Reveals Human-Like Diversification and Tolerance Checkpoints in the Mouse. PLoS ONE 7, e35497. doi:10.1371/journal.pone.0035497

Jiang, X., Wang, M., Wang, K., Estes, M.K., 1993. Sequence and Genomic Organization of Norwalk Virus. Virology 195, 51–61. doi:10.1006/viro.1993.1345

Jones, M.K., Watanabe, M., Zhu, S., Graves, C.L., Keyes, L.R., Grau, K.R., Gonzalez-Hernandez, M.B., Iovine, N.M., Wobus, C.E., Vinjé, J., Tibbetts, S.A., Wallet, S.M.,

Karst, S.M., 2014. Enteric bacteria promote human and mouse norovirus infection of B cells. Science 346, 755–759. doi:10.1126/science.1257147

Karst, S.M., Wobus, C.E., 2015. A Working Model of How Noroviruses Infect the Intestine. PLoS Pathogens 11, e1004626. doi:10.1371/journal.ppat.1004626

Kavanagh, O., Estes, M.K., Reeck, A., Raju, R.M., Opekun, A.R., Gilger, M.A., Graham, D.Y., Atmar, R.L., 2011. Serological responses to experimental Norwalk virus infection measured using a quantitative duplex time-resolved fluorescence immunoassay. Clin. Vaccine Immunol. 18, 1187–1190. doi:10.1128/CVI.00039-11

Koopmans, M., 2008. Progress in understanding norovirus epidemiology. Current Opinion in Infectious Diseases 21, 544–552. doi:10.1097/QCO.0b013e3283108965

Koopmans, M., Vinjé, J., de Wit, M., Leenen, I., van der Poel, W., van Duynhoven, Y., 2000. Molecular epidemiology of human enteric caliciviruses in The Netherlands. J Infect Dis. 181 Suppl 2, S262–9. doi:10.1086/315573

Lavinder, J.J., Horton, A.P., Georgiou, G., Ippolito, G.C., 2015. Next-generation sequencing and protein mass spectrometry for the comprehensive analysis of human cellular and serum antibody repertoires. Current Opinion in Chemical Biology 24, 112–120. doi:10.1016/j.cbpa.2014.11.007

Lavinder, J.J., Wine, Y., Giesecke, C., Ippolito, G.C., Horton, A.P., Lungu, O.I., Hoi, K.H., DeKosky, B.J., Murrin, E.M., Wirth, M.M., Ellington, A.D., Dörner, T., Marcotte, E.M., Boutz, D.R., Georgiou, G., 2014. Identification and characterization of the constituent human serum antibodies elicited by vaccination. Proc. Natl. Acad. Sci. U.S.A. 111, 2259–2264. doi:10.1073/pnas.1317793111

McDaniel, J.R., DeKosky, B.J., Tanno, H., Ellington, A.D., Georgiou, G., 2016. Ultra-high-throughput sequencing of the immune receptor repertoire from millions of lymphocytes. Nature Protocols 11, 429–442. doi:10.1038/nprot.2016.024

Mead, P.S., Slutsker, L., Dietz, V., McCaig, L.F., Bresee, J.S., Shapiro, C., Griffin, P.M., Tauxe, R.V., 1999. Food-related illness and death in the United States. Emerg. Infect. Dis. 5, 607–625. doi:10.3201/eid0505.990502

Patel, M.M., Hall, A.J., Vinjé, J., Parashar, U.D., 2009. Noroviruses: A comprehensive review. Journal of Clinical Virology 44, 1–8. doi:10.1016/j.jcv.2008.10.009

Patel, M.M., Widdowson, M.-A., Glass, R.I., Akazawa, K., Vinjé, J., Parashar, U.D., 2008. Systematic Literature Review of Role of Noroviruses in Sporadic Gastroenteritis. Emerg. Infect. Dis. 14, 1224–1231. doi:10.3201/eid1408.071114

Reddy, S.T., Ge, X., Miklos, A.E., Hughes, R.A., Kang, S.H., 2010. Monoclonal antibodies isolated without screening by analyzing the variable-gene repertoire of plasma cells. Nature.

Reeck, A., Kavanagh, O., Estes, M.K., Opekun, A.R., Gilger, M.A., Graham, D.Y., Atmar, R.L., 2010. Serological correlate of protection against norovirus-induced gastroenteritis. J Infect Dis. 202, 1212–1218. doi:10.1086/656364

Spitzer, M., Wildenhain, J., Rappsilber, J., Tyers, M., 2014. BoxPlotR: a web tool for generation of box plots. Nature Methods 11, 121–122. doi:10.1038/nmeth.2811

Treanor, J.J., Atmar, R.L., Frey, S.E., Gormley, R., Chen, W.H., Ferreira, J., Goodwin, R., Borkowski, A., Clemens, R., Mendelman, P.M., 2014. A novel intramuscular bivalent norovirus virus-like particle vaccine candidate--reactogenicity, safety, and immunogenicity in a phase 1 trial in healthy adults. J Infect Dis. 210, 1763–1771. doi:10.1093/infdis/jiu337

van Asten, L., Siebenga, J., van den Wijngaard, C., Verheij, R., van Vliet, H., Kretzschmar, M., Boshuizen, H., van Pelt, W., Koopmans, M., 2011. Unspecified Gastroenteritis Illness and Deaths in the Elderly Associated With Norovirus Epidemics. Epidemiology 22, 336–343. doi:10.1097/EDE.0b013e31821179af

Vega, E., Barclay, L., Gregoricus, N., Shirley, S.H., Lee, D., Vinjé, J., 2014. Genotypic and epidemiologic trends of norovirus outbreaks in the United States, 2009 to 2013. J. Clin. Microbiol. 52, 147–155. doi:10.1128/JCM.02680-13

Wang, B., Kluwe, C.A., Lungu, O.I., DeKosky, B.J., Kerr, S.A., Johnson, E.L., Jung, J., Rezigh, A.B., Carroll, S.M., Reyes, A.N., Bentz, J.R., Villanueva, I., Altman, A.L., Davey, R.A., Ellington, A.D., Georgiou, G., 2015. Facile Discovery of a Diverse Panel of Anti-Ebola Virus Antibodies by Immune Repertoire Mining. Scientific Reports 5, 13926. doi:10.1038/srep13926

Wine, Y., Boutz, D.R., Lavinder, J.J., Miklos, A.E., Hughes, R.A., Hoi, K.H., Jung, S.T., Horton, A.P., Murrin, E.M., Ellington, A.D., Marcotte, E.M., Georgiou, G., 2013. Molecular deconvolution of the monoclonal antibodies that comprise the polyclonal serum response. Proc. Natl. Acad. Sci. U.S.A. 110, 2993–2998. doi:10.1073/pnas.1213737110

Wine, Y., Horton, A.P., Ippolito, G.C., Georgiou, G., 2015. Serology in the 21st century: the molecular-level analysis of the serum antibody repertoire. Current opinion in immunology 35, 89–97. doi:10.1016/j.coi.2015.06.009

Zanini, B., Ricci, C., Bandera, F., Caselani, F., Magni, A., Laronga, A.M., Lanzini, A., 2012. Incidence of Post-Infectious Irritable Bowel Syndrome and Functional Intestinal Disorders Following a Water-Borne Viral Gastroenteritis Outbreak. The American Journal of Gastroenterology 107, 891–899. doi:10.1038/ajg.2012.102

Zheng, D.-P., Ando, T., Fankhauser, R.L., Beard, R.S., Glass, R.I., Monroe, S.S., 2006. Norovirus classification and proposed strain nomenclature. Virology 346, 312–323. doi:10.1016/j.virol.2005.11.015

Zheng, D.-P., Widdowson, M.-A., Glass, R.I., Vinjé, J., 2010. Molecular epidemiology of genogroup II-genotype 4 noroviruses in the United States between 1994 and 2006. J. Clin. Microbiol. 48, 168–177. doi:10.1128/JCM.01622-09

References

Abraham, J., Corbett, K.D., Farzan, M., Choe, H., Harrison, S.C., 2010. Structural basis for receptor recognition by New World hemorrhagic fever arenaviruses. Nature Publishing Group 17, 438–444. doi:10.1038/nsmb.1772

Abraham, J., Kwong, J.A., Albariño, C.G., Lu, J.G., Radoshitzky, S.R., Salazar-Bravo, J., Farzan, M., Spiropoulou, C.F., Choe, H., 2009. Host-Species Transferrin Receptor 1 Orthologs Are Cellular Receptors for Nonpathogenic New World Clade B Arenaviruses. PLoS Pathogens 5, e1000358. doi:10.1371/journal.ppat.1000358

Agnandji, S.T., Huttner, A., Zinser, M.E., Njuguna, P., Dahlke, C., Fernandes, J.F., Yerly, S., Dayer, J.-A., Kraehling, V., Kasonta, R., Adegnika, A.A., Altfeld, M., Auderset, F., Bache, E.B., Biedenkopf, N., Borregaard, S., Brosnahan, J.S., Burrow, R., Combescure, C., Desmeules, J., Eickmann, M., Fehling, S.K., Finckh, A., Goncalves, A.R., Grobusch, M.P., Hooper, J., Jambrecina, A., Kabwende, A.L., Kaya, G., Kimani, D., Lell, B., Lemaître, B., Lohse, A.W., Massinga-Loembe, M., Matthey, A., Mordmüller, B., Nolting, A., Ogwang, C., Ramharter, M., Schmidt-Chanasit, J., Schmiedel, S., Silvera, P., Stahl, F.R., Staines, H.M., Strecker, T., Stubbe, H.C., Tsofa, B., Zaki, S., Fast, P., Moorthy, V., Kaiser, L., Krishna, S., Becker, S., Kieny, M.-P., Bejon, P., Kremsner, P.G., Addo, M.M., Siegrist, C.-A., 2015. Phase 1 Trials of rVSV Ebola Vaccine in Africa and Europe. New England Journal of Medicine 374, 1647–1660. doi:10.1056/NEJMoa1502924

Agnese, G., 2007. *"Una rara enfermedad alarma a la modesta población de O'Higgins*" Análisis del discurso de la prensa escrita sobre la epidemia de Fiebre Hemorrágica Argentina de 1958 Revista de Historia & Humanidades Médicas Vol. 3 No 1, Julio 2007

Aisen, P., 2004. Transferrin receptor 1. The International Journal of Biochemistry & Cell Biology 36, 2137–2143. doi:10.1016/j.biocel.2004.02.007

Amman, B.R., Carroll, S.A., Reed, Z.D., Sealy, T.K., Balinandi, S., Swanepoel, R., Kemp, A., Erickson, B.R., Comer, J.A., Campbell, S., Cannon, D.L., Khristova, M.L., Atimnedi, P., Paddock, C.D., Crockett, R.J.K., Flietstra, T.D., Warfield, K.L., Unfer, R., Katongole-Mbidde, E., Downing, R., Tappero, J.W., Zaki, S.R., Rollin, P.E., Ksiazek, T.G., Nichol, S.T., Towner, J.S., 2012. Seasonal Pulses of Marburg Virus Circulation in Juvenile Rousettus aegyptiacus Bats Coincide with Periods of Increased Risk of Human Infection. PLoS Pathogens 8, e1002877. doi:10.1371/journal.ppat.1002877

Baize, S., Pannetier, D., Oestereich, L., Rieger, T., Koivogui, L., Magassouba, N., Soropogui, B., Sow, M.S., Keïta, S., De Clerck, H., Tiffany, A., Dominguez, G., Loua, M., Traoré, A., Kolié, M., Malano, E.R., Heleze, E., Bocquin, A., Mély, S., Raoul, H., Caro, V., Cadar, D., Gabriel, M., Pahlmann, M., Tappe, D., Schmidt-Chanasit, J., Impouma, B., Diallo, A.K., Formenty, P., Van Herp, M., Günther, S., 2014. Emergence of Zaire Ebola Virus Disease in Guinea. http://dx.doi.org/10.1056/NEJMoa1404505 371, 1418–1425. doi:10.1056/NEJMoa1404505

Barrera Oro, J.G., McKee, K.T., 1991. Toward a vaccine against Argentine hemorrhagic fever. Bulletin of PAH0 25(2), 1991

Barrette, R.W., Metwally, S.A., Rowland, J.M., Xu, L., Zaki, S.R., Nichol, S.T., Rollin, P.E., Towner, J.S., Shieh, W.-J., Batten, B., Sealy, T.K., Carrillo, C., Moran, K.E., Bracht, A.J., Mayr, G.A., Sirios-Cruz, M., Catbagan, D.P., Lautner, E.A., Ksiazek, T.G., White, W.R., McIntosh, M.T., 2009. Discovery of Swine as a Host for the Reston ebolavirus. Science 325, 204–206. doi:10.1126/science.1172705

Bermejo, M., Rodríguez-Teijeiro, J.D., Illera, G., Barroso, A., Vilà, C., Walsh, P.D., 2006. Ebola Outbreak Killed 5000 Gorillas. Science 314, 1564–1564. doi:10.1126/science.1133105

Bok, K., Parra, G.I., Mitra, T., Abente, E., Shaver, C.K., Boon, D., Engle, R., Yu, C., Kapikian, A.Z., Sosnovtsev, S.V., Purcell, R.H., Green, K.Y., 2011. Chimpanzees as an animal model for human norovirus infection and vaccine development. Proc. Natl. Acad. Sci. U.S.A. 108, 325–330. doi:10.1073/pnas.1014577107

Bolotin, D.A., Poslavsky, S., Mitrophanov, I., Shugay, M., 2015. MiXCR: software for comprehensive adaptive immunity profiling. Nature.

Bonifait, L., Charlebois, R., Vimont, A., 2015. Detection and quantification of airborne norovirus during outbreaks in healthcare facilities. Clinical Infectious ….

Borio, L., Inglesby, T., Peters, C.J., Schmaljohn, A.L., Hughes, J.M., Jahrling, P.B., Ksiazek, T., Johnson, K.M., Meyerhoff, A., O'Toole, T., Ascher, M.S., Bartlett, J., Breman, J.G., Edward M Eitzen, J., Hamburg, M., Hauer, J., Henderson, D.A., Johnson, R.T., Kwik, G., Layton, M., Lillibridge, S., Nabel, G.J., Osterholm, M.T., Perl, T.M., Russell, P., Tonat, K., Biodefense, F.T.W.G.O.C., 2002. Hemorrhagic Fever Viruses as Biological Weapons: Medical and Public Health Management. JAMA 287, 2391–2405. doi:10.1001/jama.287.18.2391

Boutz, D.R., Horton, A.P., Wine, Y., Lavinder, J.J., Georgiou, G., Marcotte, E.M., 2014.

Proteomic Identification of Monoclonal Antibodies from Serum. Anal. Chem. 86, 4758–4766. doi:10.1021/ac4037679

Bowen, E., Lloyd, G., Harris, W.J., Platt, G.S., 1977. Viral haemorrhagic fever in southern Sudan and northern Zaire: preliminary studies on the aetiological agent. The Lancet.

Bradbury, A.R.M., Sidhu, S., Dübel, S., McCafferty, J., 2011. Beyond natural antibodies: the power of in vitro display technologies. Nat Biotechnol 29, 245–254. doi:10.1038/nbt.1791

Carette, J.E., Raaben, M., Wong, A.C., Herbert, A.S., Obernosterer, G., Mulherkar, N., Kuehne, A.I., Kranzusch, P.J., Griffin, A.M., Ruthel, G., Cin, P.D., Dye, J.M., Whelan, S.P., Chandran, K., Brummelkamp, T.R., 2011. Ebola virus entry requires the cholesterol transporter Niemann-Pick C1. Nature 477, 340–343. doi:10.1038/nature10348

Carroll, S.A., Towner, J.S., Sealy, T.K., McMullan, L.K., Khristova, M.L., Burt, F.J., Swanepoel, R., Rollin, P.E., Nichol, S.T., 2013. Molecular evolution of viruses of the family Filoviridae based on 97 whole-genome sequences. J. Virol. 87, 2608–2616. doi:10.1128/JVI.03118-12

Charrel, R.N., Coutard, B., Baronti, C., Canard, B., 2011. Arenaviruses and hantaviruses: from epidemiology and genomics to antivirals. Antiviral Research.

Chaudhury, S., Berrondo, M., Weitzner, B.D., Muthu, P., Bergman, H., Gray, J.J., 2011. Benchmarking and Analysis of Protein Docking Performance in Rosetta v3.2. PLoS ONE 6, e22477. doi:10.1371/journal.pone.0022477

Chen, G., Koellhoffer, J.F., Zak, S.E., Frei, J.C., Liu, N., Long, H., Ye, W., Nagar, K., Pan, G., Chandran, K., Dye, J.M., Sidhu, S.S., Lai, J.R., 2014. Synthetic Antibodies with a Human Framework That Protect Mice from Lethal Sudan Ebolavirus Challenge. ACS Chem. Biol. 9, 2263–2273. doi:10.1021/cb5006454

Choe, H., Jemielity, S., Abraham, J., Radoshitzky, S.R., Farzan, M., 2011. Transferrin receptor 1 in the zoonosis and pathogenesis of New World hemorrhagic fever arenaviruses. Current opinion in microbiology 14, 476–82. doi:10.1016/j.mib.2011.07.014

Chachu, K.A., LoBue, A.D., Strong, D.W., Baric, R.S., Virgin, H.W., 2008a. Immune Mechanisms Responsible for Vaccination against and Clearance of Mucosal and Lymphatic Norovirus Infection. PLoS Pathogens 4, e1000236.

doi:10.1371/journal.ppat.1000236

Chachu, K.A., Strong, D.W., LoBue, A.D., Wobus, C.E., Baric, R.S., Virgin, H.W., 2008b. Antibody is critical for the clearance of murine norovirus infection. J. Virol. 82, 6610–6617. doi:10.1128/JVI.00141-08

Clarke, L.E., Warf, B.M., Flake, D.D., Hartman, A.-R., Tahan, S., Shea, C.R., Gerami, P., Messina, J., Florell, S.R., Wenstrup, R.J., Rushton, K., Roundy, K.M., Rock, C., Roa, B., Kolquist, K.A., Gutin, A., Billings, S., Leachman, S., 2015. Clinical validation of a gene expression signature that differentiates benign nevi from malignant melanoma. J. Cutan. Pathol. 42, 244–252. doi:10.1111/cup.12475

Coimbra, T.L.M., Nassar, E.S., de Souza, L.T.M., Ferreira, I.B., Rocco, I.M., Burattini, M.N., da Rosa, A.P.A.T., Vasconcelos, P.F.C., Pinheiro, F.P., LeDuc, J.W., Rico-Hesse, R., Gonzalez, J.-P., Tesh, R.B., Jahrling, P.B., 1994. New arenavirus isolated in Brazil. The Lancet 343, 391–392. doi:10.1016/S0140-6736(94)91226-2

Corti, D., Voss, J., Gamblin, S.J., Codoni, G., Macagno, A., Jarrossay, D., Vachieri, S.G., Pinna, D., Minola, A., Vanzetta, F., Silacci, C., Fernandez-Rodriguez, B.M., Agatic, G., Bianchi, S., Giacchetto-Sasselli, I., Calder, L., Sallusto, F., Collins, P., Haire, L.F., Temperton, N., Langedijk, J.P.M., Skehel, J.J., Lanzavecchia, A., 2011. A neutralizing antibody selected from plasma cells that binds to group 1 and group 2 influenza A hemagglutinins. Science 333, 850–856. doi:10.1126/science.1205669

Cox, J., Michalski, A., Mann, M., 2011. Software Lock Mass by Two-Dimensional Minimization of Peptide Mass Errors. J. Am. Soc. Mass Spectrom. 22, 1373–1380. doi:10.1007/s13361-011-0142-8

Cuevas, C.D., Lavanya, M., Wang, E., Ross, S.R., 2011. Junin virus infects mouse cells and induces innate immune responses. J. Virol.

Datta, S., Budhauliya, R., Das, B., Chatterjee, S., Vanlalhmuaka, Veer, V., 2015. Next-generation sequencing in clinical virology: Discovery of new viruses. World Journal of Virology 4, 265–276. doi:10.5501/wjv.v4.i3.265

Daugherty, M.D., Malik, H.S., 2012. Rules of Engagement: Molecular Insights from Host-Virus Arms Races. http://dx.doi.org/10.1146/annurev-genet-110711-155522 46, 677–700. doi:10.1146/annurev-genet-110711-155522

de Graaf, M., Fouchier, R.A.M., 2014. Role of receptor binding specificity in influenza A virus transmission and pathogenesis. The EMBO Journal 33, 823–841. doi:10.1002/embj.201387442

DeKosky, B.J., Ippolito, G.C., Deschner, R.P., Lavinder, J.J., Wine, Y., Rawlings, B.M., Varadarajan, N., Giesecke, C., Dörner, T., Andrews, S.F., Wilson, P.C., Hunicke-Smith, S.P., Willson, C.G., Ellington, A.D., Georgiou, G., 2013. High-throughput sequencing of the paired human immunoglobulin heavy and light chain repertoire. Nat Biotechnol 31, 166–169. doi:10.1038/nbt.2492

Delgado, S., Erickson, B.R., Agudo, R., Blair, P.J., Vallejo, E., Albariño, C.G., Vargas, J., Comer, J.A., Rollin, P.E., Ksiazek, T.G., Olson, J.G., Nichol, S.T., 2008. Chapare Virus, a Newly Discovered Arenavirus Isolated from a Fatal Hemorrhagic Fever Case in Bolivia. PLoS Pathogens 4, e1000047. doi:10.1371/journal.ppat.1000047

Demogines, A., Abraham, J., Choe, H., Farzan, M., 2013. Dual host-virus arms races shape an essential housekeeping protein. PLoS biology.

Demogines, A., Farzan, M., Sawyer, S.L., 2012. Evidence for ACE2-utilizing coronaviruses (CoVs) related to severe acute respiratory syndrome CoV in bats. J. Virol.

Desai, R., Hembree, C.D., Handel, A., Matthews, J.E., Dickey, B.W., McDonald, S., Hall, A.J., Parashar, U.D., Leon, J.S., Lopman, B., 2012. Severe outcomes are associated with genogroup 2 genotype 4 norovirus outbreaks: a systematic literature review. Clin Infect Dis. 55, 189–193. doi:10.1093/cid/cis372

Dias, J.M., Kuehne, A.I., Abelson, D.M., Bale, S., Wong, A.C., Halfmann, P., Muhammad, M.A., Fusco, M.L., Zak, S.E., Kang, E., Kawaoka, Y., Chandran, K., Dye, J.M., Saphire, E.O., 2011. A shared structural solution for neutralizing ebolaviruses. Nature Structural & Molecular Biology 18, 1424–1427. doi:10.1038/nsmb.2150

Donaldson, E.F., Lindesmith, L.C., LoBue, A.D., Baric, R.S., 2010. Viral shape-shifting: norovirus evasion of the human immune system. Nature Reviews Microbiology 8, 231–241. doi:10.1038/nrmicro2296

Eswar, N., Webb, B., Marti-Renom, M.A., Madhusudhan, M.S., 2006. Curr Protoc Bioinformatics Chapter 5. doi:10.1016/j.febslet.2010.04.028/full

Farkas, T., Berke, T., Reuter, G., Szucs, G., Matson, D.O., Jiang, X., 2002. Molecular detection and sequence analysis of human caliciviruses from acute gastroenteritis outbreaks in Hungary. Journal of Medical Virology 67, 567–573. doi:10.1002/jmv.10140

Feldmann, H., Nichol, S.T., Klenk, H.-D., Peters, C.J., Sanchez, A., 1994.

Characterization of Filoviruses Based on Differences in Structure and Antigenicity of the Virion Glycoprotein. Virology 199, 469–473. doi:10.1006/viro.1994.1147

Flanagan, M.L., Oldenburg, J., Reignier, T., Holt, N., Hamilton, G.A., Martin, V.K., Cannon, P.M., 2008. New World Clade B Arenaviruses Can Use Transferrin Receptor 1 (TfR1)-Dependent and -Independent Entry Pathways, and Glycoproteins from Human Pathogenic Strains Are Associated with the Use of TfR1. J. Virol. 82, 938–948. doi:10.1128/JVI.01397-07

Gerlier, D., 2011. Emerging zoonotic viruses: new lessons on receptor and entry mechanisms. Current Opinion in Virology 1, 27–34. doi:10.1016/j.coviro.2011.05.014

Geisbert, T.W., Daddario-DiCaprio, K.M., Lewis, M.G., Geisbert, J.B., Grolla, A., Leung, A., Paragas, J., Matthias, L., Smith, M.A., Jones, S.M., Hensley, L.E., Feldmann, H., Jahrling, P.B., 2008. Vesicular Stomatitis Virus-Based Ebola Vaccine Is Well-Tolerated and Protects Immunocompromised Nonhuman Primates. PLoS Pathogens 4, e1000225. doi:10.1371/journal.ppat.1000225

Ghosh, S., Campbell, A.M., 1986. Multispecific monoclonal antibodies. Immunology Today 7, 217–222. doi:10.1016/0167-5699(86)90108-8

Gire, S.K., Goba, A., Andersen, K.G., Sealfon, R.S.G., Park, D.J., Kanneh, L., Jalloh, S., Momoh, M., Fullah, M., Dudas, G., Wohl, S., Moses, L.M., Yozwiak, N.L., Winnicki, S., Matranga, C.B., Malboeuf, C.M., Qu, J., Gladden, A.D., Schaffner, S.F., Yang, X., Jiang, P.-P., Nekoui, M., Colubri, A., Coomber, M.R., Fonnie, M., Moigboi, A., Gbakie, M., Kamara, F.K., Tucker, V., Konuwa, E., Saffa, S., Sellu, J., Jalloh, A.A., Kovoma, A., Koninga, J., Mustapha, I., Kargbo, K., Foday, M., Yillah, M., Kanneh, F., Robert, W., Massally, J.L.B., Chapman, S.B., Bochicchio, J., Murphy, C., Nusbaum, C., Young, S., Birren, B.W., Grant, D.S., Scheiffelin, J.S., Lander, E.S., Happi, C., Gevao, S.M., Gnirke, A., Rambaut, A., Garry, R.F., Khan, S.H., Sabeti, P.C., 2014. Genomic surveillance elucidates Ebola virus origin and transmission during the 2014 outbreak. Science 345, 1369–1372. doi:10.1126/science.1259657

Glass, R.I., Noel, J., Ando, T., Fankhauser, R., Belliot, G., Mounts, A., Parashar, U.D., Bresee, J.S., Monroe, S.S., 2000. The epidemiology of enteric caliciviruses from humans: a reassessment using new diagnostics. J Infect Dis. 181 Suppl 2, S254–61. doi:10.1086/315588

Gleichmann, H., 1981. Studies on the mechanism of drug sensitization: T-cell-dependent popliteal lymph node reaction to diphenylhydantoin. Clin. Immunol. Immunopathol.

18, 203–211.

Graham, D.Y., Jiang, X., Tanaka, T., Opekun, A.R., Madore, H.P., Estes, M.K., 1994. Norwalk Virus Infection of Volunteers: New Insights Based on Improved Assays. J Infect Dis. 170, 34–43. doi:10.1093/infdis/170.1.34

Graham, R.L., Baric, R.S., 2010. Recombination, reservoirs, and the modular spike: mechanisms of coronavirus cross-species transmission. J. Virol. 84, 3134–3146. doi:10.1128/JVI.01394-09

Green, J., Vinjé, J., Gallimore, C.I., Koopmans, M., Hale, A., Brown, D.W.G., 2000. Capsid Protein Diversity among Norwalk-like Viruses. Virus Genes 20, 227–236. doi:10.1023/A:1008140611929

Hall, A.J., Vinjé, J., Lopman, B., Park, G.W., Yen, C., 2011. Updated norovirus outbreak management and disease prevention guidelines.

Helguera, G., Jemielity, S., Abraham, J., Cordo, S.M., Martinez, M.G., Rodríguez, J.A., Bregni, C., Wang, J.J., Farzan, M., Penichet, M.L., Candurra, N.A., Choe, H., 2012. An antibody recognizing the apical domain of human transferrin receptor 1 efficiently inhibits the entry of all new world hemorrhagic Fever arenaviruses. Journal of virology 86, 4024–8. doi:10.1128/JVI.06397-11

Ho, M.-S., Monroe, S., Stine, S., Cubitt, D., Glass, R., Madore, H.P., Pinsky, P., Ashley, C., Caul, E.O., 1989. VIRAL GASTROENTERITIS ABOARD A CRUISE SHIP. The Lancet 334, 961–965. doi:10.1016/S0140-6736(89)90964-1

Hood, C.L., Abraham, J., Boyington, J.C., Leung, K., Kwong, P.D., Nabel, G.J., 2010. Biochemical and structural characterization of cathepsin L-processed Ebola virus glycoprotein: implications for viral entry and immunogenicity. Journal of virology 84, 2972–82. doi:10.1128/JVI.02151-09

Humes, D., Emery, S., Laws, E., Overbaugh, J., 2012. A species-specific amino acid difference in the macaque CD4 receptor restricts replication by global circulating HIV-1 variants representing viruses from recent infection. J. Virol. 86, 12472–12483. doi:10.1128/JVI.02176-12

Ippolito, G.C., Hoi, K.H., Reddy, S.T., Carroll, S.M., Ge, X., Rogosch, T., Zemlin, M., Shultz, L.D., Ellington, A.D., VanDenBerg, C.L., Georgiou, G., 2012. Antibody Repertoires in Humanized NOD-scid-IL2Rγnull Mice and Human B Cells Reveals Human-Like Diversification and Tolerance Checkpoints in the Mouse. PLoS ONE 7, e35497. doi:10.1371/journal.pone.0035497

Jiang, X., Wang, M., Wang, K., Estes, M.K., 1993. Sequence and Genomic Organization of Norwalk Virus. Virology 195, 51–61. doi:10.1006/viro.1993.1345

Johnson, K.M., Wiebenga, N.H., 1965. Virus isolations from human cases of hemorrhagic fever in Bolivia. Experimental Biology and Medicine 118, 113–118. doi:10.3181/00379727-118-29772

Jones, M.K., Watanabe, M., Zhu, S., Graves, C.L., Keyes, L.R., Grau, K.R., Gonzalez-Hernandez, M.B., Iovine, N.M., Wobus, C.E., Vinjé, J., Tibbetts, S.A., Wallet, S.M., Karst, S.M., 2014. Enteric bacteria promote human and mouse norovirus infection of B cells. Science 346, 755–759. doi:10.1126/science.1257147

Kaelber, J.T., Demogines, A., Harbison, C.E., Allison, A.B., Goodman, L.B., Ortega, A.N., Sawyer, S.L., Parrish, C.R., 2012. Evolutionary Reconstructions of the Transferrin Receptor of Caniforms Supports Canine Parvovirus Being a Re-emerged and Not a Novel Pathogen in Dogs. PLoS Pathogens 8, e1002666. doi:10.1371/journal.ppat.1002666

Katoh, K., Kuma, K.I., Toh, H., Miyata, T., 2005. MAFFT version 5: improvement in accuracy of multiple sequence alignment. Nucl. Acids Res. 33, 511–518. doi:10.1093/nar/gki198

Katoh, K., Misawa, K., Kuma, K.I., Miyata, T., 2002. MAFFT: a novel method for rapid multiple sequence alignment based on fast Fourier transform. Nucl. Acids Res. 30, 3059–3066. doi:10.1093/nar/gkf436

Kamala, T., 2007. Hock immunization: a humane alternative to mouse footpad injections. J. Immunol. Methods 328, 204–214. doi:10.1016/j.jim.2007.08.004

Karin Bok, K.Y.G., 2013. Norovirus Gastroenteritis in Immunocompromised Patients. The New England journal of medicine 368, 971–971. doi:10.1056/NEJMc1301022

Karst, S.M., Wobus, C.E., 2015. A Working Model of How Noroviruses Infect the Intestine. PLoS Pathogens 11, e1004626. doi:10.1371/journal.ppat.1004626

Kavanagh, O., Estes, M.K., Reeck, A., Raju, R.M., Opekun, A.R., Gilger, M.A., Graham, D.Y., Atmar, R.L., 2011. Serological responses to experimental Norwalk virus infection measured using a quantitative duplex time-resolved fluorescence immunoassay. Clin. Vaccine Immunol. 18, 1187–1190. doi:10.1128/CVI.00039-11

Köhler, G., Milstein, C., 1975. Continuous cultures of fused cells secreting antibody of

predefined specificity. Nature 256, 495–497. doi:10.1038/256495a0

Koellhoffer, J.F., Chen, G., Sandesara, R.G., Bale, S., Ollmann Saphire, E., Chandran, K., Sidhu, S.S., Lai, J.R., 2012. Two Synthetic Antibodies that Recognize and Neutralize Distinct Proteolytic Forms of the Ebola Virus Envelope Glycoprotein. ChemBioChem 13, 2549–2557. doi:10.1002/cbic.201200493

Kondratowicz, A.S., Lennemann, N.J., Sinn, P.L., Davey, R.A., Hunt, C.L., Moller-Tank, S., Meyerholz, D.K., Rennert, P., Mullins, R.F., Brindley, M., Sandersfeld, L.M., Quinn, K., Weller, M., McCray, P.B., Chiorini, J., Maury, W., 2011. T-cell immunoglobulin and mucin domain 1 (TIM-1) is a receptor for Zaire Ebolavirus and Lake Victoria Marburgvirus. Proc. Natl. Acad. Sci. U.S.A. 108, 8426–8431. doi:10.1073/pnas.1019030108

Koopmans, M., 2008. Progress in understanding norovirus epidemiology. Current Opinion in Infectious Diseases 21, 544–552. doi:10.1097/QCO.0b013e3283108965

Koopmans, M., Vinjé, J., de Wit, M., Leenen, I., van der Poel, W., van Duynhoven, Y., 2000. Molecular epidemiology of human enteric caliciviruses in The Netherlands. J Infect Dis. 181 Suppl 2, S262–9. doi:10.1086/315573

Lane, D., Koprowski, H., 1982. Molecular recognition and the future of monoclonal antibodies. Nature 296, 200–202. doi:10.1038/296200a0

Lavinder, J.J., Horton, A.P., Georgiou, G., Ippolito, G.C., 2015. Next-generation sequencing and protein mass spectrometry for the comprehensive analysis of human cellular and serum antibody repertoires. Current Opinion in Chemical Biology 24, 112–120. doi:10.1016/j.cbpa.2014.11.007

Lavinder, J.J., Wine, Y., Giesecke, C., Ippolito, G.C., Horton, A.P., Lungu, O.I., Hoi, K.H., DeKosky, B.J., Murrin, E.M., Wirth, M.M., Ellington, A.D., Dörner, T., Marcotte, E.M., Boutz, D.R., Georgiou, G., 2014. Identification and characterization of the constituent human serum antibodies elicited by vaccination. Proc. Natl. Acad. Sci. U.S.A. 111, 2259–2264. doi:10.1073/pnas.1317793111

Leaver-Fay, A., Tyka, M., Lewis, S.M., Lange, O.F., Thompson, J., Jacak, R., Kaufman, K., Renfrew, P.D., Smith, C.A., Sheffler, W., Davis, I.W., Cooper, S., Treuille, A., Mandell, D.J., Richter, F., Ban, Y.-E.A., Fleishman, S.J., Corn, J.E., Kim, D.E., Lyskov, S., Berrondo, M., Mentzer, S., Popović, Z., Havranek, J.J., Karanicolas, J., Das, R., Meiler, J., Kortemme, T., Gray, J.J., Kuhlman, B., Baker, D., Bradley, P., 2011. Rosetta3: An Object-Oriented Software Suite for the Simulation and Design of Macromolecules. Methods in enzymology 487, 545–574. doi:10.1016/B978-0-12-

381270-4.00019-6

LeDuc, J.W., 1989. Epidemiology of hemorrhagic fever viruses. Review of Infectious Diseases.

Le Guenno, B., Formenty, P., Wyers, M., Gounon, P., Walker, F., Boesch, C., 1995. Isolation and partial characterisation of a new strain of Ebola virus. The Lancet 345, 1271–1274. doi:10.1016/S0140-6736(95)90925-7

Leroy, E.M., Kumulungui, B., Pourrut, X., Rouquet, P., Hassanin, A., Yaba, P., Délicat, A., Paweska, J.T., Gonzalez, J.-P., Swanepoel, R., 2005. Fruit bats as reservoirs of Ebola virus. Nature 438, 575–576. doi:10.1038/438575a

Li, L., Fang, C.J., Ryan, J.C., Niemi, E.C., 2010. Binding and uptake of H-ferritin are mediated by human transferrin receptor-1. Proceedings of the ….

Lin, G., Simmons, G., Pöhlmann, S., Baribaud, F., Ni, H., Leslie, G.J., Haggarty, B.S., Bates, P., Weissman, D., Hoxie, J.A., Doms, R.W., 2003. Differential N-linked glycosylation of human immunodeficiency virus and Ebola virus envelope glycoproteins modulates interactions with DC-SIGN and DC-SIGNR. J. Virol. 77, 1337–1346. doi:10.1128/JVI.77.2.1337-1346.2003

Lindesmith, L.C., Beltramello, M., Donaldson, E.F., Corti, D., Swanstrom, J., Debbink, K., Lanzavecchia, A., Baric, R.S., 2012. Immunogenetic Mechanisms Driving Norovirus GII.4 Antigenic Variation. PLoS Pathogens 8, e1002705. doi:10.1371/journal.ppat.1002705

Lindesmith, L.C., Donaldson, E.F., Baric, R.S., 2011. Norovirus GII.4 strain antigenic variation. J. Virol. 85, 231–242. doi:10.1128/JVI.01364-10

Lipkin, W.I., 2010. Microbe hunting. Microbiol. Mol. Biol. Rev. 74, 363–377. doi:10.1128/MMBR.00007-10

Marsh, G.A., Haining, J., Robinson, R., Foord, A., Yamada, M., Barr, J.A., Payne, J., White, J., Yu, M., Bingham, J., Rollin, P.E., Nichol, S.T., Wang, L.-F., Middleton, D., 2011. Ebola Reston virus infection of pigs: clinical significance and transmission potential. J Infect Dis. 204 Suppl 3, S804–9. doi:10.1093/infdis/jir300

Martin, C., Buckler-White, A., Wollenberg, K., Kozak, C.A., 2013. The avian XPR1 gammaretrovirus receptor is under positive selection and is disabled in bird species in contact with virus-infected wild mice. J. Virol. 87, 10094–10104. doi:10.1128/JVI.01327-13

Martin, V.K., Droniou-Bonzom, M.E., Reignier, T., Oldenburg, J.E., Cox, A.U., Cannon, P.M., 2010. Investigation of Clade B New World Arenavirus Tropism by Using Chimeric GP1 Proteins. J. Virol. 84, 1176–1182. doi:10.1128/JVI.01625-09

Mattison, K., Shukla, A., Cook, A., Pollari, F., 2007. Human noroviruses in swine and cattle. Emerging infectious Diseases Vol. 13, No. 8, August 2007

Maruyama, T., Rodriguez, L.L., Jahrling, P.B., Sánchez, A., Khan, A.S., Nichol, S.T., Peters, C.J., Parren, P.W., Burton, D.R., 1999. Ebola virus can be effectively neutralized by antibody produced in natural human infection. J. Virol. 73, 6024–6030.

McDaniel, J.R., DeKosky, B.J., Tanno, H., Ellington, A.D., Georgiou, G., 2016. Ultra-high-throughput sequencing of the immune receptor repertoire from millions of lymphocytes. Nature Protocols 11, 429–442. doi:10.1038/nprot.2016.024

Mead, P.S., Slutsker, L., Dietz, V., McCaig, L.F., Bresee, J.S., Shapiro, C., Griffin, P.M., Tauxe, R.V., 1999. Food-related illness and death in the United States. Emerg. Infect. Dis. 5, 607–625. doi:10.3201/eid0505.990502

Meyer, A.G., Sawyer, S.L., Ellington, A.D., Wilke, C.O., 2014. Analyzing machupo virus-receptor binding by molecular dynamics simulations. PeerJ 2, e266. doi:10.7717/peerj.266

Meyer, A.G., Wilke, C.O., 2015. Geometric Constraints Dominate the Antigenic Evolution of Influenza H3N2 Hemagglutinin. PLoS Pathogens 11, e1004940. doi:10.1371/journal.ppat.1004940

Meyerson, N.R., Rowley, P.A., Swan, C.H., Le, D.T., Wilkerson, G.K., Sawyer, S.L., 2014. Positive selection of primate genes that promote HIV-1 replication. Virology 454-455, 291–298. doi:10.1016/j.virol.2014.02.029

Meyerson, N.R., Sawyer, S.L., 2011. Two-stepping through time: mammals and viruses. Trends in Microbiology 19, 286–294. doi:10.1016/j.tim.2011.03.006

Meyerson, N.R., Sharma, A., Wilkerson, G.K., Overbaugh, J., Sawyer, S.L., 2015. Identification of Owl Monkey CD4 Receptors Broadly Compatible with Early-Stage HIV-1 Isolates. J. Virol. 89, 8611–8622. doi:10.1128/JVI.00890-15

Miranda, M.E.G., Miranda, N.L.J., 2011. Reston ebolavirus in humans and animals in the Philippines: a review. J Infect Dis. 204 Suppl 3, S757–60. doi:10.1093/infdis/jir296

Patel, M.M., Hall, A.J., Vinjé, J., Parashar, U.D., 2009. Noroviruses: A comprehensive review. Journal of Clinical Virology 44, 1–8. doi:10.1016/j.jcv.2008.10.009

Patel, M.M., Widdowson, M.-A., Glass, R.I., Akazawa, K., Vinjé, J., Parashar, U.D., 2008. Systematic Literature Review of Role of Noroviruses in Sporadic Gastroenteritis. Emerg. Infect. Dis. 14, 1224–1231. doi:10.3201/eid1408.071114

Parker, J., Murphy, W.J., Wang, D., O'Brien, S.J., 2001. Canine and feline parvoviruses can use human or feline transferrin receptors to bind, enter, and infect cells. Journal of ….

Parren, P.W.H.I., Geisbert, T.W., Maruyama, T., Jahrling, P.B., Burton, D.R., 2002. Pre- and postexposure prophylaxis of Ebola virus infection in an animal model by passive transfer of a neutralizing human antibody. J. Virol. 76, 6408–6412. doi:10.1128/JVI.76.12.6408-6412.2002

Parrish, C.R., Holmes, E.C., Morens, D.M., Park, E.-C., Burke, D.S., Calisher, C.H., Laughlin, C.A., Saif, L.J., Daszak, P., 2008. Cross-species virus transmission and the emergence of new epidemic diseases. Microbiol. Mol. Biol. Rev. 72, 457–470. doi:10.1128/MMBR.00004-08

Parrish, C.R., Kawaoka, Y., 2005. THE ORIGINS OF NEW PANDEMIC VIRUSES: The Acquisition of New Host Ranges by Canine Parvovirus and Influenza A Viruses. http://dx.doi.org/10.1146/annurev.micro.59.030804.121059 59, 553–586. doi:10.1146/annurev.micro.59.030804.121059

Peters, C.J., 2002. Human infection with arenaviruses in the Americas. Arenaviruses I 65–74. doi:10.1007/978-3-642-56029-3_3

Peters, C.J., 1996. Emerging infections--Ebola and other filoviruses. West. J. Med. 164, 36–38.

Pirofski, L., Casadevall, A., Rodriguez, L., Zuckier, L.S., Scharff, M.D., 1990. Current state of the hybridoma technology. J Clin Immunol 10, 5S–14S. doi:10.1007/BF00918686

Qiu, X., Alimonti, J.B., Melito, P.L., Fernando, L., Ströher, U., Jones, S.M., 2011. Characterization of Zaire ebolavirus glycoprotein-specific monoclonal antibodies. Clinical Immunology 141, 218–227. doi:10.1016/j.clim.2011.08.008

Qiu, X., Wong, G., Audet, J., Bello, A., Fernando, L., Alimonti, J.B., Fausther-Bovendo,

H., Wei, H., Aviles, J., Hiatt, E., Johnson, A., Morton, J., Swope, K., Bohorov, O., Bohorova, N., Goodman, C., Do Kim, Pauly, M.H., Velasco, J., Pettitt, J., Olinger, G.G., Whaley, K., Xu, B., Strong, J.E., Zeitlin, L., Kobinger, G.P., 2014. Reversion of advanced Ebola virus disease in nonhuman primates with ZMapp. Nature. doi:10.1038/nature13777

Ravel, G., Descotes, J., 2005. Popliteal lymph node assay: facts and perspectives. J Appl Toxicol 25, 451–458. doi:10.1002/jat.1072

Radoshitzky, S.R., Abraham, J., Spiropoulou, C.F., Kuhn, J.H., Nguyen, D., Li, W., Nagel, J., Schmidt, P.J., Nunberg, J.H., Andrews, N.C., Farzan, M., Choe, H., 2007. Transferrin receptor 1 is a cellular receptor for New World haemorrhagic fever arenaviruses. Nature 446, 92–96. doi:10.1038/nature05539

Radoshitzky, S.R., Kuhn, J.H., Spiropoulou, C.F., Albariño, C.G., Nguyen, D.P., Salazar-Bravo, J., Dorfman, T., Lee, A.S., Wang, E., Ross, S.R., Choe, H., Farzan, M., 2008. Receptor determinants of zoonotic transmission of New World hemorrhagic fever arenaviruses. PNAS 105, 2664–2669. doi:10.1073/pnas.0709254105

Radoshitzky, S.R., Longobardi, L.E., Kuhn, J.H., Retterer, C., Dong, L., Clester, J.C., Kota, K., Carra, J., Bavari, S., 2011. Machupo Virus Glycoprotein Determinants for Human Transferrin Receptor 1 Binding and Cell Entry. PLoS ONE 6, e21398. doi:10.1371/journal.pone.0021398

Reddy, S.T., Ge, X., Miklos, A.E., Hughes, R.A., Kang, S.H., 2010. Monoclonal antibodies isolated without screening by analyzing the variable-gene repertoire of plasma cells. Nature.

Reddy, S.T., Swartz, M.A., Hubbell, J.A., 2006. Targeting dendritic cells with biomaterials: developing the next generation of vaccines. Trends in Immunology 27, 573–579. doi:10.1016/j.it.2006.10.005

Reeck, A., Kavanagh, O., Estes, M.K., Opekun, A.R., Gilger, M.A., Graham, D.Y., Atmar, R.L., 2010. Serological correlate of protection against norovirus-induced gastroenteritis. J Infect Dis. 202, 1212–1218. doi:10.1086/656364

Rojek, J.M., Kunz, S., 2008. Cell entry by human pathogenic arenaviruses. Cellular Microbiology 10, 828–835. doi:10.1111/j.1462-5822.2007.01113.x

Ross, S.R., Schofield, J.J., Farr, C.J., 2002. Mouse transferrin receptor 1 is the cell entry receptor for mouse mammary tumor virus. Proceedings of the ….

Saggy, I., Wine, Y., Shefet-Carasso, L., Nahary, L., Georgiou, G., Benhar, I., 2012. Antibody isolation from immunized animals: comparison of phage display and antibody discovery via V gene repertoire mining. Protein Eng. Des. Sel. 25, 539–549. doi:10.1093/protein/gzs060

Salas, R., Pacheco, M.E., Ramos, B., Taibo, M.E., Jaimes, E., Vasquez, C., Querales, J., de Manzione, N., Godoy, O., Betancourt, A., Araoz, F., Bruzual, R., Garcia, J., Tesh, R.B., Rico-Hesse, R., Shops, R.E., 1991. Venezuelan haemorrhagic fever. The Lancet 338, 1033–1036. doi:10.1016/0140-6736(91)91899-6

Sawyer, S.L., Elde, N.C., 2012. A cross-species view on viruses. Current Opinion in Virology 2, 561–568. doi:10.1016/j.coviro.2012.07.003

Sironi, M., Cagliani, R., Forni, D., Clerici, M., 2015. Evolutionary insights into host-pathogen interactions from mammalian sequence data. Nature Reviews Genetics 16, 224–236. doi:10.1038/nrg3905

Smith, G.P., 1985. Filamentous fusion phage: novel expression vectors that display cloned antigens on the virion surface. Science 228, 1315–1317. doi:10.1126/science.4001944

Spitzer, M., Wildenhain, J., Rappsilber, J., Tyers, M., 2014. BoxPlotR: a web tool for generation of box plots. Nature Methods 11, 121–122. doi:10.1038/nmeth.2811

Steinhauer, D.A., Holland, J.J., 1986. Direct method for quantitation of extreme polymerase error frequencies at selected single base sites in viral RNA. J. Virol. 57, 219–228.

Stucker, K.M., Pagan, I., Cifuente, J.O., Kaelber, J.T., 2012. The role of evolutionary intermediates in the host adaptation of canine parvovirus. Journal of ….

Team, W.E.R., 2014. Ebola Virus Disease in West Africa — The First 9 Months of the Epidemic and Forward Projections. http://dx.doi.org/10.1056/NEJMoa1411100 371, 1481–1495. doi:10.1056/NEJMoa1411100

Towner, J.S., Sealy, T.K., Khristova, M.L., Albariño, C.G., Conlan, S., Reeder, S.A., Quan, P.-L., Lipkin, W.I., Downing, R., Tappero, J.W., Okware, S., Lutwama, J., Bakamutumaho, B., Kayiwa, J., Comer, J.A., Rollin, P.E., Ksiazek, T.G., Nichol, S.T., 2008. Newly Discovered Ebola Virus Associated with Hemorrhagic Fever Outbreak in Uganda. PLoS Pathogens 4, e1000212. doi:10.1371/journal.ppat.1000212

Treanor, J.J., Atmar, R.L., Frey, S.E., Gormley, R., Chen, W.H., Ferreira, J., Goodwin, R., Borkowski, A., Clemens, R., Mendelman, P.M., 2014. A novel intramuscular bivalent norovirus virus-like particle vaccine candidate--reactogenicity, safety, and immunogenicity in a phase 1 trial in healthy adults. J Infect Dis. 210, 1763–1771. doi:10.1093/infdis/jiu337

van Asten, L., Siebenga, J., van den Wijngaard, C., Verheij, R., van Vliet, H., Kretzschmar, M., Boshuizen, H., van Pelt, W., Koopmans, M., 2011. Unspecified Gastroenteritis Illness and Deaths in the Elderly Associated With Norovirus Epidemics. Epidemiology 22, 336–343. doi:10.1097/EDE.0b013e31821179af

van Doremalen, N., Miazgowicz, K.L., Milne-Price, S., Bushmaker, T., Robertson, S., Scott, D., Kinne, J., McLellan, J.S., Zhu, J., Munster, V.J., 2014. Host species restriction of Middle East respiratory syndrome coronavirus through its receptor, dipeptidyl peptidase 4. J. Virol. 88, 9220–9232. doi:10.1128/JVI.00676-14

Van Regenmortel, M.H.V., 2014. Specificity, polyspecificity, and heterospecificity of antibody-antigen recognition. J. Mol. Recognit. 27, 627–639. doi:10.1002/jmr.2394

Vega, E., Barclay, L., Gregoricus, N., Shirley, S.H., Lee, D., Vinjé, J., 2014. Genotypic and epidemiologic trends of norovirus outbreaks in the United States, 2009 to 2013. J. Clin. Microbiol. 52, 147–155. doi:10.1128/JCM.02680-13

Walker, L.M., Huber, M., Doores, K.J., Falkowska, E., Pejchal, R., Julien, J.-P., Wang, S.-K., Ramos, A., Chan-Hui, P.-Y., Moyle, M., Mitcham, J.L., Hammond, P.W., Olsen, O.A., Phung, P., Fling, S., Wong, C.-H., Phogat, S., Wrin, T., Simek, M.D., Protocol G Principal Investigators, Koff, W.C., Wilson, I.A., Burton, D.R., Poignard, P., 2011. Broad neutralization coverage of HIV by multiple highly potent antibodies. Nature 477, 466–470. doi:10.1038/nature10373

Walker, L.M., Phogat, S.K., Chan-Hui, P.-Y., Wagner, D., Phung, P., Goss, J.L., Wrin, T., Simek, M.D., Fling, S., Mitcham, J.L., Lehrman, J.K., Priddy, F.H., Olsen, O.A., Frey, S.M., Hammond, P.W., Protocol G Principal Investigators, Kaminsky, S., Zamb, T., Moyle, M., Koff, W.C., Poignard, P., Burton, D.R., 2009. Broad and potent neutralizing antibodies from an African donor reveal a new HIV-1 vaccine target. Science 326, 285–289. doi:10.1126/science.1178746

Wang, B., Kluwe, C.A., Lungu, O.I., DeKosky, B.J., Kerr, S.A., Johnson, E.L., Jung, J., Rezigh, A.B., Carroll, S.M., Reyes, A.N., Bentz, J.R., Villanueva, I., Altman, A.L., Davey, R.A., Ellington, A.D., Georgiou, G., 2015. Facile Discovery of a Diverse Panel of Anti-Ebola Virus Antibodies by Immune Repertoire Mining. Scientific Reports 5, 13926. doi:10.1038/srep13926

Wine, Y., Boutz, D.R., Lavinder, J.J., Miklos, A.E., Hughes, R.A., Hoi, K.H., Jung, S.T., Horton, A.P., Murrin, E.M., Ellington, A.D., Marcotte, E.M., Georgiou, G., 2013. Molecular deconvolution of the monoclonal antibodies that comprise the polyclonal serum response. Proc. Natl. Acad. Sci. U.S.A. 110, 2993–2998. doi:10.1073/pnas.1213737110

Wine, Y., Horton, A.P., Ippolito, G.C., Georgiou, G., 2015. Serology in the 21st century: the molecular-level analysis of the serum antibody repertoire. Current opinion in immunology 35, 89–97. doi:10.1016/j.coi.2015.06.009

Wu, X., Yang, Z.-Y., Li, Y., Hogerkorp, C.-M., Schief, W.R., Seaman, M.S., Zhou, T., Schmidt, S.D., Wu, L., Xu, L., Longo, N.S., McKee, K., O'Dell, S., Louder, M.K., Wycuff, D.L., Feng, Y., Nason, M., Doria-Rose, N., Connors, M., Kwong, P.D., Roederer, M., Wyatt, R.T., Nabel, G.J., Mascola, J.R., 2010. Rational Design of Envelope Identifies Broadly Neutralizing Human Monoclonal Antibodies to HIV-1. Science 329, 856–861. doi:10.1126/science.1187659

Webb, B., Sali, A., 2014. Comparative Protein Structure Modeling Using MODELLER. John Wiley & Sons, Inc., Hoboken, NJ, USA. doi:10.1002/0471250953.bi0506s47

Wolfe, N.D., 2011. The Viral Storm. doi:10.1016/0169-5347(93)90160–Q

Yamashita, M., Emerman, M., 2004. Capsid is a dominant determinant of retrovirus infectivity in nondividing cells. J. Virol. 78, 5670–5678. doi:10.1128/JVI.78.11.5670-5678.2004

Yan, Y., Liu, Q., Wollenberg, K., Martin, C., Buckler-White, A., Kozak, C.A., 2010. Evolution of functional and sequence variants of the mammalian XPR1 receptor for mouse xenotropic gammaretroviruses and the human-derived retrovirus XMRV. J. Virol. 84, 11970–11980. doi:10.1128/JVI.01549-10

Zack, D.J., Wong, A.L., Stempniak, M., Weisbart, R.H., 1995. Two kappa immunoglobulin light chains are secreted by an anti-DNA hybridoma: Implications for isotypic exclusion. Molecular Immunology 32, 1345–1353. doi:10.1016/0161-5890(95)00112-3

Zanini, B., Ricci, C., Bandera, F., Caselani, F., Magni, A., Laronga, A.M., Lanzini, A., 2012. Incidence of Post-Infectious Irritable Bowel Syndrome and Functional Intestinal Disorders Following a Water-Borne Viral Gastroenteritis Outbreak. The

American Journal of Gastroenterology 107, 891–899. doi:10.1038/ajg.2012.102

Zheng, D.-P., Ando, T., Fankhauser, R.L., Beard, R.S., Glass, R.I., Monroe, S.S., 2006. Norovirus classification and proposed strain nomenclature. Virology 346, 312–323. doi:10.1016/j.virol.2005.11.015

Zheng, D.-P., Widdowson, M.-A., Glass, R.I., Vinjé, J., 2010. Molecular epidemiology of genogroup II-genotype 4 noroviruses in the United States between 1994 and 2006. J. Clin. Microbiol. 48, 168–177. doi:10.1128/JCM.01622-09